

# Characterization of Dental Pulp Pluripotent-like Stem Cells (DPPSC) and their mesodermal differentiation potential.

Ester Martínez Sarrà

**ADVERTIMENT.** La consulta d'aquesta tesi queda condicionada a l'acceptació de les següents condicions d'ús: La difusió d'aquesta tesi per mitjà del servei TDX ([www.tesisenxarxa.net](http://www.tesisenxarxa.net)) ha estat autoritzada pels titulars dels drets de propietat intel·lectual únicament per a usos privats emmarcats en activitats d'investigació i docència. No s'autoritza la seva reproducció amb finalitats de lucre ni la seva difusió i posada a disposició des d'un lloc aliè al servei TDX. No s'autoritza la presentació del seu contingut en una finestra o marc aliè a TDX (framing). Aquesta reserva de drets afecta tant al resum de presentació de la tesi com als seus continguts. En la utilització o cita de parts de la tesi és obligat indicar el nom de la persona autora.

**ADVERTENCIA.** La consulta de esta tesis queda condicionada a la aceptación de las siguientes condiciones de uso: La difusión de esta tesis por medio del servicio TDR ([www.tesisenred.net](http://www.tesisenred.net)) ha sido autorizada por los titulares de los derechos de propiedad intelectual únicamente para usos privados enmarcados en actividades de investigación y docencia. No se autoriza su reproducción con finalidades de lucro ni su difusión y puesta a disposición desde un sitio ajeno al servicio TDR. No se autoriza la presentación de su contenido en una ventana o marco ajeno a TDR (framing). Esta reserva de derechos afecta tanto al resumen de presentación de la tesis como a sus contenidos. En la utilización o cita de partes de la tesis es obligado indicar el nombre de la persona autora.

**WARNING.** On having consulted this thesis you're accepting the following use conditions: Spreading this thesis by the TDX ([www.tesisenxarxa.net](http://www.tesisenxarxa.net)) service has been authorized by the titular of the intellectual property rights only for private uses placed in investigation and teaching activities. Reproduction with lucrative aims is not authorized neither its spreading and availability from a site foreign to the TDX service. Introducing its content in a window or frame foreign to the TDX service is not authorized (framing). This rights affect to the presentation summary of the thesis as well as to its contents. In the using or citation of parts of the thesis it's obliged to indicate the name of the author.







Universitat Internacional de Catalunya

Regenerative Medicine Research Institute

*Characterization of Dental Pulp  
Pluripotent-like Stem Cells (DPPSC)  
and their mesodermal  
differentiation potential*

PhD Thesis

Ester Martínez Sarrà

Director: Prof. Maher Atari, PhD

Co-Director: Sheyla Montori Pina, PhD

*Barcelona  
2017*







# Agraïments / Acknowledgements

---

Aquesta tesi doctoral s'ha pogut realitzar gràcies a la Beca **Junior Faculty** concedida per la Universitat Internacional de Catalunya i l'Obra Social "La Caixa". Durant la durada d'aquesta, també s'ha pogut realitzar una estada d'investigació al *Stem Cell Institute* de Leuven de la Universitat KU Leuven gràcies a la beca de mobilitat atorgada per **Boehringer Ingelheim Fonds**.

En primer lloc, voldria agrair al director d'aquesta tesi, el **Dr. Maher Atari**, l'haver-me donat l'oportunitat de poder-la realitzar al seu grup d'investigació. Agrair tot el que m'has ensenyat durant aquests 4 anys sobre com créixer com a científica, com a grup i com a persona. Són innumerables les coses que he après.

Quería agradecer muy especialmente a mi codirectora de tesis, la **Dra. Sheyla Montori**, por estar siempre ahí, siguiendo los experimentos y dando ideas y sugerencias día tras otro. Contigo he aprendido a que surja el problema que surja, siempre se debe buscar cómo solucionarlo y salir adelante.

I would also like to give special thanks to **Prof. Maurilio Sampaolesi**, for giving me the opportunity to work in such a first class institute as the Stem Cell Institute (SCIL) and for always being willing to give such helpful advice and suggestions. Thank you for giving me the opportunity to learn how a high level institute works, learn new techniques and another field of expertise, meet such good researchers and, most of all, remember all the excitement that science can offer. This thesis would not have been the same without your guidance.

I would like to thank as well **Prof. Aernout Lutun**, for all his availability and advices, for teaching me so well and in detail new techniques and letting me work in his laboratory.



Al **Carlos Gil**, per haver-me ensenyat tot en arribar a la UIC, haver-me aconsellat en innumerables ocasions, tenir la paciència més gran del món amb tots nosaltres i especialment amb mi i, sobretot, per ser el millor amic que es pot demanar. Mai podré dir-te un gràcies suficientment gran.

A la **Raquel Núñez**, per haver arribat a la nostra petita família de la UIC i haver portat amb tu l'alegria, el bon humor, les ganes i l'energia. Per haver-me ensenyat a reflexionar sobre molts aspectes importants de la vida i haver-me ensenyat a créixer com a persona, per haver compartit i confiat tantes coses i perquè passar cada dia amb tu i el Carlos ha estat un veritable plaer. Perquè espero que aquesta petita família de tres no es trenqui mai.

A **Begoña Bosch**, que aunque llegaste mucho después, me has dejado una huella muy importante. Gracias por ser cada día tan maravillosa con todos nosotros, por preocuparte de todos y siempre, siempre hacernos sonreír. Porque haces que todos los demás queramos ser mejores personas.

A tothom que forma o ha format part del Laboratori de Medicina Regenerativa i ha fet el dia a dia al laboratori millor. A la **Iulia Hategan**, la **Neus Carrió**, el **Jordi Caballé**, la **Barbara Giordano** i la **Desireé Abellán**.

Als membres del **Laboratori de Ciències Bàsiques**, per compartir el vostre laboratori i tants bons moments a l'inici d'aquest llarg viatge.

To all the members of the Laboratory of Translational Cardiology of the SCIL. Special thanks for their professional help and support to **Domiziana Costamagna** and **Hanne Grosemans**, and for their daily moral support to **Alessio Rotini**, **Gaia Giovannelli**, **Giorgia Giacomazzi**, **Robin Duelen**, **Vardine Sahakyan**, **Francesco Giordano**, **Enrico Pozzo** and **Ester di Filippo**. To the other members of the SCIL and Gasthuisberg that have become more or as close as the others: **Anna Griego**, **Frederic Lluís**, **Anchel de Jaime**, **Albert Bosch**, **Marta Aguirre**, **Rita Khoeiry**, **Michela Bartocchetti** and **Juan García**. Thank you all for being my family away from home.

A la meva **família**, per tot el recolzament que m'ha donat durant aquests 4 anys. Perquè encara que no entenguin el món de la ciència o a què em dedico, sempre estan orgullosos del què faig. Perquè m'han fet veure, i sobretot recentment comprovar, que sempre puc i podré comptar amb ells quan més els necessiti. Gràcies.

A en **Marc**, per tot el que aquesta tesi ens ha costat. Per haver compartit amb mi durant bona part d'aquest llarg viatge les alegries i mal de caps que m'ha portat. Als **seus pares**, per sempre escoltar-me i animar-me a seguir endavant.

Als biotecs, per haver-nos conegut quan només érem uns nens gràcies al nostre amor per la ciència i haver esdevingut amb els anys persones imprescindibles. Perquè començo a sospitar que és ben cert el que diuen de que els amics de la universitat són els amics per tota la vida. A en **Carlos**, els **Marc**s, l'**Eva**, la **Marcel·la**, la **Núria**, la **Judit**, la **Tere** i en **Dani**.

Uno speciale ringraziamento ad **Alessio**, per essermi stato vicino quando ne ho avuto più bisogno e per aver condiviso con me l'ultima parte di questo cammino.

Gràcies a tothom que ha fet possible aquesta tesi.



## TABLE OF CONTENTS

<b>Agraïments / Acknowledgements .....</b>	<b>7</b>
<b>ABBREVIATIONS .....</b>	<b>15</b>
<b>INTRODUCTION .....</b>	<b>19</b>
STEM CELLS .....	21
Embryonic Stem Cells .....	21
Induced Pluripotent Stem Cells .....	22
Adult Stem Cells .....	23
Stem Cells in Regenerative Medicine .....	25
MESODERM-DERIVED CELLS AND TISSUES .....	28
Endothelial differentiation from Stem Cells .....	33
Smooth Muscle differentiation from Stem Cells .....	34
Skeletal Muscle differentiation from Stem Cells .....	36
<b>OBJECTIVES .....</b>	<b>39</b>
<b>HYPOTHESES .....</b>	<b>43</b>
<b>MATERIALS AND METHODS .....</b>	<b>47</b>
Patient selection .....	49
Isolation and culture of DPPSC .....	49
Isolation and culture of DPMSC .....	50
Culture of HUVEC .....	50

TABLE OF CONTENTS

Culture of C2C12 .....50

Lentiviral transduction .....51

Images of optical microscopy .....51

Short-Comparative Genomic Hybridization .....51

RT-PCR analyses .....52

Immunofluorescence analyses .....52

Alkaline Phosphatase staining .....54

Endothelial differentiation *in vitro*.....55

Matrigel assay .....55

Smooth muscle differentiation *in vitro*.....55

Skeletal muscle differentiation *in vitro* .....56

Wound healing assay *in vivo* .....56

Haematoxylin and Eosin staining .....57

Sirius Red staining .....58

DPPSC injection in two models of dystrophic mice .....58

Statistical analyses .....59

**RESULTS .....61**

DPPSC CHARACTERIZATION.....63

DPPSC morphology, growth rate, genetic stability and gene and protein expression.....63

DPPSC pluripotency through passages .....67

DPPSC pluripotency using different seeding and splitting densities .....70

DPPSC pluripotency using different growth media .....74

DPPSC MESODERMAL DIFFERENTIATION POTENTIAL .....	85
DPPSC endothelial differentiation <i>in vitro</i> .....	85
DPPSC smooth muscle differentiation <i>in vitro</i> .....	93
DPPSC skeletal muscle differentiation <i>in vitro</i> .....	95
Wound healing assay <i>in vivo</i> .....	98
DPPSC injection in two different models of dystrophic mice.....	108
<b>DISCUSSION .....</b>	<b>117</b>
DPPSC CHARACTERIZATION.....	119
DPPSC MESODERMAL DIFFERENTIATION POTENTIAL .....	125
Endothelial differentiation .....	125
Smooth muscle differentiation .....	128
Skeletal muscle differentiation.....	130
<b>CONCLUSIONS .....</b>	<b>133</b>
<b>BIBLIOGRAPHY .....</b>	<b>137</b>
<b>APPENDIX - SUPPLEMENTARY DATA.....</b>	<b>155</b>
Supplementary figures and tables .....	157
Ethics Committee approvals.....	164
Doctorate School Academic Committee approvals.....	167



# **ABBREVIATIONS**

---





$\alpha$ SMA: Alpha Smooth Muscle Actin

yc: Common gamma chain / Interleukin 2 receptor subunit gamma

AP / ALP: Alkaline Phosphatase

ASC: Adult Stem Cells

BM: Bone Marrow

BM-MSC: Bone Marrow Mesenchymal Stromal Cells

BMP-4: Bone Morphogenic Protein 4

CD31/PECAM-1: Cluster of differentiation 31 / Platelet endothelial cell adhesion molecule 1

DFPC: Dental Follicle Precursor Cells

DMD: Duchenne Muscular Dystrophy

DMEM: Dulbecco's Modified Eagle's Medium

DNMT3B: DNA methyltransferase 3 beta

DPMSC: Dental Pulp Mesenchymal Stem Cells

DPSC: Dental Pulp Stem Cells

DPPSC: Dental Pulp Pluripotent-like Stem Cells

DGC: Dystrophin Glycoprotein Complex

DYS: Dystrophin

EC: Endothelial Cells

EGF: Epidermal Growth Factor

EGM-2: Endothelial Growth Medium 2

ESC: Embryonic Stem Cells

FBS: Foetal Bovine Serum

FGF: Fibroblast Growth Factor

GAPDH: Glyceraldehyde 3-phosphate dehydrogenase

GMP: Good manufacturing practices

hESC: Human Embryonic Stem Cells

HLA-DR: Human Leukocyte Antigen - antigen D Related

HS: Human Serum

HUVEC: Human Umbilical Endothelial Cells

iPS/iPSC: Induced Pluripotent Stem (Cells)

KLF4: Kruppel-like factor 4

LA-BSA: Linoleic Acid Bovine Serum Albumin

LMNA: Lamin A/C

LEFTY2/EBAF: Left-right determination factor 2

LIF: Leukemia Inhibitory Factor

ABBREVIATIONS

MAPC: Multipotent Adult Progenitor Cells

MD: Muscular Dystrophy

MyHC: Myosin Heavy Chain

MIAMI: Marrow Isolated Adult Multilineage Inducible

MPC: Mesenchymal Progenitor Cells

MSC: Mesenchymal Stromal Cells

OCT4/POU5F1: Octamer-binding Transcription Factor 4

PBS: Phosphate Buffer Saline

PCR: Polymerase Chain Reaction

PDGF: Human Platelet-derived growth factor

PDLSC: Periodontal Ligament Stem Cells

Rag2: Recombination activating gene 2

REX1: ZFP42 Zinc Finger Protein

RT-PCR: Retrotranscriptase PCR

SC: Stem Cells

SCAP: Stem Cells from Apical Papilla

sCGH: short-Comparative Genomic Hybridization

Scid: Severe Combined Immunodeficiency

Sgcb: Beta-Sarcoglycan

SHED: Stem Cells from Human Exfoliated Deciduous Teeth

SMC: Smooth muscle cells

SOX2: Sex determining region Y-box2

SSEA: Stage Specific Embryonic Antigen

TDGF1:Teratocarcinoma-derived growth factor 1

tGFP: Turbo Green Fluorescent Protein

TGF-β: Transforming growth factor beta

TRA-1-60: Tumor-rejection Antigen-1-60

TRA-1-81: Tumor-rejection Antigen-1-81

VE-CAD: Vascular Endothelial Cadherin

VEGFR2/FLK1/KDR/: Vascular Endothelial Growth Factor Receptor 2

VSEL: Very Small Embryonic like

VSMC: Vascular Smooth Muscle Cells

vWF: von Willebrand Factor

# **INTRODUCTION**

---



## STEM CELLS

Stem cells (SC) are undifferentiated cells that have the ability to self-renew and to generate mature, differentiated cells with specialized functions (1). In humans, stem cells have been identified in the inner cell mass of the early embryo, some fetal tissues, the umbilical cord, the placenta and in several adult organs. For the last decades, research on stem cells has provided important information on developmental, morphological, and physiological processes that govern tissue and organ formation, maintenance, regeneration and repair after injuries (2). More recently, significant advancements in our understanding of stem cell biology have provoked great interest and hold high therapeutic promise based on the possibility of stimulating their *ex vivo* and *in vivo* expansion and differentiation into functional progeny that could regenerate injured tissues/organs in humans (3).

So far, different types of stem cells have been used in regenerative medicine studies: (i) embryonic stem cells (ESC), which are pluripotent stem cells that can differentiate into any adult tissue, but they however present donor-recipient immunocompatibility problems and ethical controversy (4); (ii) adult stem cells (ASC), which are multipotent and can only repair and regenerate the tissue in which they reside, limiting their therapeutic use, and (iii) induced pluripotent stem cells (iPSC), somatic cells reprogrammed to a pluripotent state (5), which however present safety issues that impair their use in clinical applications.

### Embryonic Stem Cells

ESC are derived from the blastocyst, an early-stage embryo. Fertilization of an oocyte by a sperm cell results in a single totipotent cell called zygote, the earliest embryonic stage. This zygote, during the first hours after fertilization, divides into identical totipotent cells, which can develop into any of the three germ layers of a human organism (ectoderm, mesoderm or endoderm), into cells of the syncytiotrophoblast layer of the placenta and into the cytotrophoblast layer. When they reach a 16-cell

## INTRODUCTION

stage, called morula, the totipotent cells can undergo differentiation. They can turn into cells that will eventually become either the blastocyst's inner cell mass or the outer trophoblasts. Approximately five days after fertilization, and after several more cycles of cell division, the morula cells begin to commit, forming a hollow sphere of cells, called a blastocyst. The outer layer of the blastocyst is called the trophoblast, and the cluster of cells inside the sphere is called the inner cell mass. At this stage, there are about 70 trophoblast cells and about 30 cells in the inner cell mass. The cells of the inner cell mass, the source of ESC, have become pluripotent stem cells that give rise to all cell types of the major tissue layers (ectoderm, mesoderm, and endoderm) of the embryo (6). The use of ESC in research is controversial, since the isolation of the inner cell mass results in the destruction of the fertilized human embryo, which raises ethical issues (7).

Human embryonic stem cell (hESC) lines express many markers that are common to pluripotent and undifferentiated cells, such as octamer-binding transcription factor 4 (OCT4), NANOG, Sex determining region Y-box2 (SOX2), alkaline phosphatase (ALP), LIN28, ZFP42 Zinc Finger Protein (REX1), teratocarcinoma-derived growth factor 1 (TDGF1/Cripto), DNA methyltransferase 3 beta (DNMT3B), CD9, CD24, left-right determination factor 2 (LEFTY2/EBAF), and Thy-1, as well as stage-specific embryonic antigen-3 and 4 (SSEA-3 and SSEA-4) and tumor-rejection antigen-1-60 and 1-81 (TRA-1-60 and TRA-1-81) (8).

## Induced Pluripotent Stem Cells

In 2006, *Takahashi et al.* (5) showed that the introduction of four specific genes encoding transcription factors (OCT4, SOX2, c-MYC and KLF4) could convert mouse adult cells (fibroblasts) into pluripotent stem cells known as iPSC. These cells have the ability to propagate indefinitely, to give rise to every cell in the adult body and they are similar to ESC in morphology, proliferation and teratoma capacity formation. In 2007, iPSC were obtained from human adult stem cells by two different groups and gene introduction: *Takahashi et al.* (5) using the same 4 genes (OCT4, SOX2, c-MYC and KLF4) and *Yu et al.* using OCT4, NANOG, SOX2 and LIN28 (9).

## **Adult Stem Cells**

ASC are undifferentiated cells that reside in most of adult tissues/organs, including bone marrow, heart, brain, lungs, liver, skin and eyes (10-15). They can renew themselves in the body, making identical copies of themselves, or become specialized to yield the cell types of the tissue of origin (16). The use of ASC in research and therapy is not controversial, unlike ESC, as they are extracted from adult tissue samples rather than destroyed human embryos.

One type of ASC, mesenchymal stromal cells (MSC), has generated great interest in the fields of regenerative medicine and immunotherapy due to their unique biologic properties. MSC were first discovered in 1968 by Friedenstein and colleagues (17) as adherent fibroblast-like cells in the bone marrow (BM) capable of differentiating into bone. It was subsequently shown that MSC could be isolated from various tissues such as BM, adipose tissue (18), and umbilical cord blood (19). These cells can be expanded *in vitro*, which allows them to rapidly reach the desired cell counts for use *in vivo*. Using different strategies, several laboratories have identified, isolated, and cultured MSC with specific properties (20).

### ***Dental Pulp Stem Cells***

SC can be classified based on their capacity for differentiation, but also on their tissue of origin, such as bone marrow mesenchymal/stromal cells (BM-MSC), hematopoietic SC, umbilical cord blood SC, epithelial SC, and SC from the dental pulp. The dental pulp is a soft connective tissue within the dental crown thought to be derived from migratory neural crest cells during development. It has been shown to harbor various populations of multipotent stem/progenitor cells. Since their very first isolation in 2000 by Gronthos *et al.* (21), several types of adult stem cells have been isolated from teeth, including dental pulp stem cells (DPSC), stem cells from human exfoliated deciduous teeth (SHED), periodontal ligament stem cells (PDLSC), dental follicle precursor cells (DFPC), and stem cells from apical papilla (SCAP)(21-25).

These populations have MSC-like qualities, namely the capacity for self-renewal, the potential to differentiate into multiple lineages including osteoblasts and chondroblasts,



## INTRODUCTION

and a potential for in vitro differentiation into cell types from various embryonic layers, including adipose, bone, endothelial and neural-like tissue. They are often compared to BM-MSC and share many similarities with them, but they differ in that dental stem cells seem to be committed to an odontogenic fate, more so than to an osteogenic one. Since they have a neural crest origin, they have stronger neurogenesis capabilities but weaker adipogenesis and chondrogenesis (26).

DPSC are isolated by enzymatic digestion of pulp tissue after separating the crown from the roots. These cells are morphologically similar to fibroblasts, very proliferative and clonogenic. DPSC are multipotent cells that proliferate extensively, can be safely cryopreserved, possess immunosuppressive properties and express markers such as CD13, CD29, CD44, CD59, CD73, CD90, CD105, CD146, and STRO-1, but do not express CD14, CD24, CD34, CD45, CD19 and HLA-DR (Human Leukocyte Antigen - antigen D Related). They have the ability to differentiate into odontoblast-like cells, osteoblasts, adipocytes, neural cells, cardiomyocytes, myocytes, and chondrocytes in vitro. DPSC represent less than 1% of the total cell population present in the dental pulp (27).

### ***Dental Pulp Pluripotent-like Stem Cells***

In previous studies, our group has described a new population of adult stem cells called Dental Pulp Pluripotent-like Stem Cells (DPPSC) (28-30). These cells are isolated from the dental pulp of the third molars, express pluripotency markers such as OCT4, NANOG and SOX2, and show embryonic-like behaviour differentiating into tissues of the three embryonic layers.

These cells are not the first SC population isolated from adult tissues with pluripotency-like capacities. Indeed, several populations have been identified in recent years: very small embryonic-like (VSEL) (31), multipotent adult progenitor cells (MAPC) (32), mesodermal progenitor cells (MPC) (33) and marrow-isolated adult multilineage inducible (MIAMI) cells (34).

Compared to other populations, DPPSC have as the main advantage the fact that the third molars are a very accessible source of cells, because wisdom tooth extraction is

widely performed and the teeth are usually considered to be medical waste. Since the third molar is the last tooth to develop in humans, it is normally in an early stage of development and is capable of yielding an optimum quantity of dental pulp tissue for the isolation of stem cells. Although the percentage of DPPSC decreases with age, a population of these cells is always present (28).

DPPSC and DPSC share the same isolation protocol, as well as some characteristics. However, they differ in the expression levels of embryonic markers as well as some membrane proteins such as CD73. The culture conditions between them are also different; DPPSC need low density and a specific medium that contains growth factors such as epidermal growth factor (EGF), platelet-derived growth factor (PDGF) and leukemia inhibitory factor (LIF) to allow maintenance of the pluripotent state of DPPSC. The characteristics unique to these cells are still under investigation, but the current evidence gain insights for future comparative studies of the regenerative potency of DPPSC and SC from other sources. It has been demonstrated, for instance, that DPPSC have a greater capacity for generating bone-like cells in comparison with DPSC (30).

In addition, DPPSC have pluripotent-like properties that have not been found in cells of any other adult source: the ability to form EB-like and teratoma-like structures (28), which had been thought to be exclusive to ESC and iPSC (35, 36).

## **Stem Cells in Regenerative Medicine**

Regenerative medicine is an emerging interdisciplinary field of research and clinical applications focused on the repair, replacement or regeneration of cells, tissues or organs to restore impaired function resulting from any cause, including congenital defects, disease, trauma and aging (37). Organ regeneration is distinct from organ repair as an endpoint of a healing process following injury. Repair is an adaptation to loss of normal organ mass and leads to restoration of the interrupted continuity by synthesis of scar tissue without restoration of the normal tissue. By contrast, regeneration restores the interrupted continuity by synthesis of the missing organ mass

## INTRODUCTION

at the original anatomical site, yielding a regenerate (38). Therefore, the ultimate aim of regenerative medicine is to regenerate cells, tissues or organs.

This field holds the promise of providing therapeutic treatment for conditions where current therapies are inadequate by stimulating the body's own repair mechanisms to functionally heal previously irreparable tissues or organs or by growing tissues and organs in the laboratory and implanting them when the body cannot heal itself (39). It uses a combination of several technological approaches that moves it beyond traditional transplantation and replacement therapies. These approaches may include, but are not limited to, the use of soluble molecules administered alone or as a secretion by infused cells (immunomodulation therapy), gene therapy, cell transplantation (cell therapy), transplantation of *in vitro* grown organs and tissues (tissue engineering) and the reprogramming of cell and tissue types (40, 41).

Some of the biomedical approaches within the field of regenerative medicine may involve the use of stem cells (42), named stem-cell therapy. Human body has an endogenous system of regeneration through stem cells, where adult stem cells are found almost in every type of tissue. Their main post-natal function is to repair and regenerate the tissues in which they reside. That is why, the idea is that restoration of function is best accomplished by these cells (39).

Stem cells can overcome one of the most limiting aspects of cell therapy and tissue regeneration, which is obtaining enough quantity of cells (43), since they have a high self-renewal potential. Moreover, they can help in the regeneration process via a paracrine effect. If regeneration is achieved using autologous cells, i. e. adult stem cells, it would potentially solve the problem of the shortage of organs available for donation, the problem of organ transplant rejection due to immune complications and the problem of possible transfer of inherent infections from another donor. Taking into account all these aspects, the use of autologous adult stem cells is highly explored in regenerative medicine.

As said before, other types of stem cells, such as ESC, have a great potential due to their characteristics but their use is limited by ethical considerations and donor-

recipient immunocompatibility (39). Another type of stem cells, iPSC, presents disadvantages regarding safety issues that impair their use in clinical applications.

A limiting aspect that cell therapy using adult stem cells can present is the difficulty to harvest the cells, since it can require an invasive procedure to the patient that can cause large donor site morbidity (43). However, dental pulp tissue represents an easily accessible source of adult stem cells with low morbidity. As said before, since the third molar is the last tooth to develop in humans, it is normally in an early stage of development and is capable of yielding an optimum quantity of dental pulp tissue for the isolation of stem cells.

In *Rotter et al. (43)* it was stated that high numbers of stem cells with an effective and reliable potential for differentiation are needed for clinical applications. Thus, the identification of new stem cell sources and the establishment of optimized cell culture conditions that allow for the amplification of stem cells are of utmost relevance. In addition, the isolation procedure should ideally be minimally invasive and possibly be performed under local anesthesia (43). As said before, DPPSC, adult stem cells from the dental pulp, present a minimally invasive isolation protocol, and their effective and reliable potential for differentiation is currently under investigation, with promising results already obtained (28, 30). Nevertheless, more studies to test the differentiation capacity of DPPSC to multiple cell types are still needed.

## INTRODUCTION

**MESODERM-DERIVED CELLS AND TISSUES**

Mesoderm-derived cell types are osteogenic cells, chondrogenic cells, adipogenic cells, skeletal muscle cells, smooth muscle cells, cardiac muscle cells and endothelial cells. Although the osteogenic differentiation potential of DPPSC is quite established, little is known about their endothelial and smooth and skeletal muscle cell differentiation capability.

A key tissue regenerative process related to any stem cell-based application is the angiogenesis, the generation of new blood vessels. Indeed, blood vessels deliver oxygen and nutrients to all of the tissues and organs in the body. The two major cellular components of blood vessels are endothelial cells (EC) and vascular smooth muscle cells (VSMC). Both EC and VSMC are required for vascular function, including blood pressure control, interactions with immune cells, and the uptake of nutrients (44). As pointed out before, these two cellular types derive from the mesodermal germ layer of the very early embryo, although some smooth muscle cells (SMC) originate from the neural crest (45).

Blood vessels can be divided in three major types: arteries (and arterioles), veins (and venules) and capillaries. Arteries carry the blood away from the heart, veins carry it to the heart and capillaries are the ones in which gas, nutrients and wastes exchange with the tissues actually takes place. Regarding their structure, arteries and veins have the same three layers of tissue in their walls, while capillaries, which are much thinner, only present the most internal one of them. These layers are: (i) the tunica interna or intima, which is the thinnest of the three and is formed by EC; (ii) the tunica media, which is rich in VSMC; and (iii) the tunica externa or adventitia, made of connective tissue (Fig. 11).

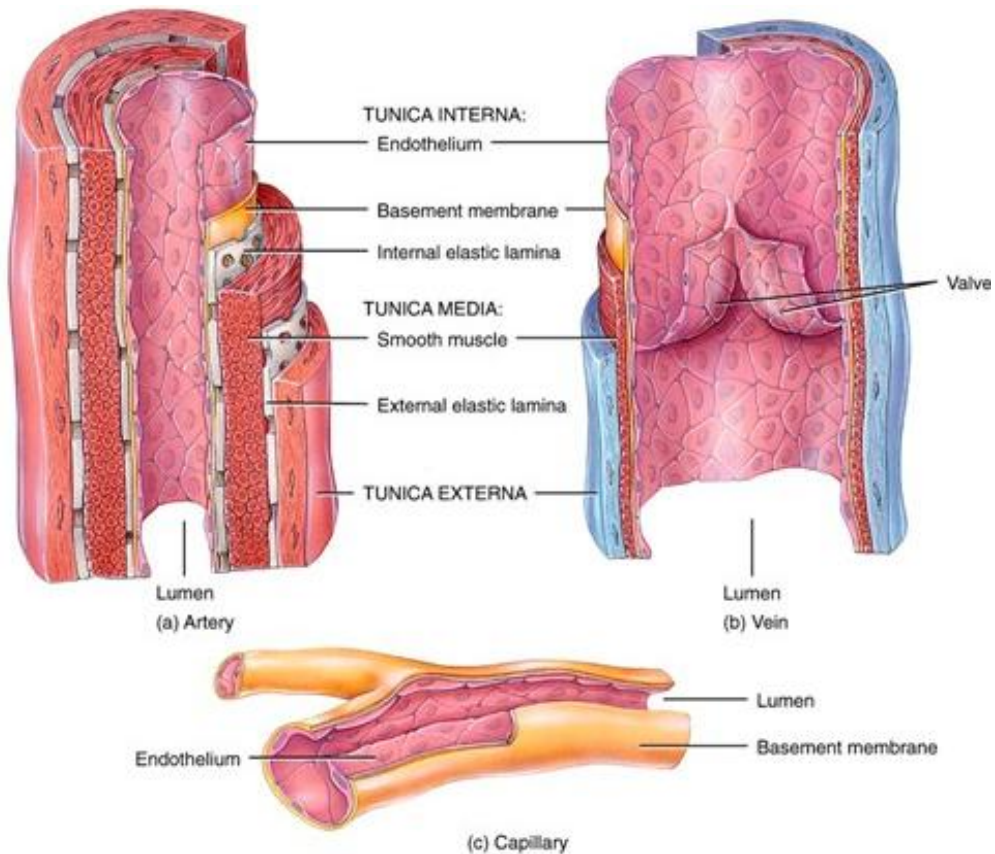


**Figure 11:** Structure of the three major types of blood vessels. Extracted from Tortora et al. (46).

Both EC and VSMC play various major physiological and pathological roles in the blood vessels. EC are responsible for subendothelial matrix proteins synthesis, homeostasis, thrombolysis, vasomotor properties, antigen presentation and synthesis of growth factors such as PDGF, insulin-like growth factor 1 (IGF-1) and FGF, which promote cell growth of VSMC (47, 48). VSMC also play physiological and pathological major roles, since they must continually repair arterial injuries and maintain functional mass in response to changing demands upon the vessel wall. Vascular smooth muscle is composed of multifunctional cells that exhibit spontaneous and agonist-induced contractile properties, secrete and assemble a wide variety of extracellular matrix

## INTRODUCTION

proteins, display migratory and proliferative responses to tissue injury, and both produce and respond to a variety of paracrine-acting growth factors (49).

Currently, there is a growing list of diseases with high incidences with an etiology that is related to blood vessels (50). More than 500 million people worldwide may benefit from pro- or anti-angiogenesis treatments (51). Tissue regeneration and stimulation of angiogenesis are important therapeutic considerations in the treatment of myocardial infarction, peripheral vascular disease, and stroke (52). In addition, angiogenesis is a key process in tissue engineering. If blood supply cannot be established rapidly, there is insufficient oxygen and nutrient transport and necrosis of the implanted tissue will occur (53). For all these reasons, EC and VSMC differentiation are studied in regenerative medicine approaches.

Another important mesoderm-derived tissue for regenerative medicine is skeletal muscle, which is the largest mesoderm-derived organ and is responsible for the voluntary movement of the body. The smallest unit of skeletal muscle is the muscle fibre or myofibre, which is a long cylindrical cell that contains many nuclei, mitochondria, and sarcomeres. The latter, made of actin and myosin filaments represent the functional unit of the muscle and are responsible for muscle contraction.

Each muscle fibre is surrounded by a thin layer of connective tissue called the endomysium (Fig. I2). Approximately 20–80 of these muscle fibres are grouped together in a parallel arrangement called a muscle fascicle or fibre bundle that is encapsulated by a perimysium, which is thicker than the epimysium, enclosing each of the bundled muscle fibres. A distinct muscle is formed by enveloping a large number of muscle fascicles in a thick collagenous external sheath extending from the tendons called the epimysium (Fig. I2).

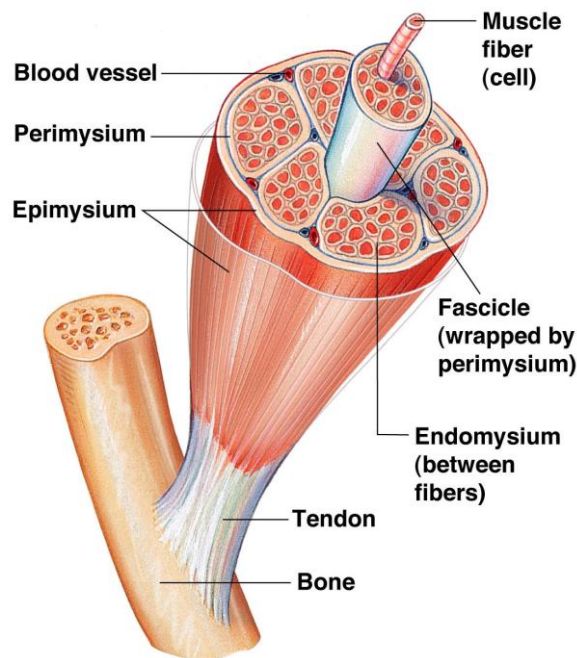


**Figure 12:** Structure of a skeletal muscle. Copyright © 2006 Pearson Education, Inc., publishing as Benjamin Cummings.

As said before, the smallest units of skeletal muscle are cylindrical, multinucleated muscle fibres. These structures are established during embryogenesis, when mononuclear cells known as myoblasts fuse into immature myofibres (myotubes). The myofibre nuclei (myonuclei) are postmitotic and under normal conditions cannot re-enter a proliferative state to contribute additional nuclei. Thus, during postnatal life, myofibres growth, homeostasis, and repair only rely on satellite cells, myogenic stem cells residing between the basal lamina and the muscle fibre membrane (54-57).

Many diseases that affect the musculature belong to the group of muscular dystrophies (MD). MD refers to a group of more than 30 genetic diseases that cause progressive weakness and degeneration of skeletal muscles used during voluntary movement. These disorders vary in age of onset, severity, and pattern of affected muscles. All forms of MD grow worse as muscles progressively degenerate and weaken. At the



INTRODUCTION

end, many individuals eventually can lose the ability to walk. For all this, skeletal muscle differentiation is also studied in regenerative medicine approaches.

The proteins that result affected in these diseases reside inside the so called Dystrophin Glycoprotein Complex (DGC) (Fig. I3). The most important, dystrophin (DYS), which results mutated in Duchenne Muscular Dystrophy (DMD), connects the sarcolemmal cytoskeleton to the extra-cellular matrix. This is accomplished through a series of interactions with a large group of membranous proteins, that belong for instance to the DGC. Other dystrophies show mutations in genes encoding for sarcoglycans, proteins that are thought to stabilize the DGC and indeed are thought to be part of it (Fig. I3).

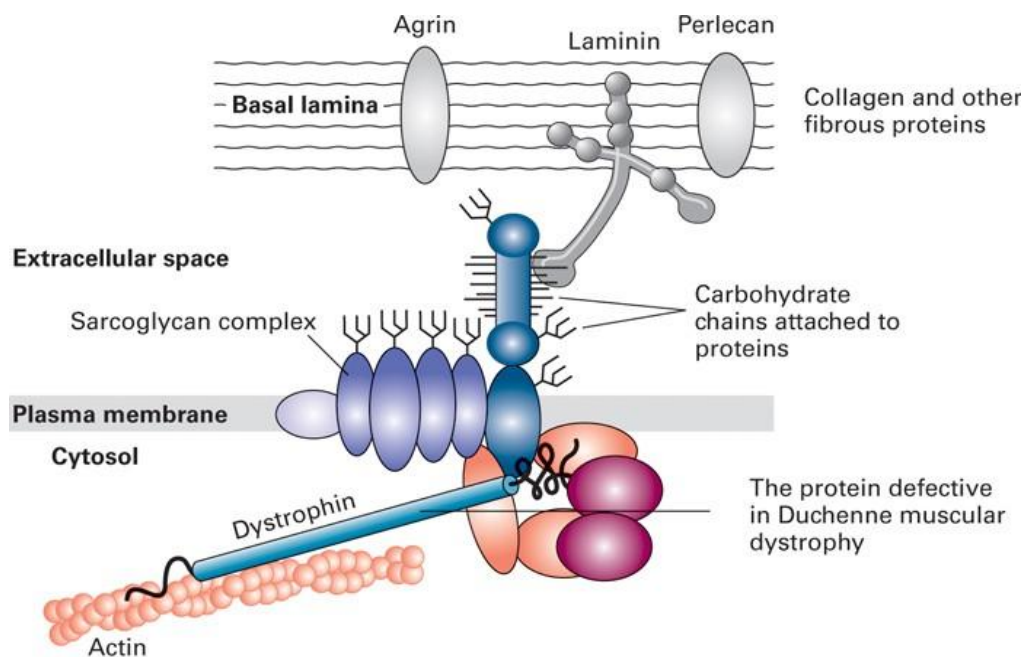


**Figure I3:** The dystrophin glycoprotein complex (DGC) in skeletal muscle cells. Extracted from Lodish et al. (58).

## **Endothelial differentiation from Stem Cells**

Currently available vascular grafts cannot reproduce the complex functions of native vessels (59). In this regard, it has been proved that presence of functional endothelial cells (EC) in the grafts can improve these functions (60). Cells assigned to cover the tissue engineered vessels have been already isolated from several human sources such as blood vessels, bone marrow and adipose tissue. However, these grafts are difficult to prepare due to insufficient autologous sources of EC (61) or the difficulty to obtain them.

To increment the number of obtained cells, stem cell differentiation has been explored, since EC derived from hESC may be used to generate a large supply of transplantable, healthy, functional cells for the repair of ischemic tissues (52). To date, there exist two commonly used methods to induce vascular cell differentiation from human pluripotent stem cells: i) embryoid body (EB) formation (62, 63) and ii) monolayer-directed differentiation (52, 64). EB formation results in differentiation of human pluripotent stem cells into various cell types, including vascular cells, albeit inefficiently (1%–5%) (62, 65, 66). Current monolayer differentiation methods offer increased efficiencies (5–20%) but depend on undefined supplements, co-culture (64, 67), heterogeneous cell aggregates (68), conditioned medium (52, 69), or lack consistent yields of vascular cells (70).

There have also been studies concerning the differentiation of adult stem cells into EC, mostly using MSC (71, 72). MSC derived from bone marrow are able to differentiate into various cell lineages of bone, cartilage, adipose, myocardial, and to some extent also into EC (73-75). The disadvantages of BM–MSC are the invasive harvesting procedure and the long lasting differentiation process. Therefore, other possible sources with less traumatizing intervention are necessary. MSC from adipose tissue represent an abundant and accessible source of such cells, which can as well differentiate into a number of mesodermal lineages, including EC (18, 76, 77). The capacity of these cells to differentiate into the endothelial cell lineage is however limited (71). Furthermore, in several studies, endothelial progenitor cells, have also been used for autologous transplantation therapy and have been shown to promote the

## INTRODUCTION

regeneration of ischemic tissues (78-81). However, difficulties in obtaining sufficient numbers of adult endothelial progenitor cells, still limit autologous stem cell therapies (82, 83). This stresses an urgent need for an easily accessible stem cell source with a high proliferation rate that can also provide sufficient cell numbers for transplantation (53).

In a preliminary study from this group (28), DPPSC showed potential to differentiate to the endothelial lineage. In the project here presented, therefore, we wanted to further investigate DPPSC capacity to undergo endothelial differentiation *in vitro*, optimizing their differentiation protocol, as well as testing their angiogenic potential *in vivo*. For the latest, we used a nude mice model to study the wound healing assay process in terms of wound closure, wound matrix organization and wound revascularization.

### **Smooth Muscle differentiation from Stem Cells**

The alterations in the differentiated state in smooth muscle cells (SMC) contribute to a variety of major cardiovascular diseases such as atherosclerosis, hypertension, restenosis and vascular aneurysm (45, 84). A better understanding of the cellular and molecular mechanisms that control VSMC differentiation is essential to help develop new approaches to both prevent and treat these diseases. Therefore, development of reliable and reproducible *in vitro* cellular models to study SMC differentiation is needed, yet it has been problematic due to intrinsic peculiarities of SMC (85, 86). In addition, smooth muscle differentiation is exploited by tissue engineering techniques to design new organ structures consisting of smooth muscle, e.g. vascular constructs or bladder reconstruction substrates (87).

SMC differentiation is a complex and poorly defined process, although much progress has been made in identifying molecular mechanisms controlling the expression of SMC specific genes (85). Accumulating evidence has shown that a precisely coordinated molecular network orchestrates the SMC differentiation program involved in a range of signaling pathways, including transforming growth factor beta (TGF- $\beta$ ).

VSMC originate from at least five different sources of progenitors during embryonic development, including neural crest, proepicardium, serosal mesothelium, secondary heart field and somites (45, 88); and SMC responses to environmental signals, such as growth factors, have been observed to vary depending on the developmental origins of SMC (45). In addition, SMC can undergo phenotypic changes, *in vitro* and *in vivo*, switching between secretory and contractile phenotypes, thus obscuring our conceptual reference to terminal differentiation in these cells (86).

Several *in vitro* model systems have been developed to mimic the SMC differentiation *in vivo* including using embryonic stem cells, embryoid bodies, neural crest cells, pluripotent C3H10T1/2 cells and multipotent A404 cells. Although these models have significantly contributed to the understanding of SMC differentiation, each of these models has its limitations (85). Human embryonic stem cell can differentiate to both EC and SMC populations in the same differentiation conditions. Though the cells are excellent for *in vivo* neoangiogenesis and regeneration of blood vessels, they may not be ideal for precisely dissecting the molecular mechanism governing SMC differentiation because SMC differentiated from embryonic stems cells are heterogenic and thus contain a mixed population. In *Shi et al. 2015* (85), human embryonic stem cell-derived mesenchymal cells derived from H9 human embryonic were studied. These stem cells are natural SMC progenitors for mesoderm-derived SMC that account for most of the vascular SMC (45) and could be robustly differentiated to SMC phenotype upon TGF- $\beta$  stimulation and exhibit a morphology resembling functional SMC.

In this project, we studied the DPPSC ability to undergo smooth muscle differentiation *in vitro* and *in vivo* in a mouse model of wound healing and in two mice model of dystrophy. Regarding the different developmental origins of SMC, it would be interesting to evaluate their differentiation from DPPSC, which have an ectomesodermal origin.

## INTRODUCTION

**Skeletal Muscle differentiation from Stem Cells**

Muscular dystrophies are particularly challenging from a therapeutic point of view and stem cell based therapy is considered to be one of the most promising methods for treating muscular dystrophies. Because of the properties of satellite cells, they represented the first candidate and there have been several clinical trials since the early 1980s involving the transplant by intramuscular injections of these cells into several locations of a single muscle or at most a few muscles (89, 90). Although results in treating DMD patients have been encouraging, this method has been limited by: (i) the necessity of a huge number of injections; (ii) immune responses toward injected satellite cells; and (iii) the rapid death of most of the satellite cells in the first 72 hours following injection (91, 92). In order to overcome these issues, many studies were addressed to find a population of ideal stem cells that could fulfill several criteria needed for the transplantation. Many studies focused on stem cells usually derived from adult bone marrow, hematopoietic SC and MSC. The latter can be obtained from fat, skin, periosteum, synovial membrane and muscle as well. MSC are multipotent and capable of differentiating into several connective tissue types including osteocytes, chondrocytes, adipocytes, tenocytes and myoblasts (93). They can also impose an additional anti-inflammatory and paracrine effect on differentiation and tissue regeneration via cytokine pathways, have anti-apoptotic features (94-96) and can produce extracellular matrix molecules (97). Compared with pluripotent ESC or iPSC, MSC have a greater biosafety profile and lower risk of tumorigenicity, and perhaps that is why numerous MSC-based therapies have made it to the clinical trial stage (98, 99). Regarding DPSC, it has been shown that upon infusion into cardiotoxin-induced muscle defects, cloned DPSC engraft and colonize host muscle, as well as express dystrophin and myosin heavy chain more efficaciously than their parent heterogeneous cells. Another study also showed the ability of pre-differentiated DPSC to regenerate dystrophin-expressing myofibres within the injected host muscles, although the number of fibres was very limited (100). These cells also showed enhancement of angiogenesis in the tissue.

All these data suggested that DPPSC could have therapeutic potential in MD. In this study, we investigated the myogenic potential of DPPSC *in vitro* and *in vivo* in an *mdx* mouse model and in a *β-sarcoglycan-null* mouse model, which represent two reliable mice models of dystrophies.



# **OBJECTIVES**

---





## Main objectives

- To characterize DPPSC and to evaluate their pluripotency capacity.
- To evaluate the mesodermal differentiation potential of DPPSC.

## Secondary objectives

- To study whether the pluripotency capacity of DPPSC changes through cell passages.
- To study whether modifications in the culture conditions such as the cellular seeding density and splitting confluence affect the pluripotency capacity of DPPSC.
- To find a GMP-approved growth medium for DPPSC that maintains the pluripotency capacity of the cells and therefore facilitates their future application in regenerative medicine.
- To evaluate the endothelial differentiation potential of DPPSC *in vitro* (optimizing the differentiation protocol) and *in vivo*.
- To evaluate the smooth muscle differentiation potential of DPPSC *in vitro* and *in vivo*.
- To evaluate the skeletal muscle differentiation potential of DPPSC *in vitro* and *in vivo*.



# **HYPOTHESES**

---



- H<sub>1</sub> 1: DPPSC have pluripotency potential.
- H<sub>0</sub> 1: DPPSC do not have pluripotency potential.
  - H<sub>1</sub> 1.1: The pluripotency capacity of DPPSC changes through cell passages.
  - H<sub>0</sub> 1.1: The pluripotency capacity of DPPSC does not change through cell passages.
  - H<sub>1</sub> 1.2: DPPSC pluripotency capacity is influenced by culture conditions such as the cellular seeding density and splitting confluence.
  - H<sub>0</sub> 1.2: DPPSC pluripotency capacity is not influenced by culture conditions such as the cellular seeding density and splitting confluence.
  - H<sub>1</sub> 1.3: DPPSC can be cultured in a GMP-approved growth medium that maintains the pluripotency capacity of the cells and facilitates their future application in regenerative medicine.
  - H<sub>0</sub> 1.3: DPPSC cannot be cultured in a GMP-approved growth medium that maintains the pluripotency capacity of the cells and facilitates their future application in regenerative medicine.
- H<sub>1</sub> 2: DPPSC have the ability to differentiate into different cells from the mesodermal lineage *in vitro* and *in vivo*.
- H<sub>0</sub> 2: DPPSC do not have the ability to differentiate into different cells from the mesodermal lineage *in vitro* and *in vivo*.
  - H<sub>1</sub> 2.1: DPPSC can differentiate into endothelial cells *in vitro*.
  - H<sub>0</sub> 2.1: DPPSC cannot differentiate into endothelial cells *in vitro*.
  - H<sub>1</sub> 2.2: DPPSC can differentiate into endothelial cells *in vivo*.
  - H<sub>0</sub> 2.2: DPPSC cannot differentiate into endothelial cells *in vivo*.
  - H<sub>1</sub> 2.3: DPPSC can differentiate into smooth muscle cells *in vitro*.
  - H<sub>0</sub> 2.3: DPPSC cannot differentiate into smooth muscle cells *in vitro*.
  - H<sub>1</sub> 2.4: DPPSC can differentiate into smooth muscle cells *in vivo*.
  - H<sub>0</sub> 2.4: DPPSC cannot differentiate into smooth muscle cells *in vivo*.

HYPOTHESES

- $H_1$  2.5: DPPSC can differentiate into skeletal muscle cells *in vitro*.
- $H_0$  2.5: DPPSC cannot differentiate into skeletal muscle cells *in vitro*.
- $H_1$  2.6: DPPSC can differentiate into skeletal muscle cells *in vivo*.
- $H_0$  2.6: DPPSC cannot differentiate into skeletal muscle cells *in vivo*.

# **MATERIALS AND METHODS**

---





## Patient selection

DPPSC and DPMSC (Dental Pulp Mesenchymal Stem Cells) were isolated from healthy human third molars extracted for orthodontic and prophylactic reasons from 15 patients with ages comprised between 14 and 21 year old. All patients provided informed consent before obtaining the samples. For patients under 18 years old, a legal guardian authorised the procedure. Experiments were performed following the guidelines on human stem cell research issued by the Committee on Bioethics of the UIC Barcelona. The approved protocol code of this study is BIO-ELB-2013-04 (see appendix – supplementary data). Clinical information about the patients and the third molars can be found in the supplementary data (Supplementary Table 1).

## Isolation and culture of DPPSC

After extraction, teeth were washed using gauze soaked in 70% ethanol. A second wash was performed with distilled water. The dental pulp was then extracted from the teeth using a sterile nerve-puller file 15 and forceps if the apexes were still open or, otherwise, fracturing the teeth and taking the dental pulp using forceps. The dental pulp was placed in falcon tubes containing sterile 1X phosphate-buffered saline (PBS) with 5% of 0.25% trypsin-EDTA (Life Technologies) and 1% Penicillin-Streptomycin (PAA). The samples were then transferred to the laboratory. The tissues from the dental pulp were disaggregated by digesting the dental pulp tissue with collagenase type I (3 mg/ml; Sigma) for 60 minutes at 37°C. After that, the cells were cultivated in DPPSC medium, which consisted of 60% Dulbecco's modified Eagle's medium (DMEM)-low glucose (Life Technologies) and 40% MCDB-201 (Sigma) supplemented with 1X insulin-transferrin-selenium (ITS; Sigma), 1X linoleic acid-bovine serum albumin (LA-BSA; Sigma),  $10^{-9}$  M dexamethasone (Sigma),  $10^{-4}$  M ascorbic acid 2-phosphate (Sigma), 100 units of penicillin/1000 units of streptomycin (PAA), 2% foetal bovine serum (FBS; Sigma), 10 ng/ml human PDGF-BB (R&D Systems), 10 ng/ml EGF (R&D Systems), 1000 units/ml human LIF (Millipore), Chemically Defined Lipid Concentrate (Gibco), 0.8 mg/ml BSA (Sigma) and 55 mM  $\beta$ -mercaptoethanol (Sigma) in 650 ml flasks precoated overnight with 100 ng/ml fibronectin at 37°C in a 5% CO<sub>2</sub>

## MATERIALS AND METHODS

incubator. During the 2 weeks of primary culture, the medium was changed every 4 days. To propagate DPPSC, the cells were detached at 30% confluence (after 3-4 days of culture) by adding PBS containing 0.25% trypsin-EDTA (Life Technologies) and replated at a density of 100 cells/cm<sup>2</sup>. Seeding DPPSC at the appropriate cell density with uniform distribution and correct timing of passage entails the most crucial part of DPPSC culture. Too low cell density results in cell death whereas too high cell density could result in differentiation into MSC lineage.

### **Isolation and culture of DPMSC**

Adult human DPMSC were isolated from the dental pulp of third molar teeth as described above and then suspended in DMEM with 4.5 g/l glucose (Life Technologies) supplemented with 10% FBS (Hyclone) and 1X Penicillin/Streptomycin (PAA). Cells were grown in 650 ml flasks at 37°C in a 5% CO<sub>2</sub> incubator. The medium was changed after 3 days and every 2 days thereafter. To propagate the DPMSC, the cells were detached at 90% confluence by the addition of PBS containing 0.25% trypsin-EDTA (Life Technologies) and replated at a density of 5-10x10<sup>3</sup> cells/cm<sup>2</sup>. DPMSC were used as controls to compare against DPPSC growth rate and genetic stability, as well as differentiation potential to endothelial lineage. DPMSC and DPPSC from the same donors were always used for direct comparison.

### **Culture of HUVEC**

Human Umbilical Vein Endothelial Cells were maintained with EGM-2 (Lonza), the medium was changed every 2 days and the cells were expanded when they reached 70-85% confluence using PBS containing 0.25% trypsin-EDTA (Life Technologies) and replated at a density of 2.5x10<sup>3</sup> cells/cm<sup>2</sup>. HUVEC were used as a positive control for endothelial differentiation of DPPSC, as well as for co-cultures differentiation systems or obtaining conditioned medium.

### **Culture of C2C12 cells**

The mouse immortalised line C2C12 of skeletal myoblasts was maintained using DMEM 4.5 g/l glucose supplemented with 10% FBS (Hyclone), 1% Glutamine (Sigma),

1% Sodium Pyruvate (Life Technologies) and 1% Penicillin/Streptomycin (Life Technologies). They were used as a positive control for skeletal muscle differentiation of DPPSC, as well as for co-cultures differentiation systems or obtaining conditioned medium. This technique was performed during a stay in the Laboratory of Translational Cardiomyology of the Stem Cell Biology and Embryology Unit, Department of Development and Regeneration of the KU Leuven.

## **Lentiviral transduction**

DPPSC at a density of 500, 1000 or 2000 cells/cm<sup>2</sup> were seeded and transduced at 50-70% confluence with the lentiviral vector shc003 (Sigma) containing turbo Green Fluorescent Protein (tGFP) from Pontellina Plumata for 24 hours. The transduced cells were analysed in terms of tGFP expression, proliferation and mRNA pluripotency expression, and cells from donor 8 seeded at 500 cells/cm<sup>2</sup> and transduced at 60% confluence were used for subsequent experiments. This technique was performed during a stay in the Laboratory of Translational Cardiomyology of the Stem Cell Biology and Embryology Unit, Department of Development and Regeneration of the KU Leuven.

## **Images of optical microscopy**

Images of optical microscopy were taken from the OX.3040 Euromex binocular microscope for phase contrast using the camera DC.10000c CMEX-10 digital 10 Mpix USB-2 CMOS.

## **Short-Comparative Genomic Hybridization**

The short-Comparative Genomic Hybridization (sCGH) technique was performed as described in *Rius M. et al.* (101) catching single cells from a homogeneous DPPSC or DPMS culture. All samples were analysed in triplicate. The DNA control used for the hybridization was XXY. This technique was performed by an external service in the Unitat de Biologia Cel·lular i Genètica Mèdica Eugin-UAB.

## MATERIALS AND METHODS

## RT-PCR analyses

Samples of total RNA were extracted from undifferentiated or differentiated cells using Trizol (Invitrogen). RNA was isolated following manufacturer's instructions. Two (2)  $\mu$ g of total RNA with a ratio 260/280 between 1.8 and 2 were treated with DNase I (Invitrogen) and reverse-transcribed using Transcriptor First Strand cDNA Synthesis Kit (Roche). PCR was performed using the primers on *Table M1* for the amplification of the desired cDNA using TopTaq MasterMix kit (Qiagen) for regular PCR or FastStart Universal SYBR Green Master (Roche) for Real-Time PCR using a CFX96 Real-Time PCR Detection System (Bio-Rad).

Gene	Forward	Reverse	Size (bp)
OCT4A	CTTCGCAAGCCCTCATTTCACC	CCAGGTCCGAGGATCAACC	158
NANOG	AACAGGTGAAGACCTGGTTCC	CTGAGGCCTTCTGCGTCACA	102
GAPDH	CTGGTAAAGTGGATATTGTTGCCAT	TGGAATCATATTGGAACATGTAAACC	81
CD73	GCAACATGGGCCAACCTGATT	TGGATTCCATTGTTGCGTTCA	145
SOX2	TGG CGA ACC ATC TCT GTG GT	CCA ACG GTG TCA ACC TGC AT	111
LIN28	GGA GGC CAA GAA AGG GAA TAT GA	AAC AAT CTT GTG GCC ACT TTG ACA	60
VEGFR2	TGG CAT CGC GAA AGT GTA TC	AAA GGG AGG CGA GCA TCT C	151
CD31	ACT GCA CAG CCT TCA ACA GA	TTT CTT CCA TGG GGC AAG	92
vWF	GTC GAG CTG CAC AGT GAC AT	CCA CGT AAG GAA CAG AGA CCA	64

**Table M1:** List of primers used for cDNA amplification in PCR.

## Immunofluorescence analyses

For *in vitro* analyses, wells containing cells were fixed with 4% paraformaldehyde for 15 minutes at room temperature and then, after 3 PBS washes, permeabilized with 1%BSA + 0.2% or 0.5% triton for 30-45 minutes at room temperature to increase permeability. Cells were then incubated for 30 minutes with 10% donkey serum at room temperature and after that overnight at 4°C with the primary antibody (Table M2).

The day after, after 3 PBS washes, they were incubated for 1-2 hours at room temperature with the secondary antibody and washed again 3 times. DAPI 1:3000 was used, the cells were washed 3 times again and the immunofluorescence was closed using FluorSave (Millipore). The cells were examined by fluorescence microscopy using Nikon Eclipse Ti. Images were merge using ImageJ.

For *in vivo* analyses from cryosections, slides were fixed with 4% paraformaldehyde for 15 minutes or Ethanol-Acetone 1:1 for 4 minutes at room temperature and permeabilized with 1%BSA + 0.5% triton for 30 minutes at room temperature. Cells were incubated sequentially 60 minutes with 10% donkey serum, 2h at room temperature or 4°C overnight with the primary antibody (Table M2) and 1-2 hours at room temperature with the secondary antibody. DAPI 1:3000 was used and the immunofluorescence was closed using FluorSave (Millipore). Washes were performed as in the *in vitro* analyses. These techniques were performed during a stay in the Laboratory of Translational Cardiomyology of the Stem Cell Biology and Embryology Unit, Department of Development and Regeneration of the KU Leuven.

For *in vivo* analyses from paraffin-embedded sections, deparaffinization and rehydration of the sections were needed, followed by an antigen recovery step (putting the slides in citrate buffer pH=6 for 20 min in the microwave or in trypsin 1:80 in 0.01% CaCl at 37°C for 7 minutes). Samples were washed with Tris-buffered saline (TBS), incubated 20 minutes with MeOH-H<sub>2</sub>O<sub>2</sub> and washed again. They were then permeabilized using 0.5% triton, washed with TBS, blocked in 20% donkey serum or Tris-NaCl-blocking buffer and incubated with the primary antibody (Table M2) overnight. Samples were washed with Tris-NaCl-Tween buffer, incubated with the secondary antibody and washed again. mCD31 (mouse cluster of differentiation 31) was amplified using TSA Fluorescein System (Perkin Elmer). Samples were mounted using Prolong Gold with DAPI (Life Technologies). This technique was performed during a stay in the Laboratory of Translational Cardiomyology of the Stem Cell Biology and Embryology Unit, Department of Development and Regeneration of the KU Leuven in collaboration with the Centre for Molecular and Vascular Biology of the KU Leuven.

## MATERIALS AND METHODS

Antibody against	Company	Cat. Number	Dilution
OCT4	Abcam	ab27985	1:200
NANOG	Abcam	ab80892	1:100
SOX2	Santa Cruz Biotechnology	sc-17320	1:50
VE-CAD	Santa Cruz Biotechnology	Sc-9989	1:50
vWF	Abcam	ab6994	1:400
CD31 (in vitro)	Millipore	04-1074	1:100
Calponin	Abcam	ab46794	1:200
$\alpha$ SMA (in vitro and paraffin-embedded sections)	Sigma	C6198	1:200
Lamin A/C (in vitro)	Epitomics	2966-1	1:600
MyHC	Hybridoma Bank	-	1:5
tGFP	Evrogen	AB513	1:500
mCD31 (in vivo)	BD Biosciences	BD557355	1:500
Lamin A/C (in vivo)	Novocastra	NCL-LAM-A/C	1:100
Laminin	Sigma	L9393	1:300
Dystrophin 1	Novocastra	NCL-DYS1	1:100
Dystrophin 2	Novocastra	NCL-DYS2	1:300
Dystrophin 3	Novocastra	NCL-DYS3	1:100
SGCB	Novocastra	NCL-b-SARC	1:75
$\alpha$ SMA (cryosections)	Sigma	A2547	1:300

**Table M2:** List of antibodies used for protein detection in immunofluorescence analyses.

## Alkaline Phosphatase staining

SIGMAFAST™ BCIP®/NBT (Sigma) for the detection of alkaline phosphatase (AP) activity was used following manufacturer's instructions. Briefly, one tablet was dissolved in 10ml of water, and 1 ml was added in a 24-well containing undifferentiated DPPSC. The solution was kept for 2 hours at 37°C. Fibroblasts were used as a

negative control. This technique was performed during a stay in the Laboratory of Translational Cardiomyology of the Stem Cell Biology and Embryology Unit, Department of Development and Regeneration of the KU Leuven.

## **Endothelial differentiation *in vitro***

For the DPPSC and DPMSC endothelial differentiation potential experiment, cells from donor 5 at passage 6 were seeded in 24-well plates at  $4 \times 10^4$  cells/cm<sup>2</sup> using EGM-2 medium for 25 days. The medium was changed every 2-3 days. Matrigel assay was performed at day 7, 14 and 25 of differentiation and RNA extraction at day 25.

For the DPPSC endothelial differentiation optimization, DPPSC were seeded in 24-well plates at 3 different densities: (1)  $4 \times 10^4$  cells/cm<sup>2</sup>, (2)  $2 \times 10^4$  cells/cm<sup>2</sup> or (3)  $5 \times 10^3$  cells/cm<sup>2</sup>. They were cultured using 3 different media or differentiation protocols: (1) EGM-2 (Lonza), (2) EGM-2 conditioned for 24h with HUVEC (and then filtrated with 0.22 µm diameter pores to eliminate any HUVEC) or (3) using a transwell system in which DPPSC and HUVEC were co-cultured without direct cell contact, using ThinCert™ Cell Culture Inserts (Greiner Bio-One). The medium was changed every 2-3 for 28 days. RNA extraction and matrigel assay was performed at day 7, 14, 21 and 28 of differentiation. Immunofluorescence analysis was performed at day 28.

## **Matrigel assay**

DPPSC or DPMSC were detached using PBS containing 0.25% trypsin-EDTA (Life Technologies) and 50.000 cells were replated in EGM-2 medium in a 24-well coated with Matrigel™ Basement Membrane Matrix Growth Factor Reduced (BD Biosciences). Matrigel coating was performed following manufacturer's instructions for the Thin Gel Method assay, adding 250 µl of matrigel in a 24-well and keeping it 30 minutes at 37°C. After 24 hours, tube-like structures were analysed.

## **Smooth muscle differentiation *in vitro***

DPPSC from 2 different donors (donor 5 and donor 8) and 2 passages (passage 5 and passage 10) were differentiated to smooth muscle using differentiation media



## MATERIALS AND METHODS

consisting of High Glucose DMEM (Life Technologies) supplemented with 2% Horse serum (Life Technologies), 1% Sodium Pyruvate (Life technologies), 1% Glutamine (Sigma), 1% Pen-Strep (Life technologies) and 50ng/ml transforming growth factor  $\beta$ 1 (TGF- $\beta$ 1, Peprotech). Cells were plated in 24-well plates at 500 cells/cm<sup>2</sup> and differentiation was started when they reach 60% confluence. If cells proliferated too much during differentiation, they were split 1:3. Medium was changed every 2-3 days for 10 days. This technique was performed during a stay in the Laboratory of Translational Cardiomyology of the Stem Cell Biology and Embryology Unit, Department of Development and Regeneration of the KU Leuven.

### **Skeletal muscle differentiation *in vitro***

DPPSC from 3 different donors (donor 5, 6 and 8) and 2 passages (passage 5 and passage 10) were differentiated to skeletal muscle using differentiation media consisting of High Glucose DMEM (Life Technologies) supplemented with 2% Horse serum (Life Technologies), 1% Glutamine (Sigma), 1% Sodium Pyruvate (Life technologies) and 1% Pen-Strep (Life technologies). Cells were differentiated alone, using conditioned media from C2C12 cells for 24 hours (followed by subsequent filtering) and in direct co-culture with C2C12 cells at 1:1 and 1:3 ratio (1 DPPSC cell every 3 C2C12 cells). The cells were plated in 24-well plates at a density of 1x10<sup>4</sup> cells/cm<sup>2</sup> and induction was started when cells reached 70% confluence. Medium was changed every 2-3 days for 5-7 days. This technique was performed during a stay in the Laboratory of Translational Cardiomyology of the Stem Cell Biology and Embryology Unit, Department of Development and Regeneration of the KU Leuven.

### **Wound healing assay *in vivo***

8-week-old male athymic nude mice (Foxn1, Charles River) were treated with DPPSC or sham operated as controls (n=5 for each group). The mice were injected with anti-NK to eliminate natural killer cell activity 24 hours before starting the surgery. Full thickness wounds (0.5-cm diameter) were made on the back of the mice, splinted with a silicone ring and treated with tGFP<sup>+</sup> DPPSC from donor 8 at P10 (1x10<sup>6</sup> cells per mice) or PBS. A dressing with moisture was added to protect the wound area. All

wounded mice were housed individually to avoid fighting and to prevent removal of the occlusive wound dressing. Every other day, digital pictures of the wounds were taken (using a NikonD1 camera and Camera-Control-Pro software) under isoflurane anaesthesia and the dressings were renewed. Presence of DPPSC was monitored at day 5 and 10 using fluorescence microscopy. Wound contraction was evaluated by comparing relative wound area (RWA) over time. RWA was calculated using ImageJ software (NIH, Baltimore, Maryland) by dividing the healing wound area by the fixed reference area inside the silicone ring and expressing it as a %. To account for small inter-animal variations, for each time point, relative wound area of each individual animal was expressed as percentage compared to the relative wound area at day 0. Wound contraction (%) was calculated as the complement of relative wound area (100-RWA). At day 11 after wounding, mice were sacrificed and skin fragments including the wound area and a rim of normal skin were dissected out, fixed, separated in two pieces at the midline and processed for paraffin embedding. For all stainings and analyses, 7µm microtome sections were used. To analyse the tissue, Haematoxylin/Eosin and Sirius Red stainings were performed, as well as immunofluorescence analyses. These experiments were performed during a stay in the Laboratory of Translational Cardiology of the Stem Cell Biology and Embryology Unit, Department of Development and Regeneration of the KU Leuven in collaboration with the Centre for Molecular and Vascular Biology of the KU Leuven. Mouse procedures were performed according to the guidelines of the Institutional Animal Care and Use of KU Leuven, under the approved project with protocol code ECD N°P018/2015 issued by the *Ethische Commissie Dierproeven* of the KU Leuven (see appendix – supplementary data).

## **Haematoxylin and Eosin staining**

Sections in paraffin were heated in the oven at 60°C for 1 hour, deparaffinised and rehydrated. The samples were then soaked in distilled water for 5 minutes, Harris haematoxylin for 4 minutes and washed afterwards in running tap water for 2 minutes. After that, the sections were subsequently soaked for 1 minute each in acid alcohol, running water, bluing reagent, running water, eosin, 95% ethanol, 100% ethanol and

## MATERIALS AND METHODS

histoclear. The slides were then mounted with DPX and left in a slide heater overnight. The staining was then observed and photographed using Nikon Eclipse Ti microscope. These experiments were performed during a stay in the Laboratory of Translational Cardiomyology of the Stem Cell Biology and Embryology Unit, Department of Development and Regeneration of the KU Leuven in collaboration with the Centre for Molecular and Vascular Biology of the KU Leuven.

### **Sirius Red staining**

Sirius Red solution was prepared mixing 0.2g of Direct Red 80 (Sigma) with saturated aqueous solution of picric acid (prepared mixing 8g of picric acid in 200ml of distilled water). Sections in paraffin were deparaffinised and rehydrated, put in tap water for 10 minutes, distilled water for 5 minutes and Sirius Red solution for 90 minutes. After that, the slides were washed with HCL 0.01N for 2 minutes and dehydrated with ethanol 70% for 45 seconds and ethanol 100% for 5 minutes (twice). Lastly, samples were cleared in xylol for 5 minutes (twice) and mounted with DPX. These experiments were performed during a stay in the Laboratory of Translational Cardiomyology of the Stem Cell Biology and Embryology Unit, Department of Development and Regeneration of the KU Leuven in collaboration with the Centre for Molecular and Vascular Biology of the KU Leuven.

### **DPPSC injection in two models of dystrophic mice**

Ten (10) 3-months-old *Scid/mdx* mice (an immunodeficient mouse model for Duchenne Muscular Dystrophy, available at KUL SPF animal care facility, Belgium), 5 males and 5 females, and 4 3-months-old *Sgcb-null Rag2-null  $\gamma$ c-null* mice (an immunodeficient mouse model for Limb-Girdle Muscular Dystrophy type 2E, available at KU Leuven SPF animal care facility, Belgium), 3 males and 1 female, were injected in the left Tibialis Anterior with  $2.5 \times 10^5$  cells per mice. DPPSC from 3 different donors (donor 5, 6 and 8) at P5-P10 were used. Right limbs were used as controls. After 20-30 days, mice were sacrificed and muscles were frozen and kept at  $-80^\circ\text{C}$ . The samples were then cut in  $7\mu\text{m}$  sections using a cryostat machine (Leica). Immunofluorescence analyses were performed to study the tissue. These experiments were performed during a stay

in the Laboratory of Translational Cardiomyology of the Stem Cell Biology and Embryology Unit, Department of Development and Regeneration of the KU Leuven. Mouse procedures were performed according to the guidelines of the Institutional Animal Care and Use of KU Leuven, under the approved project with protocol code ECD N°P095/2012 issued by the *Ethische Commissie Dierproeven* of the KU Leuven (see appendix – supplementary data).

## Statistical analyses

Data from the different experiments were analysed using the statistical program Statgraphics Centurion XVI. Two-tailed Student's test or one-way ANOVA were used to compare interrelated samples, while two-way ANOVA was used to analyse multiple factors. Confidence intervals were fixed at 95% ( $p < 0.05$ ), 99% ( $p < 0.01$ ) and 99.9% ( $p < 0.001$ ). GraphPad Prism was used to graph the results as the average  $\pm$  standard error of the mean (see figure legends for specific information regarding the number of independent experiments or biological replicates).



# RESULTS

---



## DPPSC CHARACTERIZATION

### DPPSC morphology, growth rate, genetic stability and gene and protein expression

DPPSC and DPMSC from different donors were isolated and cultivated as described. DPPSC were cultivated at very low density (100 cells/cm<sup>2</sup>) using DPPSC growth medium and expanded when the culture reached a confluence of 30% (3-4 days). As described before, DPPSC presented a small size with large nuclei and low cytoplasm content, resembling MAPC, and without the typical flat and elongated MSC appearance (Fig. 1A). This morphology was maintained for more than 15 passages (Fig. 1A1-A5). DPMSC presented a larger cell size compared to DPPSC with the typical spindle-shaped morphology of MSC (Fig. 1B), a feature that increased through passages (Fig. 1B1-B5).

To further characterize the cells, the growth rate of DPPSC and DPMSC was studied in cells from 15 different donors during 15 passages. The population doubling time of DPPSC was found significantly lower than DPMSC (Fig. 2A). The number of divisions per passage was also studied and DPMSC presented a significant higher number of divisions (Fig. 2B), due to the fact that DPMSC are split at much more confluence than DPPSC.

Since the potential application of stem cells in regenerative medicine depends on their ability to undergo a large scale *in vitro* amplification without genetic instability, and it has been reported that in other cell types as MSC this instability appears, it was crucial to analyse DPPSC genetic stability. DPPSC from 10 different donors at passage 15 were analysed by sCGH and all of them showed no chromosomal abnormalities (Fig. 2C and Fig. S1 and S2). DPMSC were also analysed by sCGH at passage 15 and showed chromosomal instability (Fig. 2D).



RESULTS

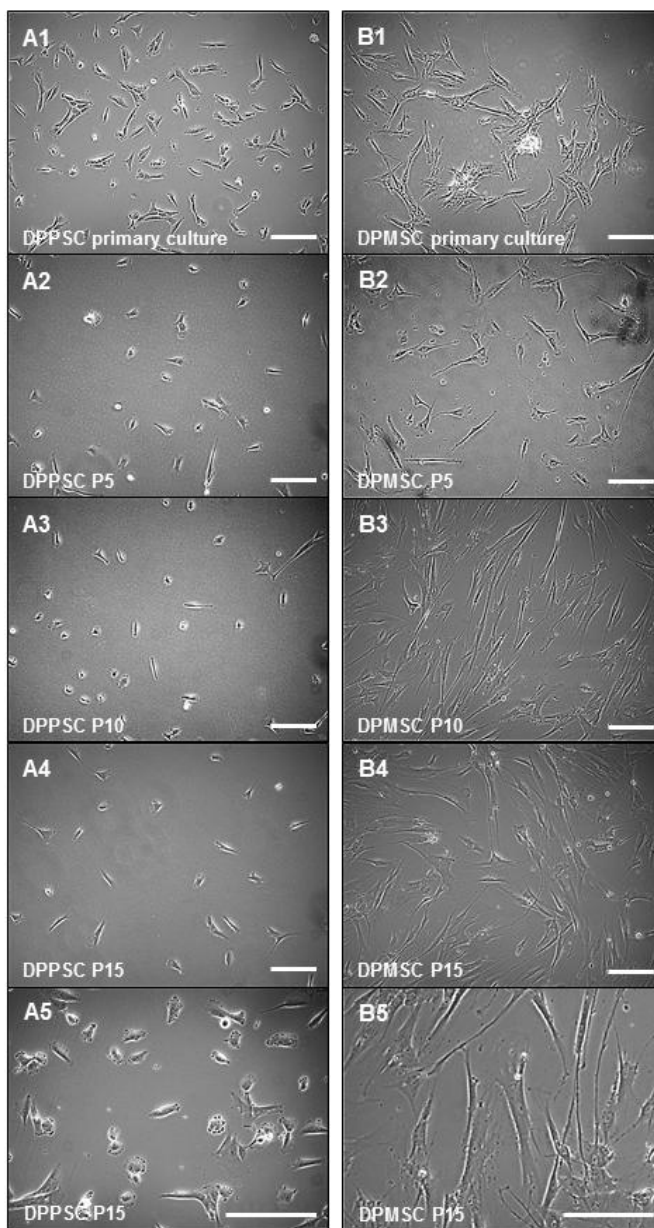


**Figure 1: Cell morphology of DPPSC and DPMSC. A)** Phase contrast image of DPPSC morphology in the primary culture (A1), passage 5 (A2), passage 10 (A3) and passage 15 (A4, A5). **B)** Phase contrast image of DPMSC morphology from the same donor in the primary culture (B1), passage 5 (B2), passage 10 (B3) and passage 15 (B4, B5). Scale bars: 200  $\mu$ m.

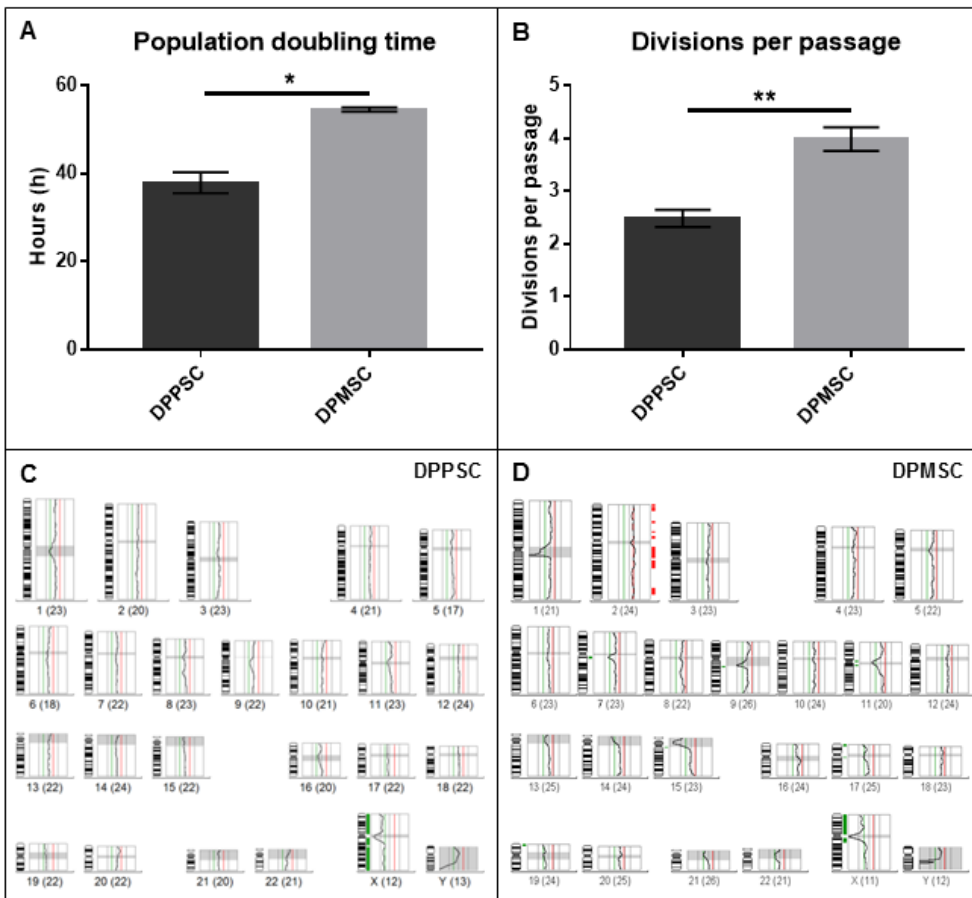


**Figure 2: Population doubling and genetic stability of DPPSC and DPMSC.**  
**A)** Population doubling time in hours of DPPSC and DPMSC for 15 passages, showing faster division in DPPSC. \* $p < 0.05$ ,  $n = 15$  different donors. **B)** Number of divisions per passage of DPPSC and DPMSC for 15 passages, showing DPMSC divide more times per passage. \*\* $p < 0.01$ ,  $n = 15$  different donors. **C)** Example of a short-Comparative Genomic Hybridization in DPPSC from one donor at passage 15 showing no chromosomal abnormalities. sCGH from several other donors can be found in the supplementary data (Fig. S1 and Fig. S2). **D)** Short-Comparative Genomic Hybridization in DPMSC from the same donor and passage showing chromosomal abnormalities (chromosome 2). The DNA control used for the hybridization was XXY, therefore the observed loss of chromosome X indicates these cells are from a male donor.

RESULTS

In order to confirm the phenotype of DPPSC, mRNA expression of the pluripotency markers OCT4A and NANOG was analysed by RT-PCR in cells from 8 different donors at different passages. As described before, the cells showed expression of both markers in all passages (Fig. 3A and Fig. S3).

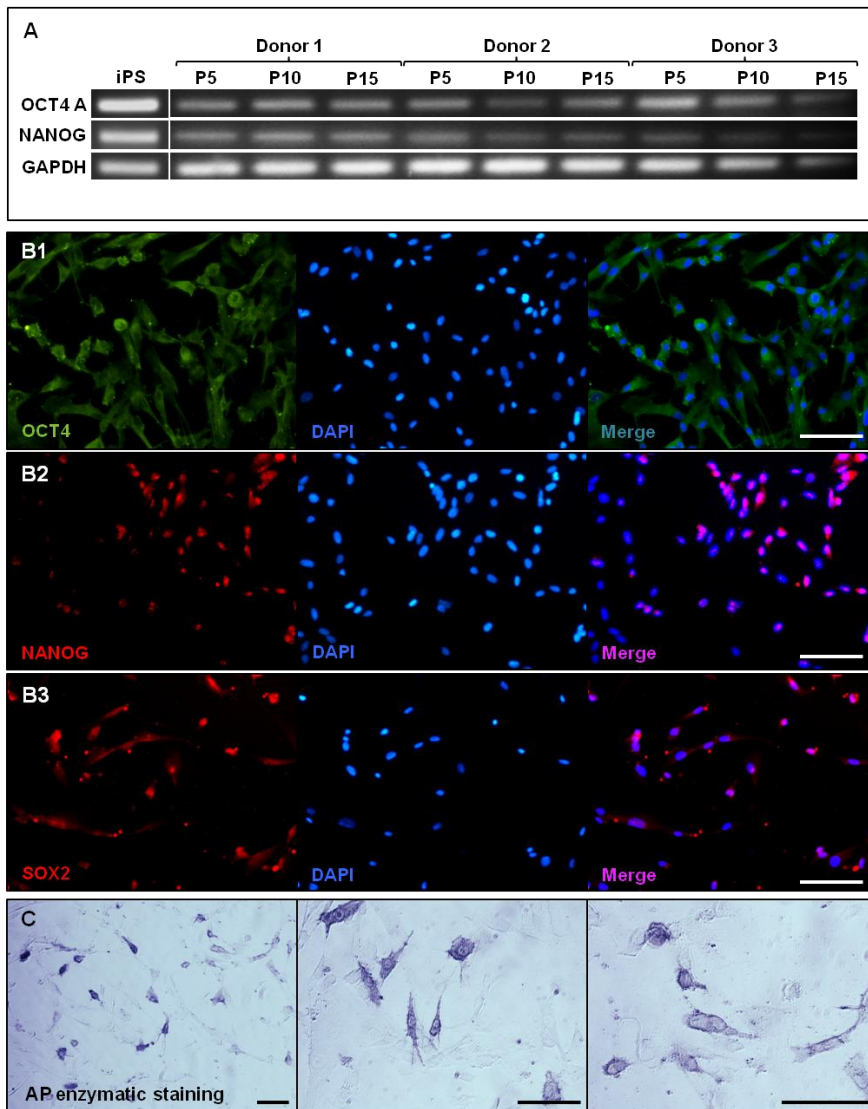


**Figure 3: RT-PCR, immunofluorescence and immunohistochemistry analyses of undifferentiated DPPSC. A)** Analysis of mRNA expression of the pluripotency markers OCT4A and NANOG by RT-PCR in DPPSC from 3 different

*donors at passage 5, 10 and 15. GAPDH was used as a housekeeping control. iPS cells were used as positive control. RT-PCR analysis for 5 other donors at the same passages can be found in the supplementary data (Fig. S3). **B**) Immunofluorescence analysis for the pluripotency markers OCT4 (green), NANOG (red) and SOX2 (red) in undifferentiated DPPSC at passage 10. Nuclei are counterstained with DAPI (blue). Scale bars: 100µm. **C**) Alkaline Phosphatase staining of DPPSC at passage 10. Scale bars: 100µm.*

Aiming to further characterize DPPSC, the presence of the pluripotency proteins OCT4, NANOG and SOX2, was also detected by immunofluorescence analysis (Fig. 3B). Although there is no specific commercial antibody that detects the nuclear pluripotency-related isoform of OCT4 (OCT4A) without cross-reacting with the functional non related cytoplasmic isoform (OCT4B), DPPSC were positive for OCT4 (Fig. 3B1). The nuclei of several cells were also positive for NANOG and SOX2 (Fig. 3B2-B3). In addition, DPPSC were also positive for AP enzymatic staining, a widely used assay to detect this pluripotent stem cell marker (Fig. 3C).

## **DPPSC pluripotency through passages**

As described before, DPPSC were able to maintain their characteristic small size with large nuclei and low cytoplasm for 15 passages (Fig. 1A). However, DPMSC became more elongated and spindle-shaped through cell passages (Fig. 1B). When studying their growth rate at earlier passages (passage 1 to 5), intermediate passages (passage 6 to 10) and later passages (passage 11 to 15), DPPSC showed significantly faster division at P6-10 and P11-15 compared to DPMSC, although a tendency was already observed from the beginning of the culture at P1-5 (Fig.4A). In addition, DPPSC were able to maintain the same population doubling time through all 15 passages, while DPMSC divide slower at later passages (Fig. 4B). Furthermore, DPMSC performed more divisions per passage than DPPSC at earlier passages, although at later passages this difference was reduced and no longer significant (Fig. 4C). DPPSC also maintained the number of divisions per passage stable during all the culture, while DPMSC decreased the number of divisions (Fig. 4D).

RESULTS

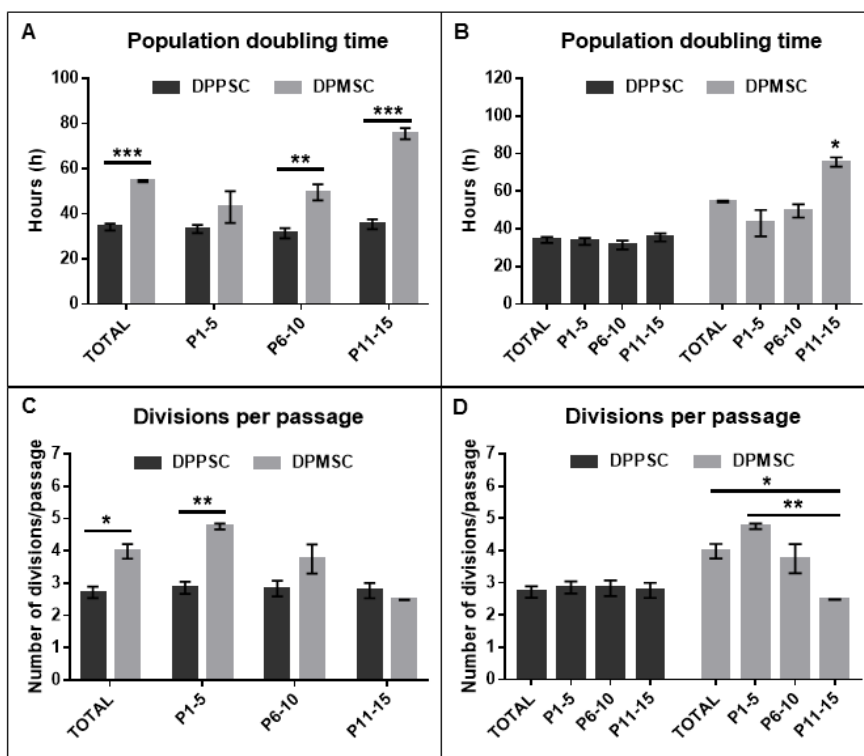


**Figure 4: Population doubling and cell divisions of DPPSC and DPMSC.** A-B) DPPSC and DPMSC population doubling time through different passages, comparing between the two populations (A) or among different passages (B). C-D) Number of DPPSC and DPMSC divisions per passage through different passages, comparing between the two populations (C) or among different passages (D). \* $p < 0.05$ , \*\* $p < 0.01$ , \*\*\* $p < 0.001$ ,  $n = 12$  different donors.

Focusing on the gene expression of DPPSC through passages, pluripotency markers OCT4A and NANOG expression was analysed by qRT-PCR analysis. These genes were found to be significantly higher expressed at passage 10 compared to passage 5 and 15 (Fig. 5A-B). In addition, the expression of OCT4A and NANOG was significantly lower at passage 15 than passage 5 or 10 (Fig. 5A-B).

Next, we hypothesised whether the decreased expression of the pluripotency markers at passage 15 compared to passage 10 was due to the lack of a constricting selection when performing the DPPSC primary culture. Indeed, other populations (such as

DPMSC) could be present in the culture at a small percentage from the beginning and finally be able to highly proliferate or somehow affect the DPPSC population. Therefore, we performed a qRT-PCR analysis for CD73, normally absent in OCT4<sup>+</sup> and SOX2<sup>+</sup> cells (putative DPPSC) and present in OCT4<sup>-</sup> and SOX2<sup>-</sup> cells (putative DPMSC). The results of the qRT-PCR analysis showed that, as we hypothesised, the expression of CD73 was significantly increased at late passages, and inversely proportional to the OCT4A and NANOG gene expression pattern (Fig. 5C).

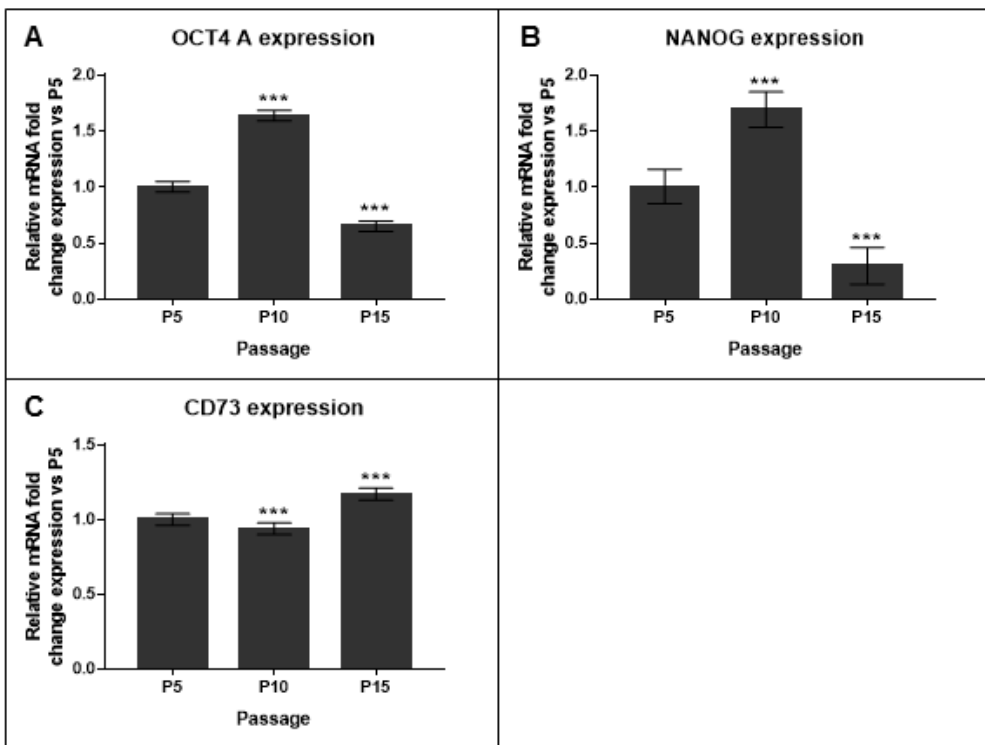


**Figure 5: qRT-PCR analysis of pluripotent and mesenchymal markers in DPPSC at different passages.** **A)** Relative mRNA fold change expression of the pluripotency marker OCT4A at passage 5, 10 and 15 compared to P5 in DPPSC from 8 different donors. **B)** Relative mRNA fold change expression of the pluripotency marker NANOG at passage 5, 10 and 15 compared to P5 in DPPSC from 8 different donors. **C)** Relative mRNA fold change expression of the mesenchymal stem cell marker CD73 at passage 5, 10 and 15 compared to P5 in DPPSC from 8 different donors. \*\*\* $p < 0.001$ ,  $n = 8$  different donors.

## RESULTS

### **DPPSC pluripotency using different seeding and splitting densities**

Since a large number of cells are needed in regenerative medicine approaches, we wanted to assess whether DPPSC can be cultured at higher densities than the established one without losing their properties, thus allowing the obtainment of more cells using the same resources. Therefore, a density study was performed in which cells at passage 6 were seeded and split at higher densities for 4 passages. Specifically, DPPSC populations from 3 different donors were seeded at a density 1.5 to 10 times higher ( $150 \text{ cells/cm}^2$  to  $1000 \text{ cells/cm}^2$ ), and split at a confluence between 1.5-2 times higher (50%).

DPPSC cultured in these conditions presented a more elongated morphology (Fig. 6A3-A6) than the control cells (Fig. 6A1-A2), although their morphology was not as spindle-shaped as the one observed in DPMSC (Fig. 1B3).

Regarding growth rate, the population doubling time of the cells did not vary significantly in any of the conditions (Fig. 6B). The number of divisions per passage increased significantly in the two lower seeding densities (Fig. 6C) due to the fact that they need to reach the same confluence starting from a lower number of cells.

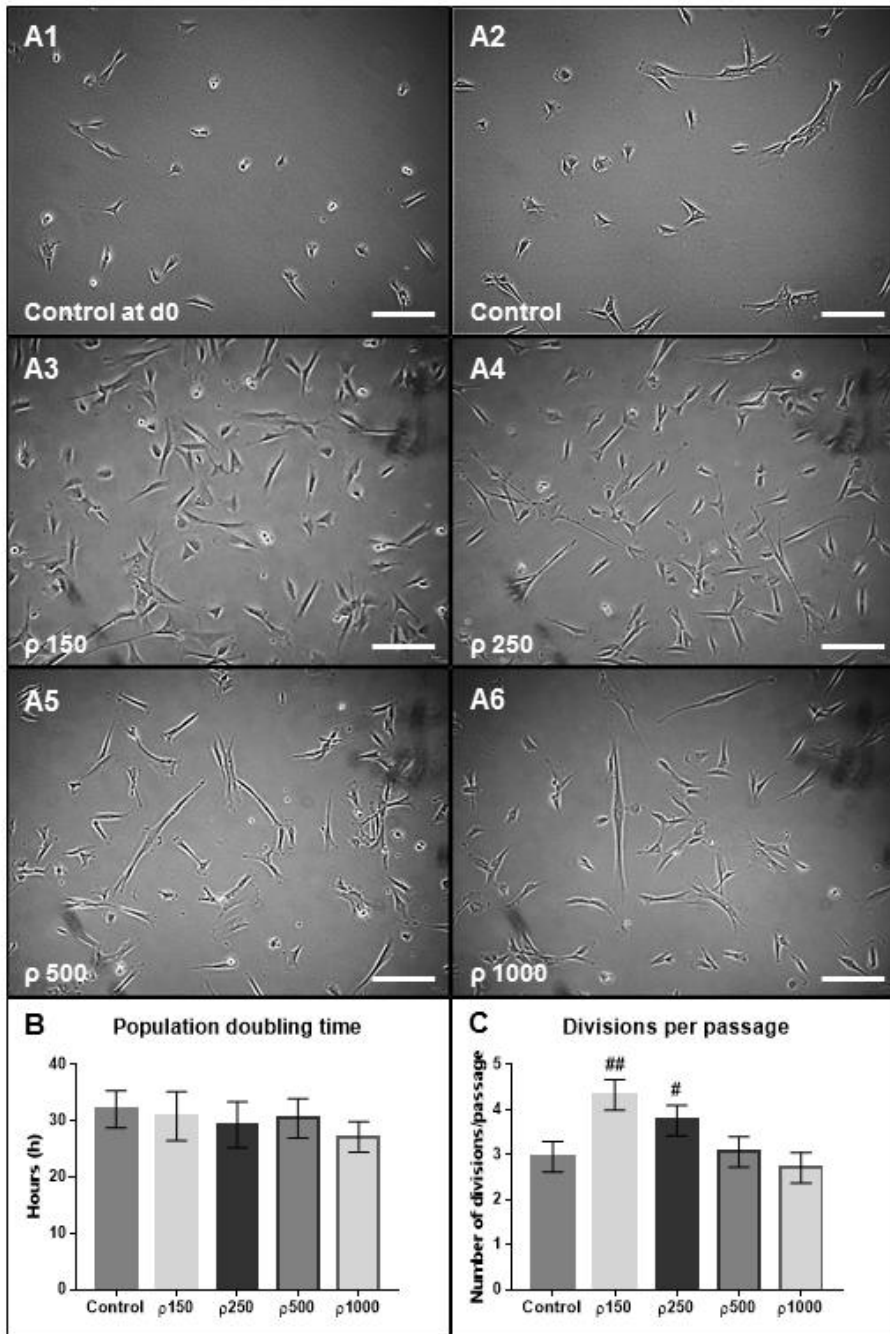


**Figure 6: Cell morphology and growth of DPPSC cultured at different seeding and splitting densities. A) Phase contrast image of DPPSC**



## RESULTS

*morphology at the regular seeding and splitting density (100 cells/cm<sup>2</sup> and 30%) (A1, A2) and at 50% splitting density with a seeding density of 150 cells/cm<sup>2</sup> (A3), 250 cells/cm<sup>2</sup> (A4), 500 cells/cm<sup>2</sup> (A5), and 1000 cells/cm<sup>2</sup> (A6). Scale bars: 200 μm. B) DPPSC population doubling time for the different seeding and splitting conditions, showing no significant differences ( $p > 0.05$ ;  $n = 3$  independent experiments). C) Number of DPPSC divisions per passage for the different seeding and splitting conditions. # $p < 0.05$ , ## $p < 0.01$  ( $p_{150}$  and  $p_{250}$  cells/cm<sup>2</sup> are not statistically significant between them but statistically significant to all the other conditions),  $n = 3$  independent experiments using populations from different donors.*

In order to analyse the gene expression of the cells in the different conditions, we performed qRT-PCR analyses for the pluripotency markers OCT4A, NANOG, SOX2 and LIN28. We noticed that, as similarly observed before (Fig. 5A-B), the control cells at the end of the experiment (passage 10) expressed higher OCT4A and NANOG expression than at day 0 (passage 6) (Fig. 7A-B). Moreover, SOX2 expression at passage 10 was also increased compared to passage 6 (Fig. 7C). In the case of the seeding density 500 cells/cm<sup>2</sup> and splitting density of 50%, the cells maintained the same levels of expression of OCT4A, NANOG and LIN28 as the control cells cultured with the conventional conditions (Fig. 7A, B, D), although SOX2 gene expression significantly decreased (Fig. 7C). The level of SOX2 was only maintained in the cells seeded at 150 cells/cm<sup>2</sup>, but this condition also showed a significantly diminished expression of OCT4A and NANOG expression.

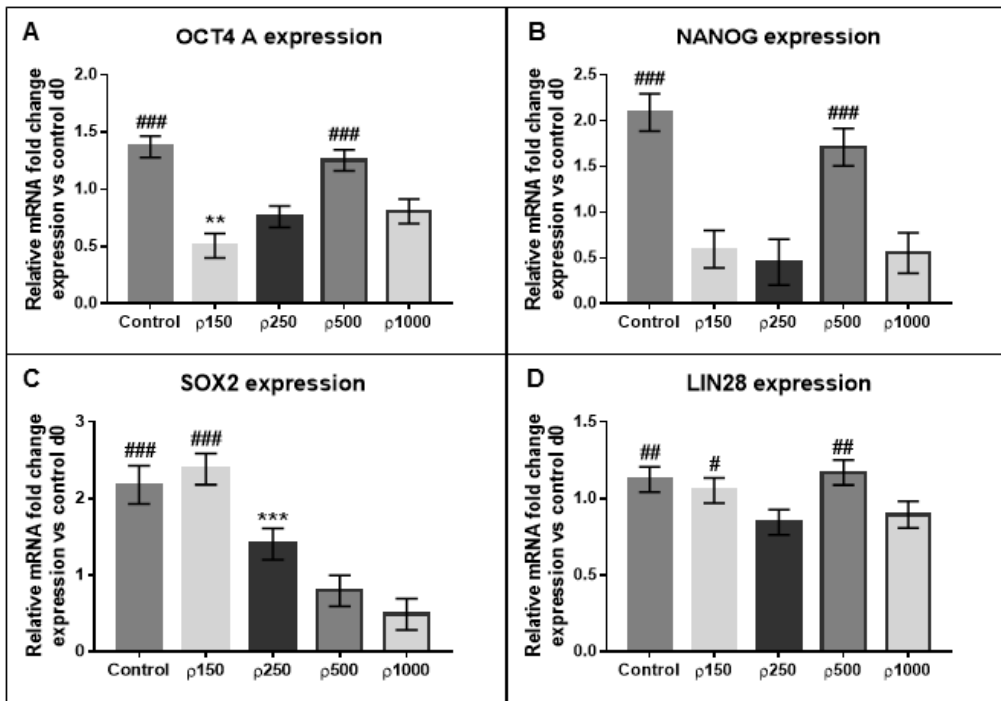


**Figure 7: Pluripotency of DPPSC cultured at different seeding and splitting densities.** **A)** qRT-PCR analysis of OCT4A expression of DPPSC at different seeding and splitting densities. \*\* $p < 0.01$  ( $\rho 150$  expression is different from all the others), ### $p < 0.001$  (expression of the control and  $\rho 500$  is not statistically significant between them but statistically significant to all the other conditions). **B)** qRT-PCR of NANOG expression of DPPSC at different seeding and splitting densities. ### $p < 0.001$  (expression of the control and  $\rho 500$  is not statistically significant between them but statistically significant to all the other conditions). **C)** qRT-PCR analysis of SOX2 expression of DPPSC at different seeding and splitting densities. \*\*\* $p < 0.001$  ( $\rho 250$  is different from all the other conditions), ### $p < 0.001$  (expression of the control and  $\rho 150$  is not statistically significant between them but statistically significant to all the other conditions). **D)** qRT-PCR analysis of LIN28 expression of DPPSC at different seeding and splitting densities. # $p < 0.05$ , ## $p < 0.01$  (expression of the control,  $\rho 150$  and  $\rho 500$  are not statistically significant among them but statistically significant to all the other conditions). For **A-D**,  $n=3$  independent experiments using populations from different donors.

## RESULTS

### **DPPSC pluripotency using different growth media**

By introducing variations in the growth medium, we aimed to establish a new culture medium with good manufacturing practices (GMP) conditions in order to facilitate the future application of the cells in clinical practice. After several modifications in the medium and foetal bovine serum replacement with serum from human origin, we established a new growth medium for DPPSC qualified for GMP conditions (GMP-approved).

We used this GMP-approved growth medium supplemented with 10% of human serum (HS) in the primary culture and to later expand DPPSC from different donors. The cells presented a morphology very similar to the ones cultured with the conventional growth medium, even at later passages (Fig. 8).

Studying the growth rate of the DPPSC cultured using the two growth media for 10 passages, we observed that the population doubling time and the number of divisions per passage were not affected by the change of the growth medium (Fig. 9A-B).

Genetic stability of the cells cultured with GMP medium was also tested, and no chromosomal abnormalities were observed (Fig. 9D and 9F).

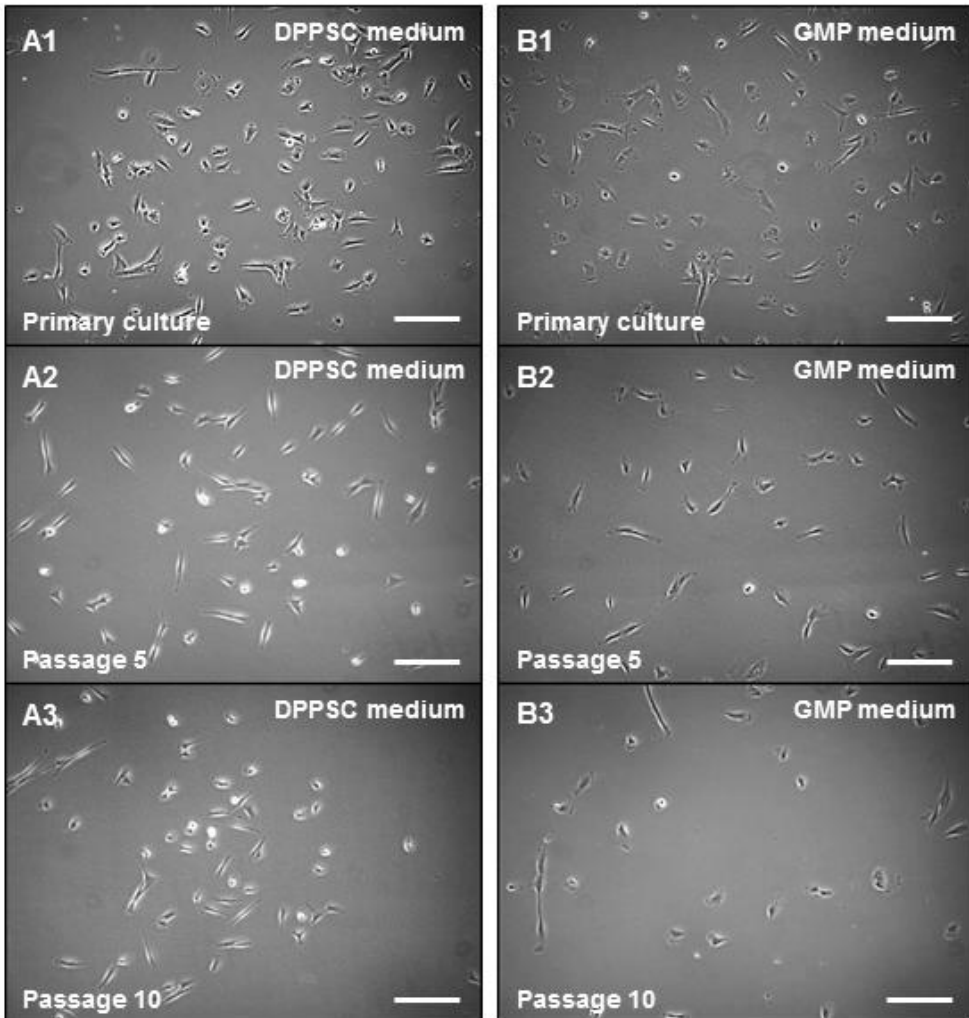


**Figure 8: Cell morphology of DPPSC cultured in different growth media (DPPSC growth medium and GMP growth medium).** **A)** Phase contrast image of DPPSC morphology cultured with DPPSC growth medium in the primary culture (**A1**), at passage 5 (**A2**) and at passage 10 (**A3**). **B)** Phase contrast image of DPPSC morphology from the same donor cultured in GMP growth medium in the primary culture (**B1**), at passage 5 (**B2**) and at passage 10 (**B3**). Scale bars: 200  $\mu\text{m}$ .

RESULTS

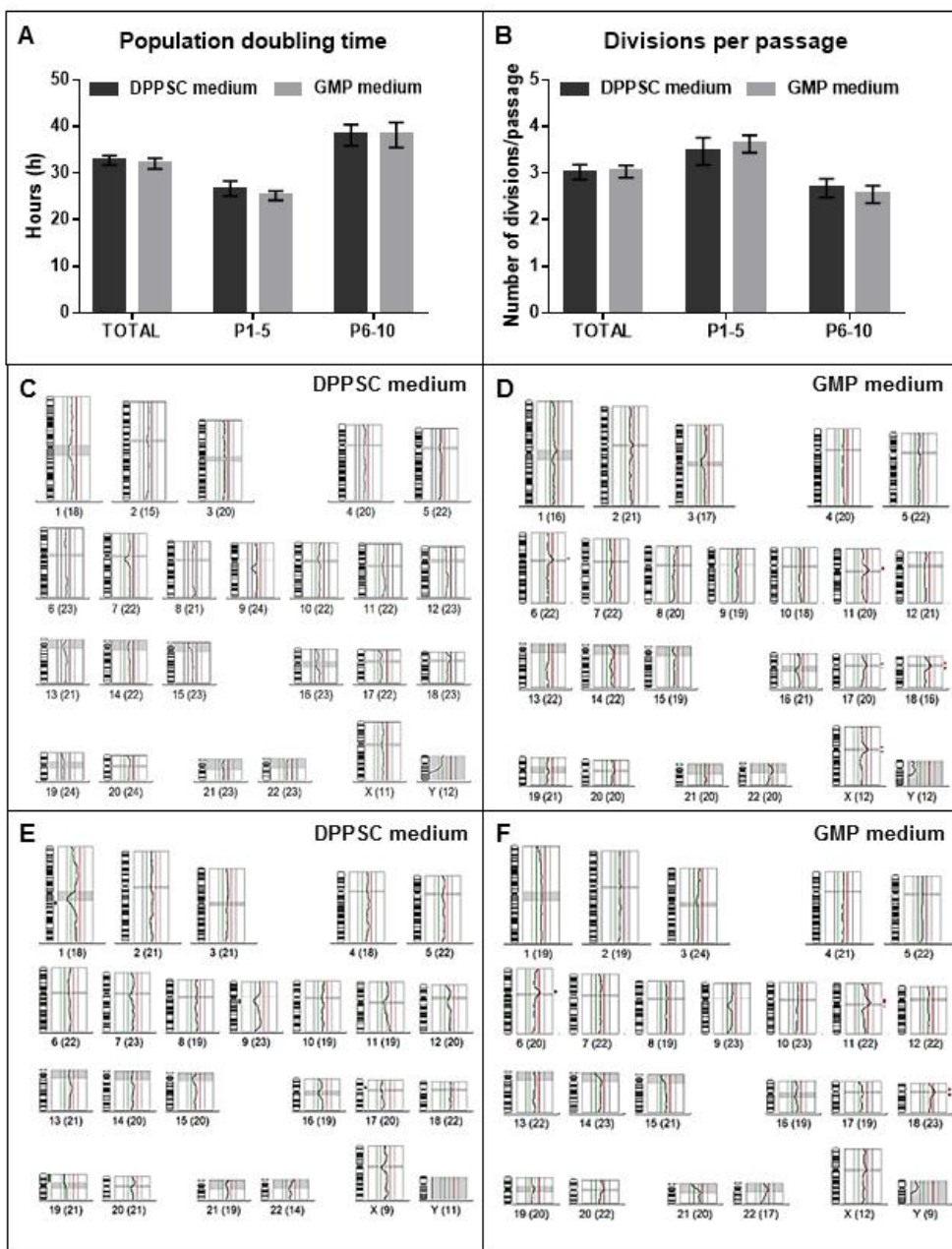


**Figure 9: Growth and genetic stability of DPPSC cultured in different growth media (DPPSC growth medium and GMP growth medium). A) Comparison studies of the population doubling time of DPPSC at different passages cultured in**

*different media show no significant differences ( $p>0.05$ ;  $n=5$ ). **B)** Comparison studies of the number of divisions per passage of DPPSC at different passages cultured in different media show no significant differences ( $p>0.05$ ;  $n=5$ ). **C-F)** Examples of short-Comparative Genomic Hybridization in DPPSC from two different donors (**C, D and E, F**) cultured in DPPSC growth medium (**C, E**) and GMP growth medium (**D, F**) showing no chromosomal abnormalities in both conditions. The DNA control used for the hybridization was XXY, therefore the observed loss of chromosome Y indicates these cells are from female donors. Differences detected in the centromeric or peri-centromeric regions (chromosome 6, 11 and 18 in **F**) are typical artefacts.*

The gene expression of the cells cultured with the two different growth media for 5 and 10 passages was assessed by qRT-PCR analyses. We observed that cells cultured with GMP medium showed higher levels of OCT4A and NANOG both at passage 5 and 10, compared to the cells cultured in DPPSC medium (Fig. 10A-B). However, SOX2 expression was dramatically reduced in GMP medium cultured cells (Fig. 10C). The levels of the pluripotency marker LIN28 did not vary significantly when using the different media (Fig. 10D).

RESULTS

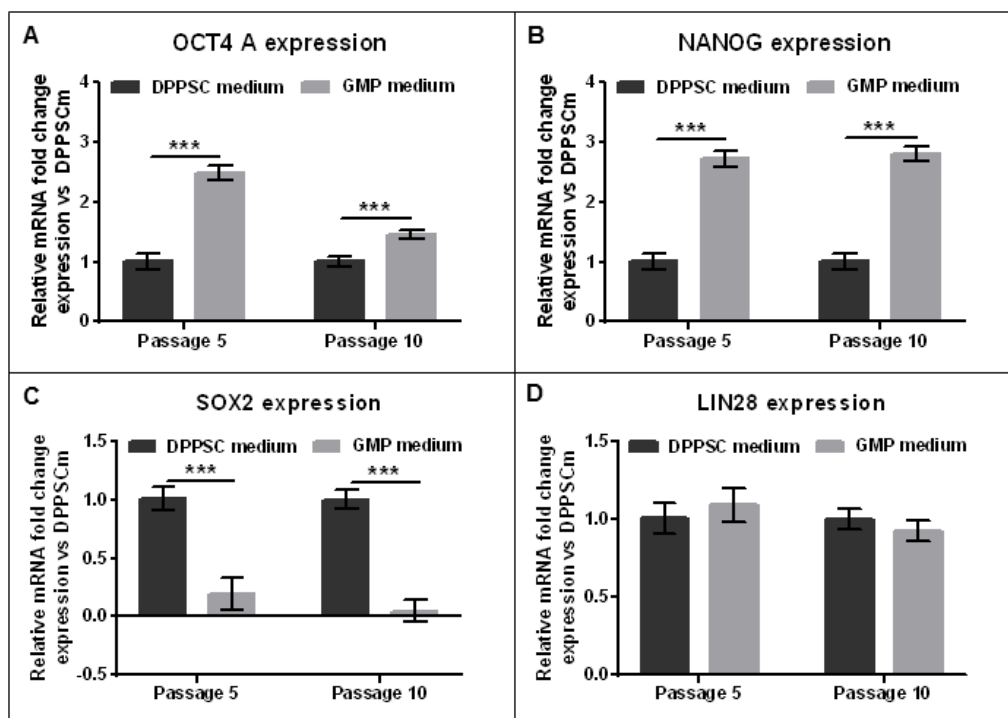


**Figure 10: Pluripotency of DPPSC cultured in different growth media (DPPSC growth medium and GMP growth medium).** **A)** qRT-PCR analysis of OCT4A expression in DPPSC cultured with the two different media for 5 and 10 passages. **B)** qRT-PCR analysis of NANOG expression of DPPSC cultured with the two different media for 5 and 10 passages. **C)** qRT-PCR analysis of SOX2 expression in DPPSC cultured with the two different media for 5 and 10 passages. For **A-C**, \*\*\* $p < 0.001$ ,  $n = 5$  independent experiments using populations from different donors. **D)** qRT-PCR analysis of LIN28 expression in DPPSC cultured with the two different media for 5 and 10 passages, showing no significant differences ( $p > 0.05$ ;  $n = 5$  independent experiments using populations from different donors).

After observing these interesting results in terms of morphology, division rate and pluripotency gene expression (at least regarding OCT4A, NANOG and LIN28), we hypothesized whether reducing the percentage of serum in the GMP medium, and thus diminishing the quantity of undefined components in the medium, could maintain (or even improve) the properties of DPPSC observed in the GMP medium. We decided to reduce the serum amount in the medium to a final dilution of 2%, 1% and 0.5%.

The morphology of the cells cultured in the GMP growth media for 5 passages was very similar to the control cells cultured in the DPPSC growth medium (Fig. 11A1-A4), except for the cells cultured with the lower serum concentration (0.5% HS), which displayed more elongated shape (Fig. 11A5). After 10 passages, the same pattern was observed, although cells cultured in the GMP medium supplemented with 2% HS and 1% HS were slightly more elongated than the control cells (Fig. 11B1-B4). Cells cultured for 10 passages in GMP medium supplemented with 0.5% HS displayed and even more elongated shape (Fig. 11B5).

We also observed that cells cultured in the GMP medium supplemented with 0.5% HS divided slower at passages 6-10 than the control cells (Fig. 12A). In addition, cells cultured with GMP supplemented with 0.5% HS and 1% HS at passages 6-10 divided less per passage than the control cells (Fig. 12B).



RESULTS

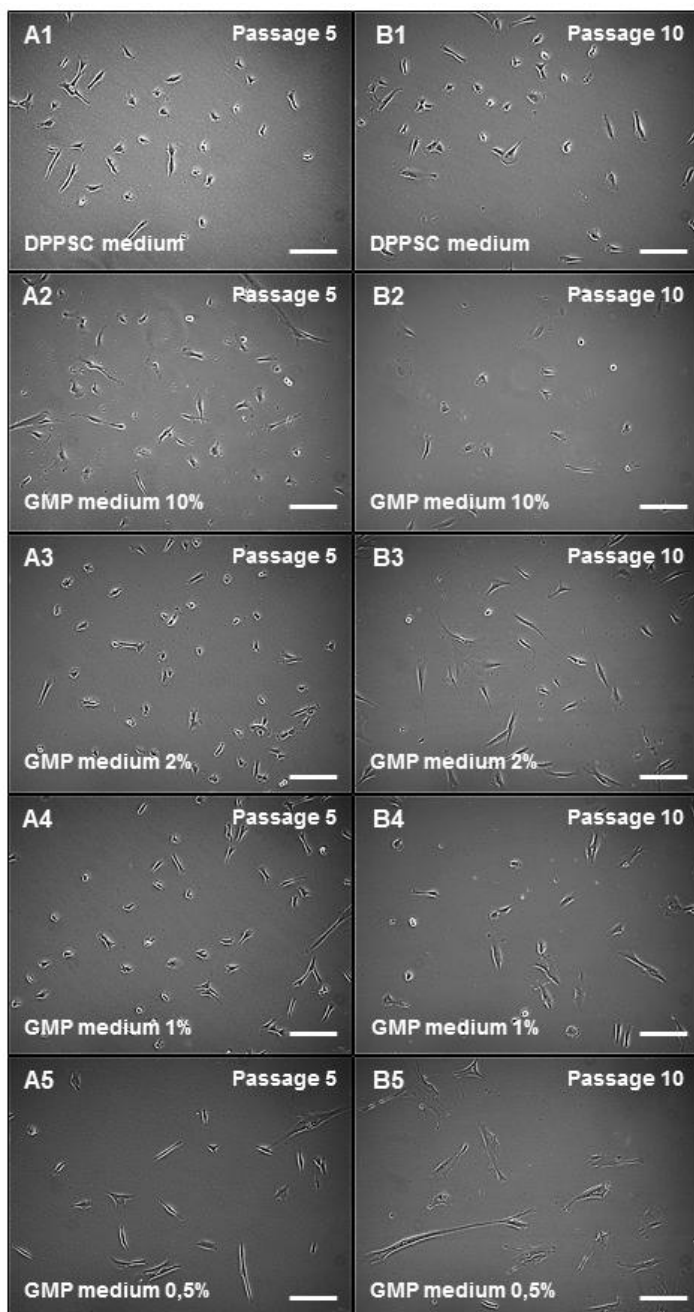


**Figure 11: Cell morphology of DPPSC cultured in different growth media (DPPSC growth medium and GMP growth medium supplemented with different human serum concentration). A) Phase contrast image of DPPSC**

morphology at passage 5 using DPPSC growth medium (A1), GMP medium supplemented with 10% serum (A2), with 2% serum (A3), with 1% serum (A4) and with 0.5% serum (A5). B) Phase contrast image of DPPSC morphology at passage 10 using DPPSC growth medium (B1), GMP medium supplemented with 10% serum (B2), with 2% serum (B3), with 1% serum (B4) and with 0.5% serum (B5). Scale bars: 200  $\mu$ m.

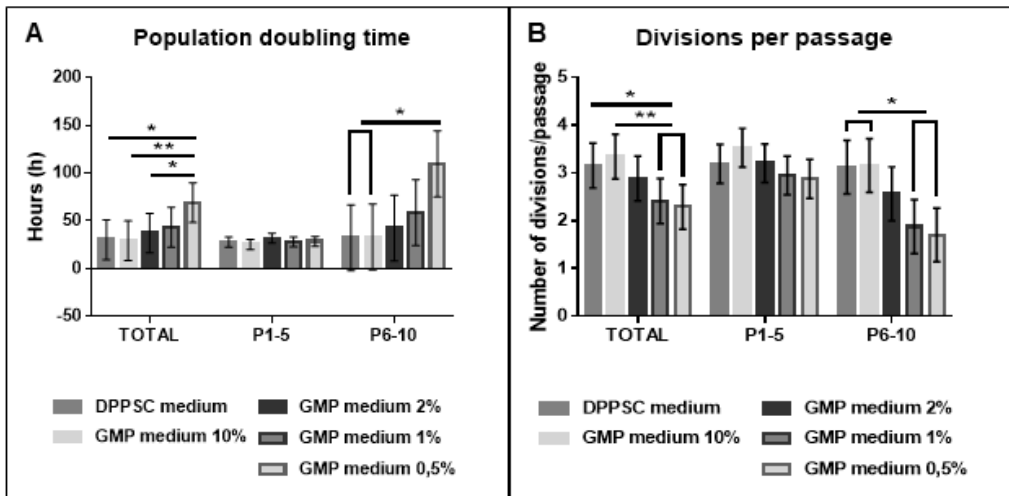


**Figure 12: Population doubling and cell divisions of DPPSC cultured in different growth media (DPPSC growth medium and GMP growth medium supplemented with different human serum concentration). A) Comparison studies of the population doubling time of DPPSC at different passages cultured in different media. B) Comparison studies of the number of divisions per passage of DPPSC at different passages cultured in different media. \* $p < 0.05$ , \*\* $p < 0.01$ ,  $n = 5$ .**

When analysing the pluripotency gene expression of the cells, we observed that at passage 5 the OCT4A and NANOG levels of the GMP supplemented with 10% HS were again significantly increased comparing to control cells cultured with the regular DPPSC medium (Fig. 13A-B). Cells cultured with GMP supplemented with 1% HS presented similar OCT4A and NANOG gene expression levels as GMP supplemented with 10% HS cells. DPPSC cultured in GMP supplemented with 2% HS expressed OCT4 and NANOG similarly to the control cells, while in cells cultured in GMP

## RESULTS

supplemented with 0.5% HS the gene expression levels significantly decreased. Regarding SOX2 expression at passage 5, while cells in GMP supplemented with 10% HS again dramatically decreased its expression (and so did the cells cultured in GMP supplemented with 2% and 0.5% HS), cells cultured in GMP supplemented with 1% HS maintained the same levels of SOX2 as the control cells (Fig. 13C). LIN28 expression at P5 was significantly increased in GMP supplemented with 1% HS cultured cells (Fig. 13D), while in cells in GMP supplemented with 2% and 0.5% HS LIN28 expression was comparable to the controls.

Focusing on cells maintained in these GMP conditions for 10 passages, GMP supplemented with 10% HS cells again expressed significantly higher levels of OCT4A and NANOG comparing to the control (Fig. 113A-B). GMP supplemented with 1% HS cultured cells also displayed significantly higher levels of NANOG compared to the control (although not as high as GMP supplemented with 10% HS). However, the expression level of OCT4A in GMP supplemented with 1% HS at P10 was decreased compared to the control cells, although not as much as the one from GMP supplemented with 2% or 0.5% HS cultured cells. NANOG expression in GMP supplemented with 2% and 0.5% HS did not vary significantly compared to the control cells. In the case of SOX2 expression at P10, all conditions except GMP supplemented with 1% HS decreased even more their expression (Fig. 13C). GMP supplemented with 1% HS not only did not diminish the expression of SOX2, but it increased it 4 times compared to the control cells in the regular DPPSC medium. Regarding LIN28, GMP supplemented with 10% and 1% HS cultured cells maintained the same expression levels, while GMP supplemented with 2% and 0.5% HS showed lower expression.

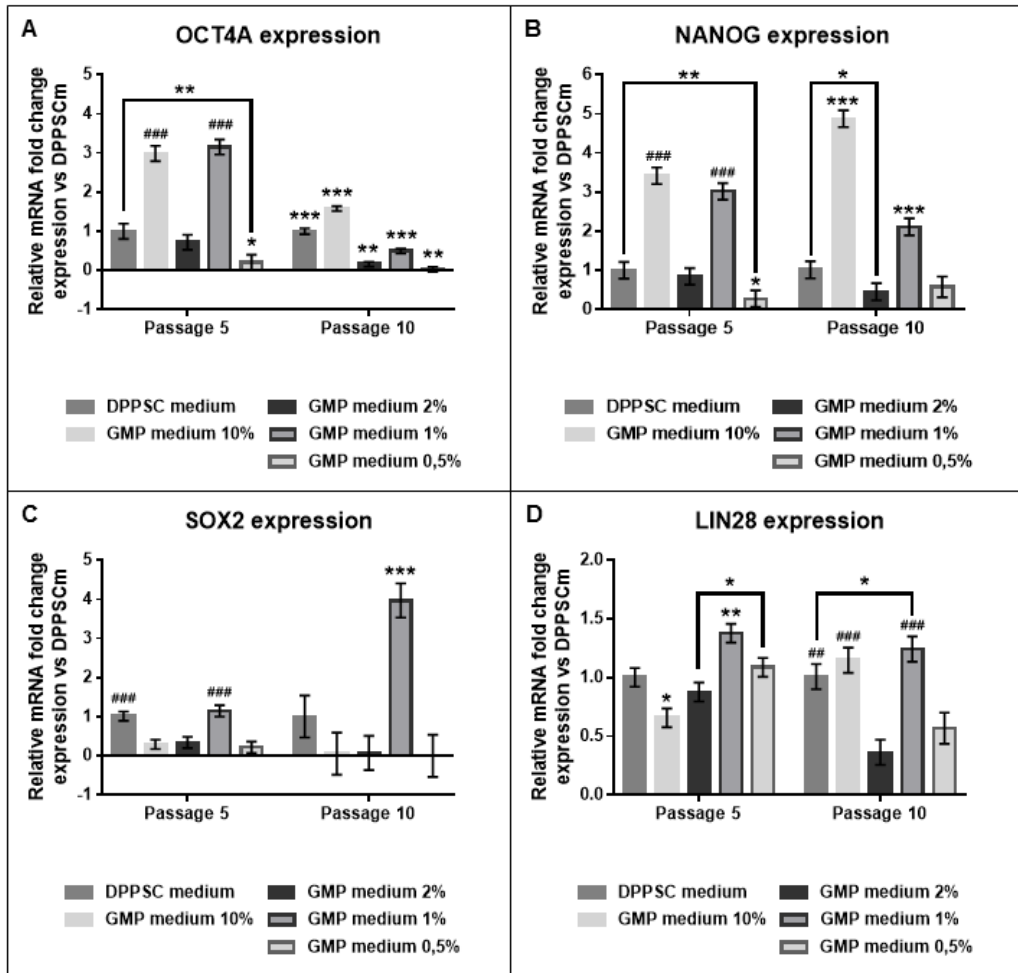


**Figure 13: Pluripotency of DPPSC cultured in different growth media (DPPSC growth medium and GMP growth medium supplemented with different human serum concentration). A)** qRT-PCR analysis of OCT4A expression of DPPSC cultured in different growth media at 5 and 10 passages. \* $p < 0.05$ , \*\* $p < 0.01$ , \*\*\* $p < 0.001$ , #### $p < 0.001$  (expression of cells cultured in GMP supplemented with 10% and 1% of serum at passage 5 is not statistically significant between them but statistically significant to all the other conditions),  $n = 3$ . **B)** qRT-PCR analysis of NANOG expression of DPPSC cultured in different growth media at 5 and 10 passages. \* $p < 0.05$ , \*\* $p < 0.01$ , \*\*\* $p < 0.001$ , #### $p < 0.001$  (expression of cells cultured in GMP supplemented with 10% and 1% of serum at passage 5 is not statistically significant between them but statistically significant to

## RESULTS

*all the other conditions), n=3. C) qRT-PCR analysis of SOX2 expression of DPPSC cultured in different growth media at 5 and 10 passages. \*\*\*p<0.001, ###p<0.001 (expression of cells cultured in DPPSC growth medium and GMP supplemented with 1% of serum at passage 5 is not statistically significant between them but statistically significant to all the other conditions), n=3. D) qRT-PCR analysis of LIN28 expression of DPPSC cultured in different growth media at 5 and 10 passages. \*p<0.05, \*\*p<0.01, ##p<0.01, ###p<0.001 (expression of cells cultured in DPPSC growth medium and GMP supplemented with 10% and 1% of serum at passage 10 is not statistically significant among them but statistically significant to all the other conditions), n=3.*

## **DPPSC MESODERMAL DIFFERENTIATION POTENTIAL**

### **DPPSC endothelial differentiation *in vitro***

The first approach to evaluate if DPPSC had endothelial differentiation potential was to culture them with a widely used commercial medium for endothelial cells and endothelial differentiation called EGM-2. DPPSC were cultured for 25 days in EGM-2 and their endothelial differentiation potential was evaluated at different time points by the functional matrigel assay for endothelial cells and at the end of the differentiation by RT-PCR of the early endothelial marker VEGFR2 (Vascular Endothelial Growth Factor Receptor 2, also known as FLK-1 or KDR). DPMSC were also differentiated in parallel in order to compare their endothelial potential with DPPSC. HUVEC were cultured in EGM-2 as a positive control for endothelial cells. At day 7 of the differentiation, it was already possible to observe some tube-like structures in the matrigel assay in DPPSC and DPMSC, confirming their endothelial potential (Fig. 14A). At day 14 of differentiation, DPPSC showed even more tube-like structures, while in DPMSC we observed the same as in day 7 (Fig. 14B). This pattern was even more noticeable at day 25 of differentiation (Fig. 14C).

The RT-PCR analysis showed that differentiated DPPSC at day 25 expressed the early endothelial marker VEGFR2 while DPMSC in the same condition did not (Fig. 14D).

The next step for DPPSC endothelial differentiation was to optimize the differentiation protocol in terms of seeding density and differentiation protocol. We decided to reduce cell density to 1:2 ( $2 \times 10^4$  cells/cm<sup>2</sup>) in respect to previous conditions ( $4 \times 10^4$  cells/cm<sup>2</sup>) and to 1:8 ( $5 \times 10^3$  cells/cm<sup>2</sup>), as previously used for osteogenic differentiation. We also adopted 3 different differentiation protocols: (1) commercial available EGM-2 endothelial cell medium, (2) HUVEC conditioned EGM-2 endothelial cell medium and (3) transwell system for the indirect co-cultures of DPPSC with HUVEC cells.

RESULTS

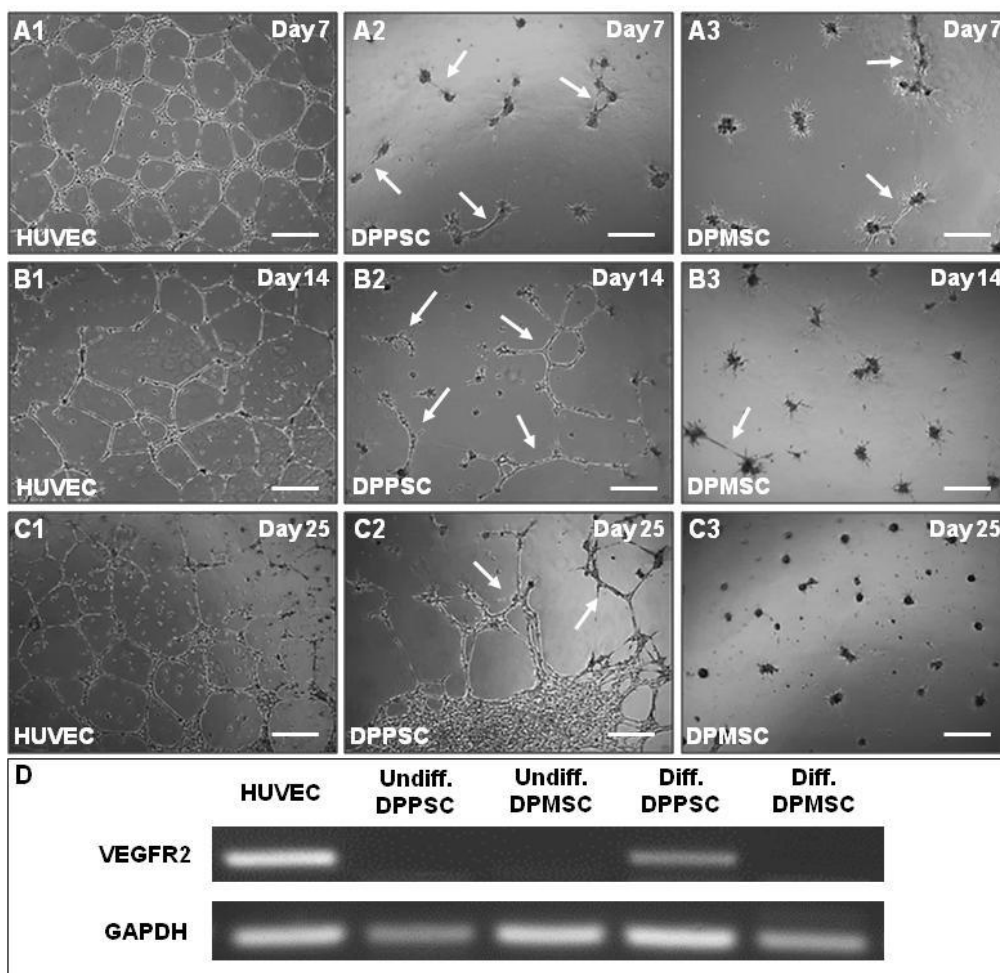


**Figure 14: In vitro endothelial differentiation potential of DPPSC and DPMSC cultured in EGM-2 for 25 days. A-C) Functional 2D Matrigel assay at 24 hours showing tube-like structures (white arrows) formed by DPPSC (A2, B2 and C2) and DPMSC (A3, B3 and C3) differentiated for 7 days (A), 14 days (B) and 25 days (C) towards the endothelial lineage using EGM-2. HUVEC (A1, B1 and C1) were used as a control. Scale bars: 500 μm. D) RT-PCR of the early endothelial marker VEGFR2 in DPPSC and DPMSC undifferentiated and differentiated for 25 days. HUVEC were used as a positive control and GAPDH as housekeeping gene.**

After DPPSC differentiation for 25 days in all these conditions, we observed by the functional matrigel assay that the middle seeding density seemed to present more tube-like structures than the highest seeding density in any of the 3 different differentiation strategies (Fig. 15A-B). Regarding the lowest density, no tube-like structures were obtained in any of the different strategies (Fig. 15C).

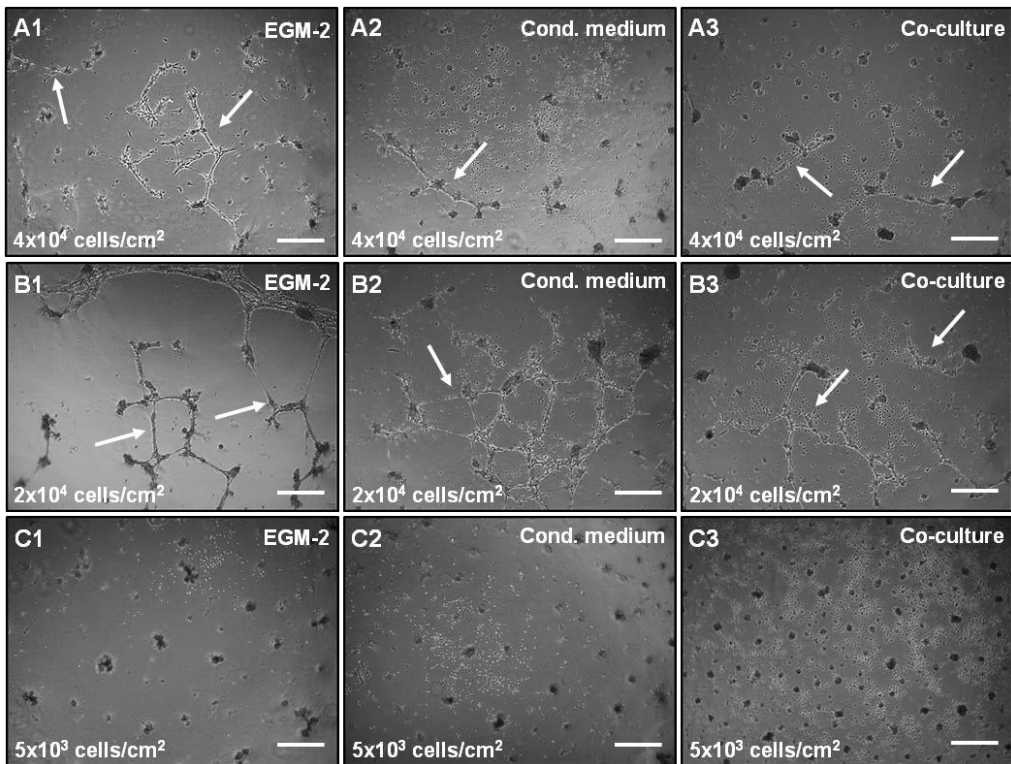


**Figure 15: *In vitro* endothelial differentiation of DPPSC using different seeding densities and differentiation protocols for 25 days.** Functional 2D Matrigel assay showing tube-like structures (white arrows) formed by DPPSC differentiated for 25 days using a seeding density of  $4 \times 10^4$  cells/cm<sup>2</sup> (**A**),  $2 \times 10^4$  cells/cm<sup>2</sup> (**B**) and  $5 \times 10^3$  cells/cm<sup>2</sup> (**C**). DPPSC were differentiated in EGM-2 medium (**A1**, **B1** and **C1**), HUVEC conditioned EGM-2 medium for 24 hours (**A2**, **B2** and **C2**) and in EGM-2 with an indirect co-culture system with HUVEC (**A3**, **B3** and **C3**). Scale bars: 500  $\mu$ m.



## RESULTS

According to these results, we decided to use the  $2 \times 10^4$  cells/cm<sup>2</sup> seeding density to proceed with the differentiation optimization, focusing on the 3 different differentiation strategies. We performed more DPPSC endothelial differentiations using these conditions and analysed their gene expression and tube-like structure formation after 4 weeks of differentiation.

Gene expression analysis by qRT-PCR revealed that DPPSC cultured in the conditioned medium and the co-cultures at day 28 significantly expressed higher levels of VEGFR2 compared to day 0 of differentiation (Fig. 16A). The expression levels of the endothelial marker von Willebrand factor (vWF) followed the same pattern, although the values did not reach statistical significance. In addition, the expression of the endothelial marker CD31 (or PECAM-1, platelet endothelial cell adhesion molecule 1) significantly increased in all conditions, being the co-cultures the ones with the highest expression.

The matrigel assay for functional endothelial cells showed again that the 3 protocols were able to generate functional endothelial cells (Fig. 16B). After quantification of the tubular structures formed, we observed that the conditioned medium protocol produced as many functional cells as the positive control (HUVEC), while the other 2 strategies produced significant less functional cells (Fig. 16C).

Seeing these results, we decided to adopt the conditioned medium differentiation protocol ( $2 \times 10^4$  cells/cm<sup>2</sup> in HUVEC conditioned-EGM-2 medium) for further experiments. In addition, this protocol is technically much easier and economically cheaper to perform compared to the co-cultures.

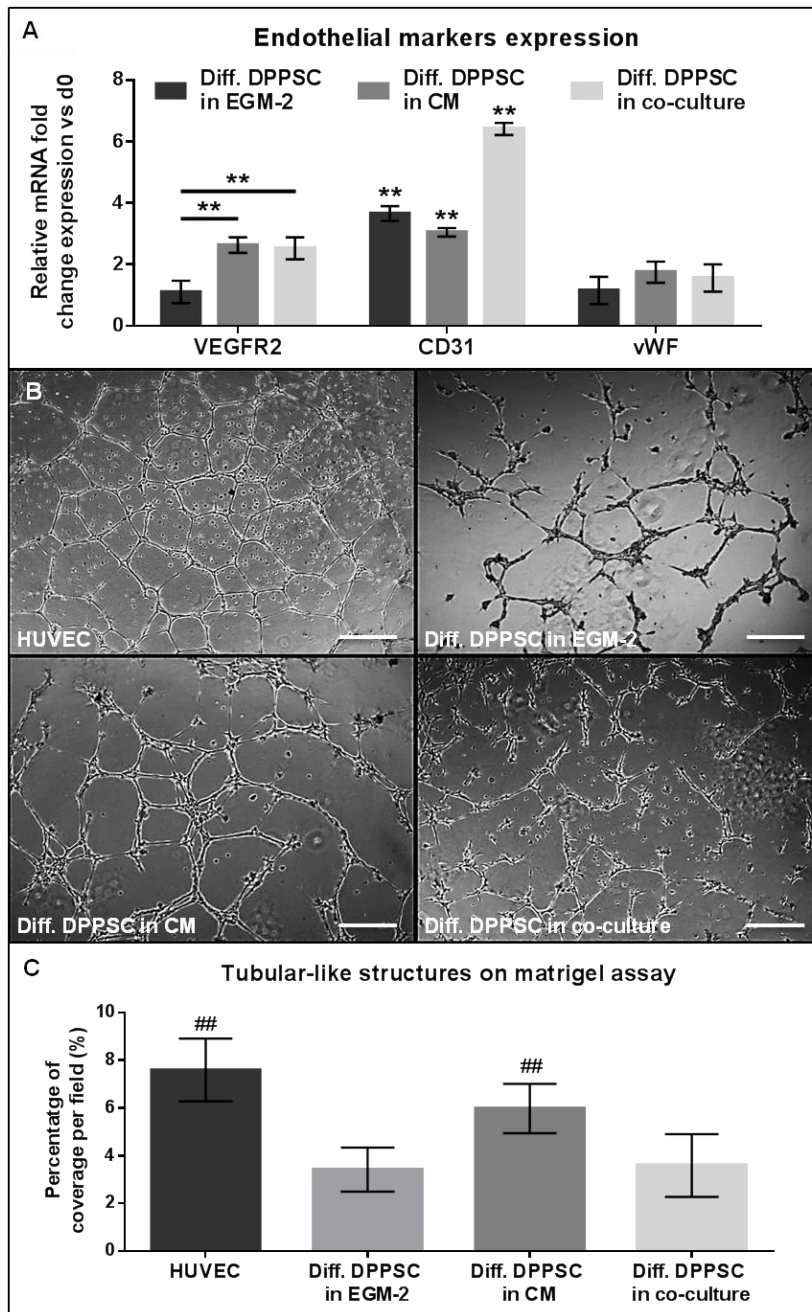


**Figure 16: In vitro endothelial differentiation of DPPSC cultured in three EGM-2-based differentiation protocols for 28 days. A)** qRT-PCR of the early endothelial marker *VEGFR2*, and the later markers *CD31* and *vWF*. HUVEC were

## RESULTS

*used as controls and GAPDH as housekeeping gene. \*\* $p < 0.01$ ,  $n = 3$ . B) Functional 2D Matrigel assay at 24 hours showing tube-like structures formed by DPPSC after 28 days of endothelial differentiation. Scale bars: 500  $\mu\text{m}$ . C) Quantitative analysis of the tubular-like structures formed in the matrigel assay. ### $p < 0.01$  (data obtained by DPPSC cultivated in conditioned medium (CM) are statistically significant comparing to those obtained in the other differentiation protocols),  $n = 3$ .*

Next, gene expression of endothelial markers VEGFR2, CD31 and vWF were analysed by qRT-PCR every week (day 7, 14, 21 and 28) in DPPSC subjected to endothelial differentiation in the adopted protocol (Fig. 17A). The expression level of the endothelial genes did not vary significantly at day 7, but at day 14 a significant up-regulation of the endothelial marker vWF compared to day 0 was observed and maintained at day 28. At day 21, the expression of CD31 increased significantly until it reached the highest value at day 28. A significant up-regulation of VEGFR2 was also observed at day 28 of the differentiation (Fig. 17A).

Regarding the functional matrigel assay, the cells show a tendency to form more tubular-like structures every week, until the 4<sup>th</sup> week (day 28) when the surface of tubular-like structures formed was significantly higher than before and as high as in the HUVEC controls (Fig. 17B-C).

Finally, the protein expression of cells seeded at  $2 \times 10^4$  cells/cm<sup>2</sup> and differentiated in conditioned media for 28 days was detected by immunofluorescence analyses. We were able to detect differentiated cells expressing the endothelial markers CD31, vWF and VE-CAD (Vascular Endothelial Cadherin) forming elongated structures all over the differentiation well (Fig. 18).

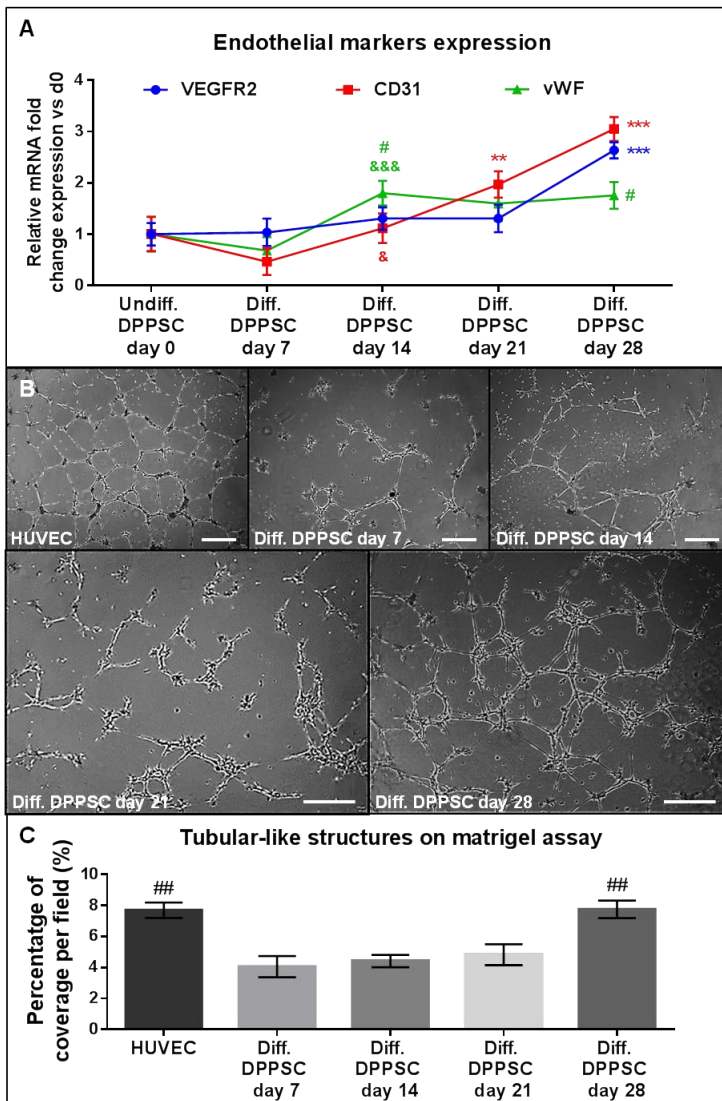


**Figure 17: In vitro endothelial differentiation of DPPSC cultured in HUVEC conditioned EGM-2 medium for 28 days.** **A)** qRT-PCR for the endothelial markers VEGFR2, CD31 and vWF at different differentiation time points. HUVEC were used as controls and GAPDH as housekeeping gene. \* $p < 0.05$ , \*\* $p < 0.01$ , \*\*\* $p < 0.001$ , # $p < 0.05$  (vWF gene expression d0 vs d14 and d0 vs d28), & $p < 0.05$  (CD31 gene expression d7 vs d14), &&& $p < 0.001$  (vWF gene expression d7 vs d14),  $n = 3$ . **B)** Functional 2D Matrigel assay at 24 hours showing tube-like structures formed by HUVEC and DPPSC after 28 days of endothelial differentiation. Scale bars: 500  $\mu\text{m}$ . **C)** Quantitative analysis of the tubular-like

## RESULTS

structures formed in the matrigel assay.  $##p<0.01$  (data obtained by DPPSC cultivated on conditioned medium for 28 days are statistically significant comparing to those obtained in the other time points),  $n=3$ .

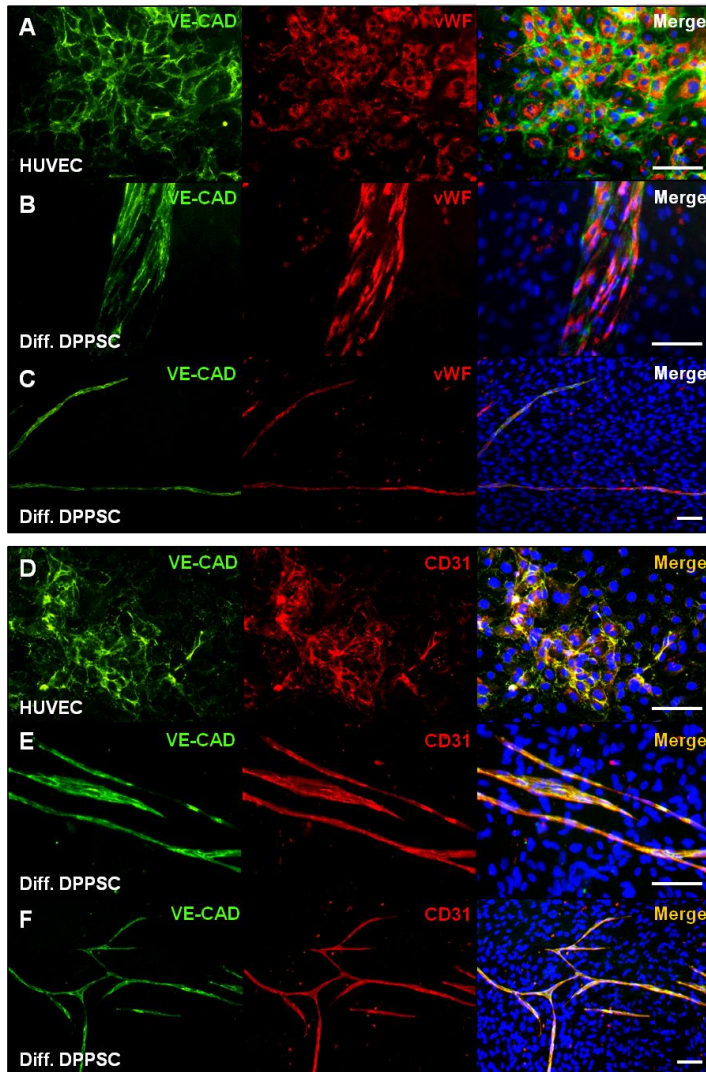


**Figure 18: In vitro endothelial differentiation of DPPSC for 28 days using HUVEC conditioned EGM-2 medium. A-C)** Immunofluorescence analysis for the endothelial markers VE-cadherin (green) and von Willebrand Factor (red) in HUVEC (A) and differentiated DPPSC (B-C). vWF and VE-cad do not colocalize and double positive cells are shown in the merge with green and red signals. **D-F)** Immunofluorescence analysis for the endothelial markers VE-cadherin (green)

and CD31 (red) in HUVEC (D) and differentiated DPPSC (E-F). VE-cadherin and CD31 colocalize and double positive cells are shown in the merge with yellow signal. Nuclei are counterstained with DAPI (blue). Scale bars: 100 $\mu$ m.

## DPPSC smooth muscle differentiation *in vitro*

To further assess the mesodermal differentiation capacity of DPPSC, the differentiation potential of DPPSC to undergo smooth muscle differentiation was evaluated using a protocol already established to differentiate other types of adult stem cells.

This experiment was performed using cells from 2 different donors at 2 different passages (passage 5 and passage 10). In addition, a population of one of these two donors that was infected with a virus containing tGFP (and thus became tGFP<sup>+</sup>) was included. These tGFP<sup>+</sup> DPPSC were later used for the *in vivo* experiments, so we wanted to first evaluate whether they could undergo smooth muscle differentiation.

To evaluate the differentiation, we focused on the morphology of the cells and observed that from day 4 they became bigger, flatter and with more apparent cytoplasm content. At day 10, immunofluorescence analysis for the smooth muscle markers  $\alpha$ SMA (alpha smooth muscle actin) and calponin was performed and all differentiated populations (but not the undifferentiated ones) contained cells positive for both markers (Fig. 19A).

As the populations coming from the different donors seemed to present different percentage of differentiated cells, we proceed to quantify the percentage of cells positive for each smooth muscle marker. We observed that cells coming from the same donor at different passages presented very similar percentages of positive cells for each marker, and bigger differences appeared between the different donors (Fig. 19B). Specifically, the percentage of double positive cells for one donor was 78.2%  $\pm$  15.9% at P5 and 76.2%  $\pm$  19.6% at P10, while in the other donor the percentage was 47.9%  $\pm$  13.8% at P5 and 44.9%  $\pm$  15.9% at P10. Nevertheless, the differences in the percentage of double positive cells were not statistically significant and the percentage of cells calponin positive (including double positive and calponin positive alone cells) remained very similar. Regarding the percentage of double positive cells in the tGFP<sup>+</sup>



RESULTS

DPPSC, which came from the second donor, we observed that the percentage decreased to 25.22% ± 15.8% (Fig. 19B).

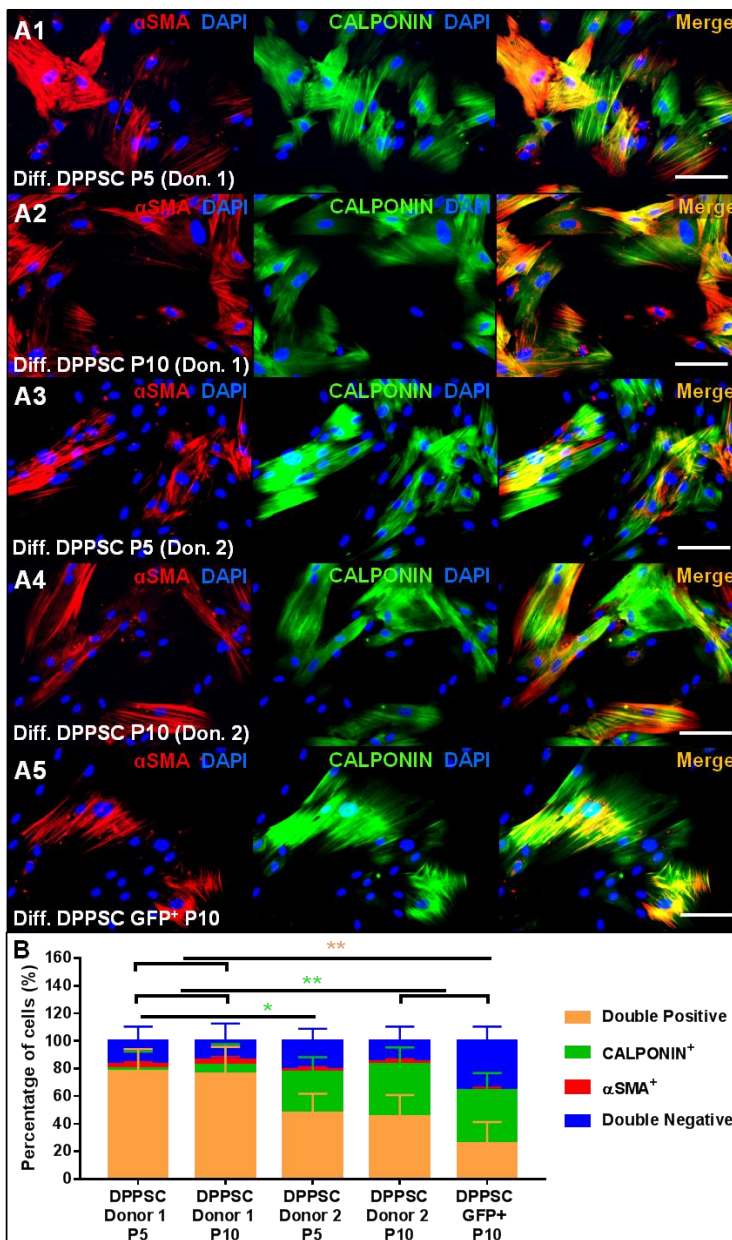


Figure 19: In vitro smooth muscle differentiation of DPPSC. A) Immunofluorescence for the smooth muscle markers αSMA (red) and Calponin

(green) in DPPSC cultured in differentiation medium for 10 days from 2 different donors at passages 5 (**A1, A3**) and 10 (**A2, A4**). *tGFP*<sup>+</sup> DPPSC at passage 10 were also analysed (**A5**). Double positive cells are shown in the merge (yellow-orange); nuclei are counterstained with DAPI (blue). Scale bars: 100 $\mu$ m. **B**) Quantitative analysis of the percentage of cells expressing both smooth muscle markers (orange), calponin alone (green),  $\alpha$ SMA alone (red) or none of them (blue). \* $p < 0.05$ , \*\* $p < 0.01$ ,  $n = 3$ .

## DPPSC skeletal muscle differentiation *in vitro*

The differentiation potential of DPPSC to generate skeletal muscle cells was also evaluated and myogenic mouse C2C12 cells were used as controls.

The skeletal muscle differentiation of DPPSC from 3 different donors at passage 5 and 10 was performed using different protocols: (1) DPPSC cultured in differentiating medium, (2) DPPSC cultured in C2C12 cells conditioned differentiation medium for 24 hours and (3) DPPSC co-cultured with C2C12 at 1:1 or 1:3 ratio.

To evaluate the myogenic potential, immunofluorescence analysis for myosin heavy chain (MyHC) and human specific lamin A/C (LMNA) was performed in order to detect formed myotubes with human nuclei generated from DPPSC.

DPPSC cultured alone in differentiation medium for 7 days did not show clear multinucleated myotube formation as observed in the control C2C12 cells, although rare multinucleated cells positive for MyHC were detected (Fig. S4).

DPPSC cultured using conditioned medium exhibit a more elongated morphology more similar to myotubes, although multinucleated myotubes were not clearly observed since the high proliferation rate hindered the visualization of nuclei inside the same cells (data not shown).

DPPSC in co-culture with C2C12 cells showed evident multinucleated myotubes in which human nuclei could be easily detected, confirming DPPSC capacity for integration in the myotubes (Fig. 20A-B). DPPSC from all the three donors and at the two different passages analysed showed comparable results (Fig. 20A-B, Fig. S5), and



## RESULTS

the different cell-cell ratio did not influence the DPPSC fusion ability (Fig. S5). tGFP<sup>+</sup> DPPSC were also tested and tGFP positive myotubes could be detected (Fig. 20C).

When comparing DPPSC-C2C12 co-cultures with C2C12 cells differentiation, we noticed that DPPSC seemed to enhance the formation of myotubes from an early time point (Fig. 20D-E). The fusion index of the co-cultures and the C2C12 cells alone at day 7 from myogenic differentiation induction was analysed and found statistically significant higher in the co-cultures (Fig. 20F). The same occurred with the number of MyHC<sup>+</sup> myotubes, much higher in the co-cultures (Fig. 20G). The area of MyHC<sup>+</sup> myotubes was also determined and found higher in the co-cultures compared to the C2C12 MyHC<sup>+</sup> myotubes, although the difference did not reach statistical significance (Fig. 20H).

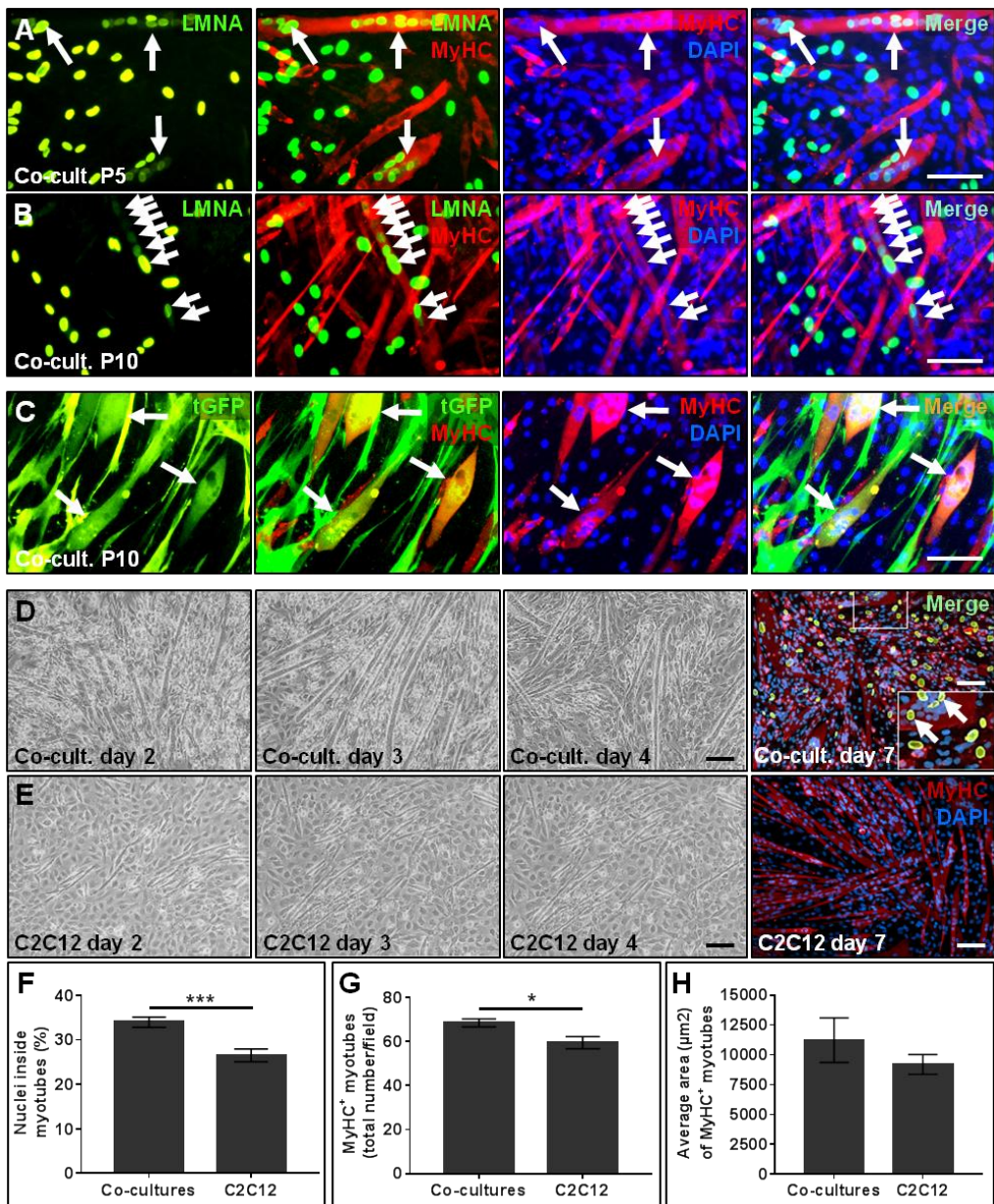


**Figure 20: In vitro myogenic differentiation contribution of DPPSC co-cultured with C2C12 cells.** A-B) DPPSC from passage 5 (A) and 10 (B) co-cultured with C2C12 cells at ratio 1:1 for 5 days. Arrows indicate the presence of human nuclei (stained for human-specific Lamin A/C in green) inside the formed myotubes expressing Myosin Heavy Chain (red). Nuclei are counterstained with

## RESULTS

DAPI (blue). Scale bars: 100  $\mu\text{m}$ . Pictures of DPPSC-C2C12 co-cultures from different donors at ratio 1:1 and 1:3 can be found in the supplementary data (Fig. S5). **C)** tGFP<sup>+</sup> DPPSC from passage 10 co-cultured with C2C12 1:1 for 5 days. Arrows indicate the presence of myotubes expressing both Myosin Heavy Chain (red) and turboGFP (green). DAPI was used as a nucleus control. Scale bar: 100  $\mu\text{m}$ . **D-E)** Co-cultures of DPPSC-C2C12 cells (**D**) and culture of C2C12 cells alone (**E**) at days 2, 3 and 4 of the myogenic differentiation. The last right panels correspond to immunofluorescence analyses at day 7 for Myosin Heavy Chain (red) and Lamin A/C (green); nuclei are counterstained with DAPI (blue). Scale bars: 100  $\mu\text{m}$ . **F)** Fusion Index of the DPPSC-C2C12 cells co-cultures is higher compared to the fusion index of C2C12 cells cultured alone, \*\*\* $p < 0.001$ ,  $n=6$ . **G)** Quantitative analysis of the number of MyHC<sup>+</sup> myotubes per field in the co-cultures compared to C2C12 cells alone, showing an increased number of positive myotubes in the co-cultures. \* $p < 0.05$ ,  $n=6$ . **H)** Average area ( $\mu\text{m}^2$ ) of MyHC<sup>+</sup> myotubes in the co-cultures are not statistically significant compared to the value obtained with myotubes formed from C2C12 cells cultured alone ( $p > 0.05$ ,  $n=6$ ).

### Wound healing assay *in vivo*

In order to evaluate the angiogenesis or vasculogenesis potential of DPPSC through endothelial and smooth muscle differentiation *in vivo*, we performed a wound healing assay in a nude mouse model. Full thickness wounds were made on the back of nude Foxn1 mice, splinted with a silicone ring (Fig. 21A) and treated with PBS or tGFP<sup>+</sup> DPPSC. tGFP<sup>+</sup> DPPSC cells were obtained using a commercial vector containing tGFP. DPPSC were transduced at different confluence and concentration of the vector. The selection of the population used on the *in vivo* assay was based on morphology, proliferation, tGFP<sup>+</sup> expression and mRNA expression of pluripotency markers (data not shown).

During the experiment, the presence of the cells in the wound area was confirmed at day 5 and 11 using fluorescence microscopy (Fig. 21A-D and Fig. S6A). Digital pictures of the wounds were also taken every two days in order to assess wound contraction, although no differences were detected between mice treated with PBS or DPPSC (Fig. S6B).

At day 11 after wounding, mice were sacrificed and skin fragments including the wound area and a rim of normal skin were processed for subsequent analyses. tGFP<sup>+</sup> DPPSC were detected in the tissue sections by immunofluorescence analysis (Fig. 21E).

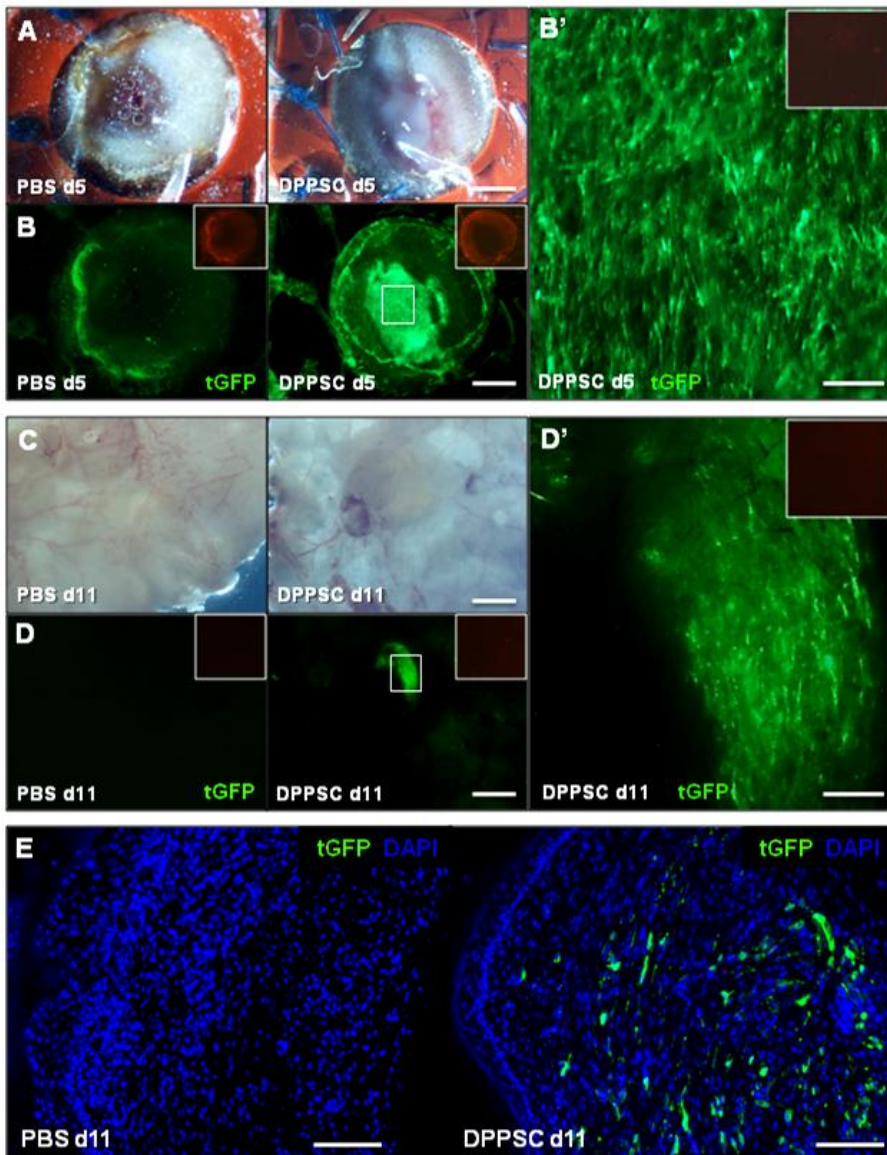


**Figure 21: Cell engraftment in the wound healing assay in vivo using DPPSC. A)** Bright field image of wounds (with silicone rings) in mice treated with PBS or DPPSC at day 5. Scale bars: 2mm. **B)** Turbo GFP expression (in green) of

## RESULTS

*DPPSC in wounds at day 5. Unspecific fluorescence in the PBS and DPPSC treated mice can be observed in the TRITC channel (upper right picture). Scale bars: 2mm. B')* Enlarged image of tGFP expression in DPPSC at day 5. Scale bars: 200 $\mu$ m. *C)* Bright field image of wounds in mice treated with PBS or DPPSC at day 11 after sacrifice. *D)* tGFP expression of DPPSC in wounds at day 11. Unspecific fluorescence in the PBS and DPPSC treated mice can be observed in the TRITC channel (upper right picture). Scale bars: 2mm. *D')* Enlarged image of tGFP expression in DPPSC at day 11. Scale bars: 200 $\mu$ m. *E)* Immunofluorescence analysis for tGFP (green) in paraffin embedded sections of the wound area of mice treated with PBS or DPPSC. Nuclei are counterstained with DAPI (blue). Scale bars: 100 $\mu$ m.

Subsequently, the wound closure in the two groups was analysed and we observed that only two of the five PBS-treated mice showed complete epithelium coverage of the wound, while all 5 DPPSC-treated mice presented complete coverage (Fig. 22A-C). In addition, the epithelium thickness in the two groups was found statistically significant, since DPPSC-treated wounds presented less thick epithelium resembling normal tissue (Fig. 22D-E).



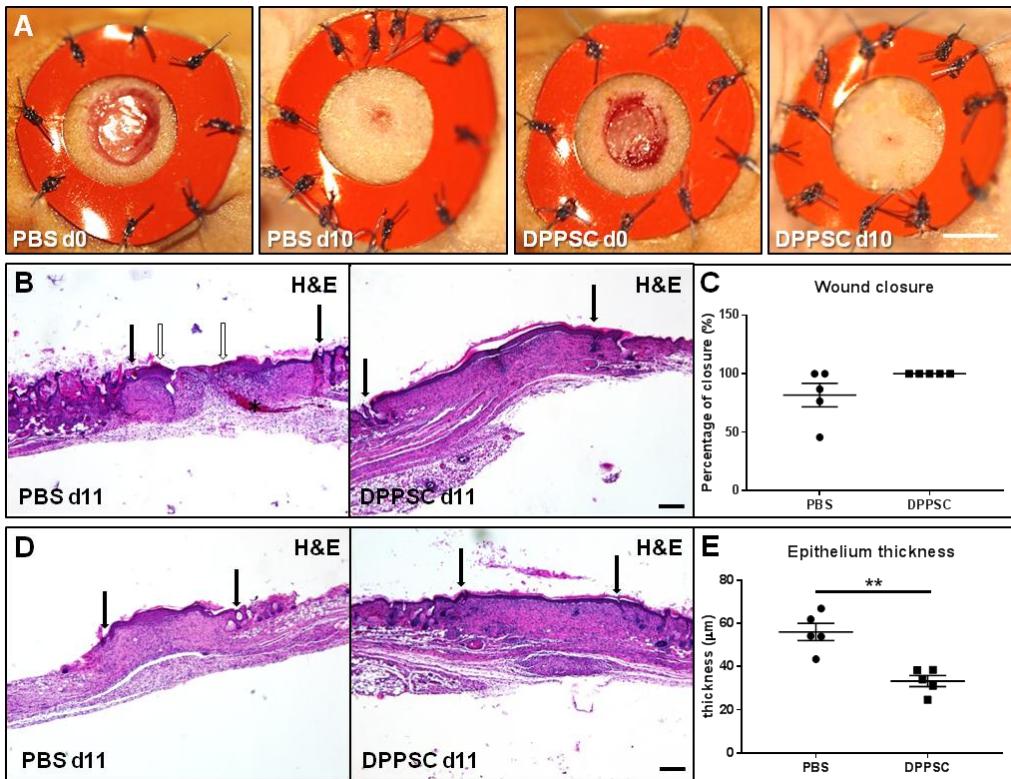


**Figure 22: Wound closure in the wound healing assay in vivo.** **A)** Bright field image of wounds (with silicone rings) in mice treated with PBS or DPPSC at day 0 and at day 10, showing wound closure through time in both conditions. Scale bar: 5mm. **B)** Haematoxylin and eosin staining of paraffin sections of the wound tissue at day 11. Wound area is delimited with black arrows. Some of the PBS treated wounds showed no complete epithelium coverage of the wound, as pointed by white arrows, while all DPPSC treated wounds were completely covered. Some leakage can be observed in the PBS treated condition (-). Scale bar: 500 µm. **C)** Quantification of wound closure (in percentage) with PBS or DPPSC treatment.  $n=5$  for each group. **D)** Haematoxylin and eosin staining of paraffin sections of the wound tissue at day 11, showing the epithelium thickness in the wound area (black arrows) in PBS and DPPSC treated mice. Scale bar: 500 µm. **E)** Quantification of the epithelium thickness in µm.  $*p<0.05$ ,  $**p<0.01$ ,  $n=5$  for each group.

## RESULTS

Next, wound revascularization was analysed. We performed a double immunofluorescence analysis for tGFP and  $\alpha$ SMA to detect DPPSC and smooth muscle cells in the regenerated area (Fig. 23A). We observed that the majority of DPPSC (tGFP<sup>+</sup>) were distributed all over the tissue although some DPPSC (tGFP and  $\alpha$ SMA double positive cells) were integrated in vessel-like structures (Fig. 23B). In addition,  $\alpha$ SMA signal with no tubular/vessel-like structure permitted to detect myofibroblasts (indicated with \* in Fig. 23A) in the tissue. Autofluorescence of blood cells also allowed the detection of leakage when no vessel was surrounding the cells (indicated with \* in Fig. 22B and # Fig. 23A). We observed that sections from PBS-treated mice seemed to present more myofibroblast and leakage presence (Fig. 23A).

Subsequently, we performed an immunofluorescence analysis for the detection of CD31 and  $\alpha$ SMA (Fig. 23C) in order to elucidate if DPPSC were able to promote angiogenesis. Quantification of CD31<sup>+</sup> vessels,  $\alpha$ SMA<sup>+</sup> vessels and the number of functional vessels (with blood cells inside), as well as their area was determined. Regarding the number and area of CD31<sup>+</sup> vessels, no significant differences were found between PBS and DPPSC-treated wounds, although the area of CD31<sup>+</sup> vessels seemed higher in the DPPSC-treated ones (Fig. S6C, S6G). The area and percentage of  $\alpha$ SMA coated vessels was significantly higher in DPPSC-treated wounds (Fig. 23D-E). Number, area and percentage of functional vessels were also found higher in DPPSC-treated wounds, although the values did not reach statistical significance (Fig. S6E, S6F, S6H).

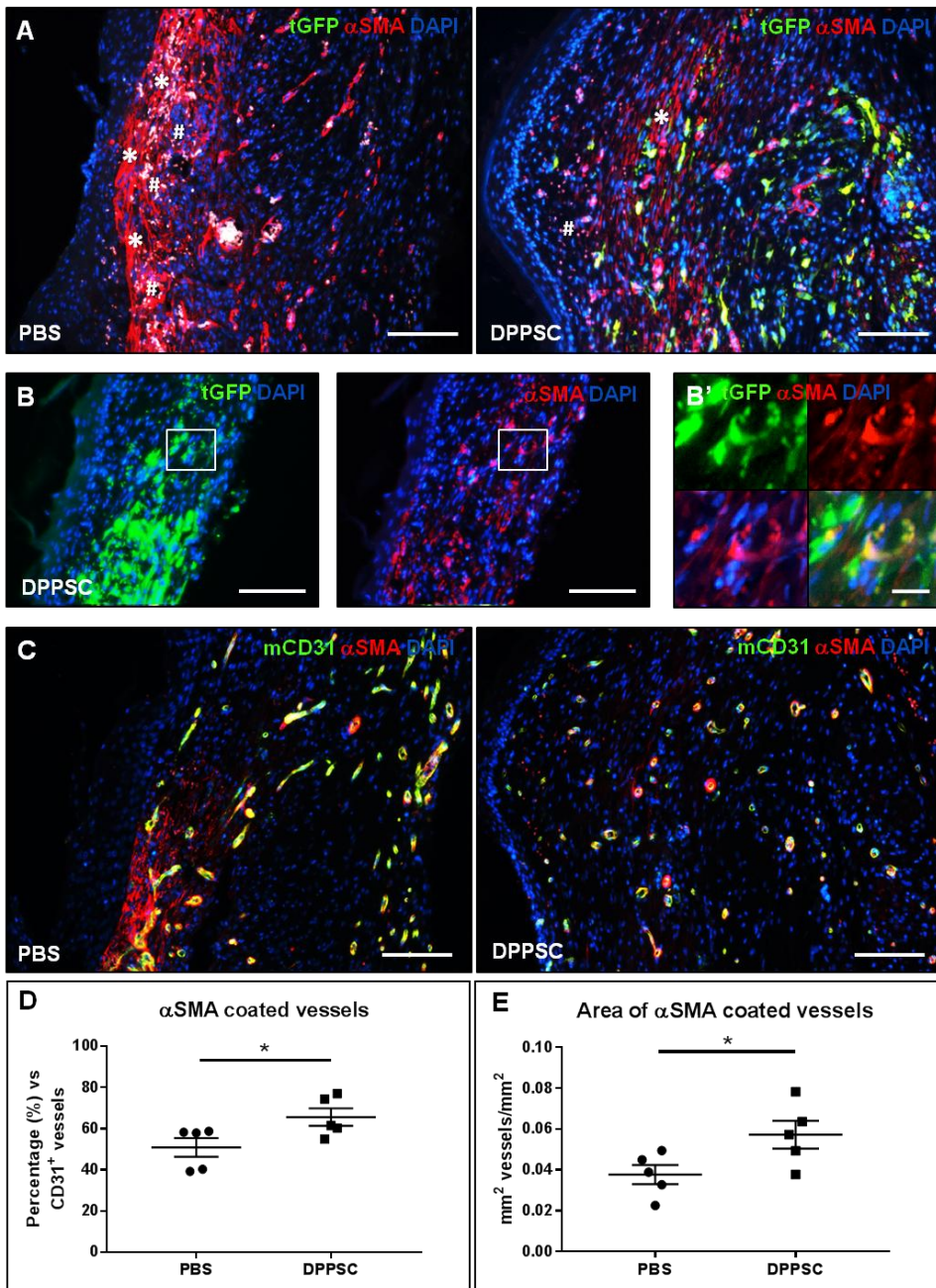


**Figure 23: Wound revascularization in the wound healing assay in vivo at day 11. A)** tGFP (green) and αSMA (red) immunofluorescence analyses in PBS or DPPSC treated mice. Nuclei are counterstained with DAPI (blue). Note that



## RESULTS

*$\alpha$ SMA staining with no tubular structures detected myofibroblasts presence (-). Autofluorescence of blood cells allowed the detection of leakage when no vessel was surrounding the cells (#). Scale bar: 100 $\mu$ m. **B, B'**) tGFP (green) and  $\alpha$ SMA (red) double positive cells (yellow) in treated wound identified DPPSC integrated in a vessel-like structure. Nuclei are counterstained with DAPI (blue). Scale bars: 100 $\mu$ m (B), 20 $\mu$ m (B'). **C**) Mouse CD31 (green) and  $\alpha$ SMA (red) immunofluorescence analysis in PBS or DPPSC treated wounds, showing the presence of CD31<sup>+</sup> vessels with  $\alpha$ SMA coverage. Nuclei are counterstained with DAPI (blue). Scale bars: 100  $\mu$ m. **D**) Quantification of  $\alpha$ SMA-coated vessels in PBS and DPPSC treated wounds, showing higher percentage of coverage in DPPSC treated wounds. \* $p$ <0.05,  $n$ =5 for each group. **E**) Quantification of the area of  $\alpha$ SMA-coated vessels in PBS and DPPSC treated wounds, showing bigger area of coverage in DPPSC treated wounds. \* $p$ <0.05,  $n$ =5 for each group.*

Finally, the wound matrix organization was analysed. Sirius red staining for the dermal collagen matrix showed that total collagen quantification was significantly higher in the centre of the DPPSC-treated wounds than the ones with PBS (Fig. 24A, 24C). The side part of the wounds, closer to the normal tissue, showed no significant difference between the two groups (Fig. S6I-J). Organized collagen, observed in red in the Sirius Red staining using polarized light, followed the same pattern, being significantly higher in the centre of the DPPSC-treated wounds compared to the controls (Fig. 24B and 24D) and no statistically significant in the side part of the wounds (Fig. S6K-L). Indeed, the values of total and organized collagen in the centre of the DPPSC-treated wounds were very similar to the uninjured tissue (present in the border of the wound of both PBS and DPPSC-treated mice, Fig. 24E-F).

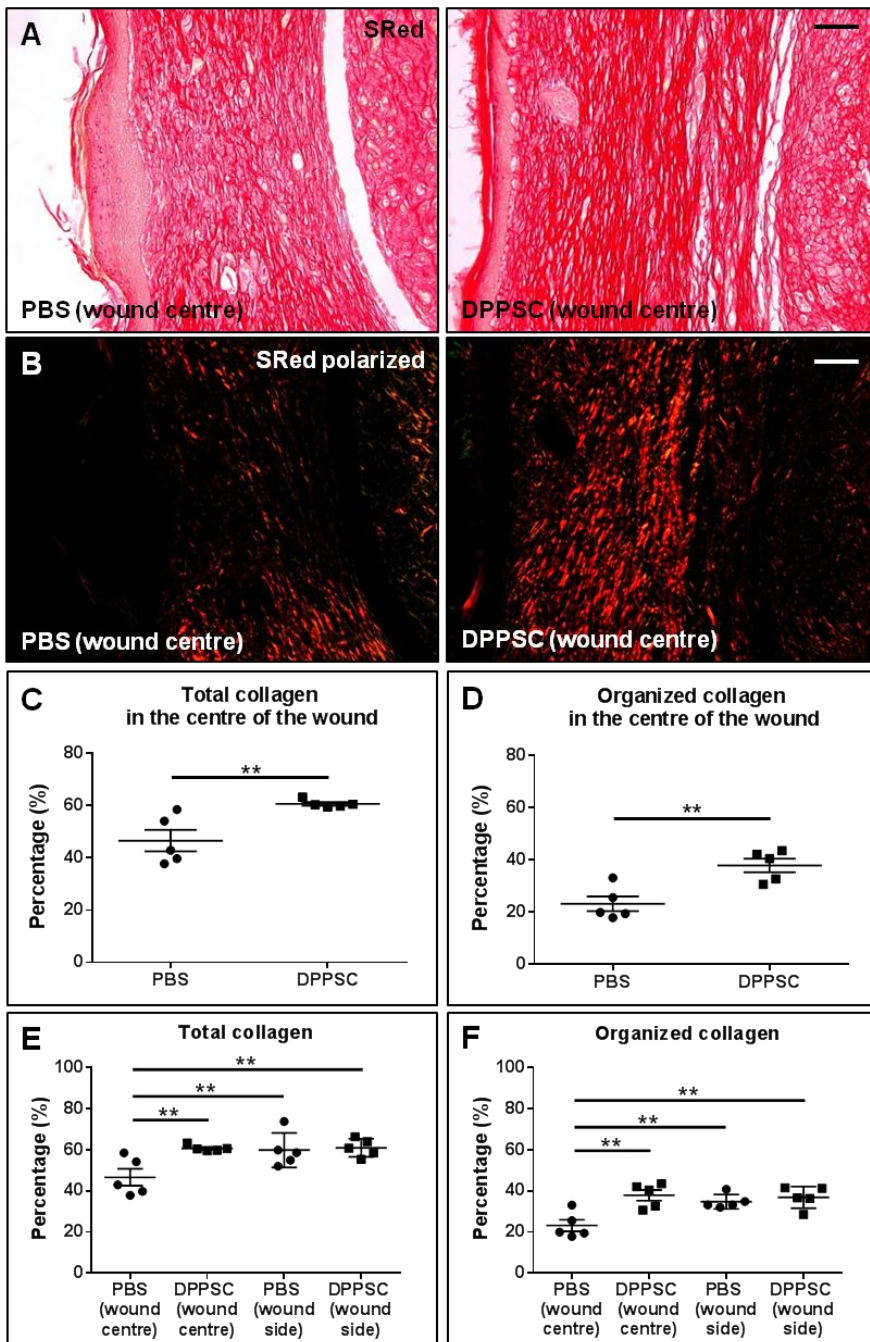


**Figure 24: Wound matrix organization in the wound healing assay in vivo at day 11. A) Sirius Red staining of the central part of wounds treated with PBS or**

## RESULTS

*DPPSC for the analysis of total collagen in the wound matrix. Scale bars: 200  $\mu\text{m}$ . **B)** Sirius Red staining of the same sections as in A using polarized light for the analysis of organized collagen (observed in red) in the wound matrix. Scale bars: 200  $\mu\text{m}$ . **C)** Quantification of the total collagen present in the central part of the wounds treated with PBS or DPPSC, showing higher percentage of collagen in DPPSC treated wounds.  $**p < 0.01$ ,  $n=5$  for each group. **D)** Quantification of the organized collagen present in the central part of the wounds treated with PBS or DPPSC, showing higher percentage of organized collagen in DPPSC treated wounds.  $**p < 0.01$ ,  $n=5$  for each group. **E)** Quantification of the total collagen present in the central and side part of the wounds treated with PBS or DPPSC.  $**p < 0.01$ ,  $n=5$  for each group. **F)** Quantification of the organized collagen present in the central and side part of the wounds treated with PBS or DPPSC.  $**p < 0.01$ ,  $n=5$  for each group.*

All numerical data obtained in the wound healing assay have been included in Table 1.

			PBS	DPPSC
<b>Wound closure from day 2 until day 10</b>				
<b>Contraction (%)</b>	Day 2		18 ± 3	17 ± 7
	Day 4		26 ± 3	28 ± 4
	Day 6		68 ± 9	88 ± 2
	Day 8		92 ± 4	92 ± 5
	Day 10		97 ± 1	98 ± 1
<b>Wound closure, revascularization and matrix organization at day 11</b>				
<b>Wound closure</b>	Epidermal closure	Complete epithelial coverage	2 out of 5	5 out of 5
		Epithelial coverage (%)	82 ± 10	100 ± 0
		Epithelium thickness	56 ± 4	33 ± 3 **
<b>Wound revascularization</b>	Number of CD31 <sup>+</sup> vessels/mm <sup>2</sup> tissue		461 ± 49	409 ± 42
	mm <sup>2</sup> CD31 <sup>+</sup> vessels/mm <sup>2</sup> tissue		0,069 ± 0,006	0,075 ± 0,015
	Number of αSMA-coated vessels/mm <sup>2</sup> tissue		252 ± 47	262 ± 31
	% αSMA-coated vessels vs CD31 <sup>+</sup> vessels		51 ± 5	66 ± 4 *
	mm <sup>2</sup> αSMA coated vessels/mm <sup>2</sup> tissue		0,038 ± 0,005	0,057 ± 0,007 *
	Number of functional vessels/mm <sup>2</sup> tissue		155 ± 4	168 ± 19
	% functional vessels vs CD31 <sup>+</sup> vessels		38 ± 4	43 ± 5
	mm <sup>2</sup> functional vessels/mm <sup>2</sup> tissue		0,038 ± 0,004	0,051 ± 0,007
	Leakage presence		High	Low
	Myofibroblasts presence		High	Low
<b>Wound matrix organization</b>	% Total collagen	in the centre of the wound	47 ± 4	61 ± 1 **
		in the side of the wound	60 ± 4	61 ± 2
	% Organized collagen	in the centre of the wound	23 ± 3	38 ± 3 **
		in the side of the wound	35 ± 1	37 ± 2

**Table 1: Effects of DPPSC treatment in the wound healing assay.** \* $p < 0.05$ , \*\* $p < 0.01$ ,  $n = 5$  for each group.

## RESULTS

### **DPPSC injection in two different models of dystrophic mice**

In order to evaluate the myogenic potential of DPPSC *in vivo* to undergo skeletal muscle differentiation, as well as their angiogenic potential *in vivo*, we injected DPPSC in two different mouse models of muscular dystrophies. Specifically, *Scid/mdx*, immunodeficient mice that lack functional dystrophin, and *Sgcb-null Rag2-null γc-null*, immunodeficient mice beta-sarcoglycan null, were used. Mice were injected with undifferentiated DPPSC in the *tibialis anterior* muscles.

At day 20-30 after injection, mice were sacrificed and muscles were processed for subsequent molecular and histological analyses. DPPSC engraftment in the muscle tissue was detected by immunofluorescence analysis for human specific lamin A/C. DPPSC were found present in the muscle of both mouse models (Fig. 25A-B). Focusing on DPPSC localization in the muscle, DPPSC were observed in the interstitial space between groups of fibres (Fig. 25A-B) and in the basal lamina of the fibres (Fig. 25C1 and 25D1). Human nuclei were also detected in regenerating fibres in *Scid/mdx* (Fig. 25C2-C5) and *Sgcb-null Rag2-null γc-null* (Fig. 25D2-D5). Finally, DPPSC were also detected in both mice models integrated in vessel-like structures (Fig. 25C6 and 25D6).

Focusing on the DPPSC myogenic differentiation *in vivo*, we wanted to assess whether we could find fibres expressing either dystrophin (in *mdx*) or beta-sarcoglycan (in *Sgcb-null*). More dystrophin positive fibres were observed in the DPPSC injected *Scid/mdx* muscles than in the controls (Fig. 26A-B). We could also detect, in serial sections, dystrophin expression in the same zones where we detected lamin A/C positive DPPSC (Fig. 26C), suggesting a DPPSC direct myogenic contribution. Regarding *Sgcb-null Rag2-null γc-null mice*, beta-sarcoglycan positive fibres were detected only in DPPSC injected muscles, while no beta-sarcoglycan positive fibres were detected in the controls (Fig. 26D-G).

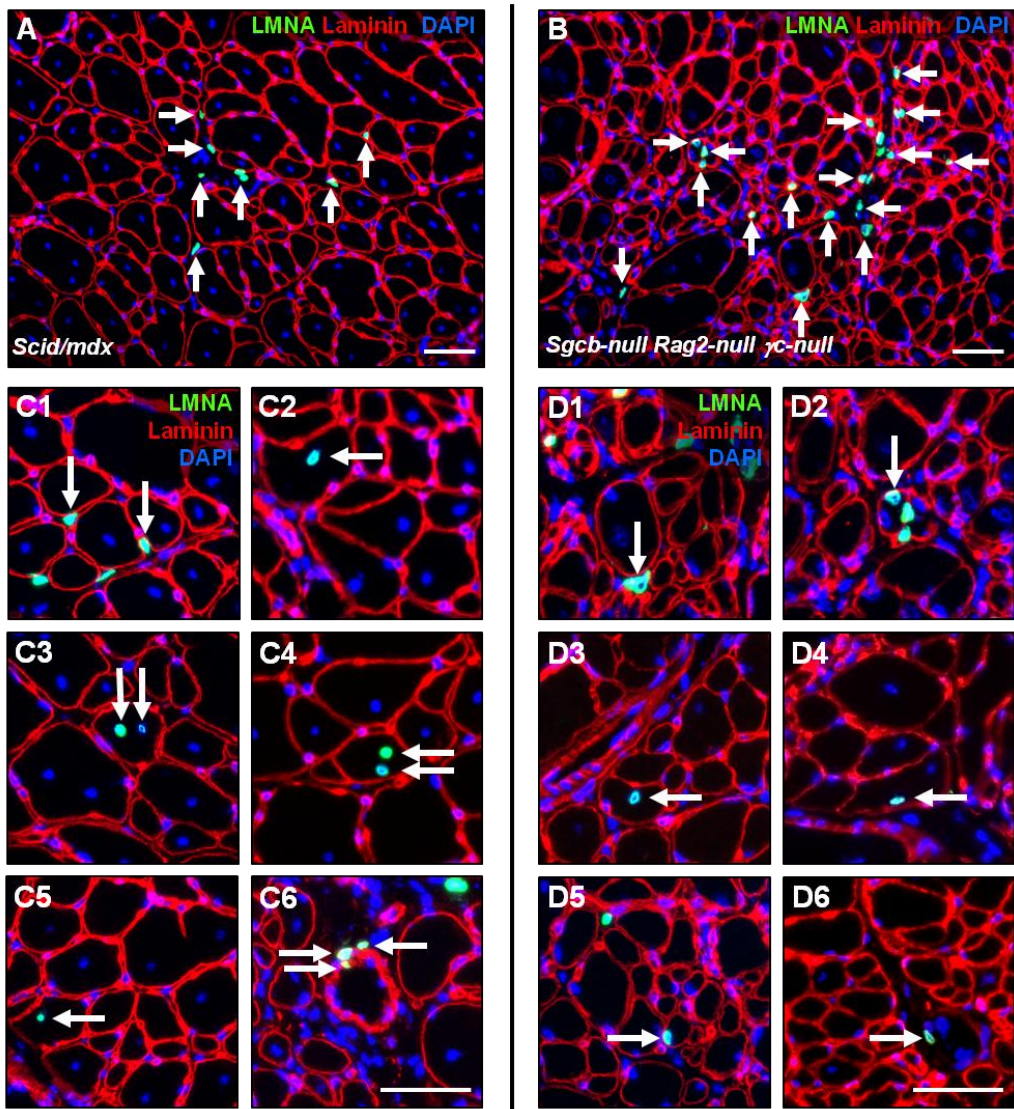


**Figure 25: DPPSC localization after injection in dystrophic mice. A-B)** Immunofluorescence analysis for human specific Lamin A/C (green) and Laminin (red), showing DPPSC engraftment (white arrows) in *Scid/mdx* (A) and *Sgcb-null Rag2-null γc-null* (B) mice. **C-D)** Immunofluorescence analysis for hLMNA (green) and laminin (red) in *Scid/mdx* (C) and *Sgcb-null Rag2-null γc-null* (D), showing localization of DPPSC (white arrows) outside the muscular fibres in the basal lamina (C1, D1), inside the newly formed regenerative fibres (C2-C5, D2-D5), and



RESULTS

*in vessel-like structures (C6, D6). Nuclei are counterstained with DAPI (blue). Scale bars: 50  $\mu$ m.*

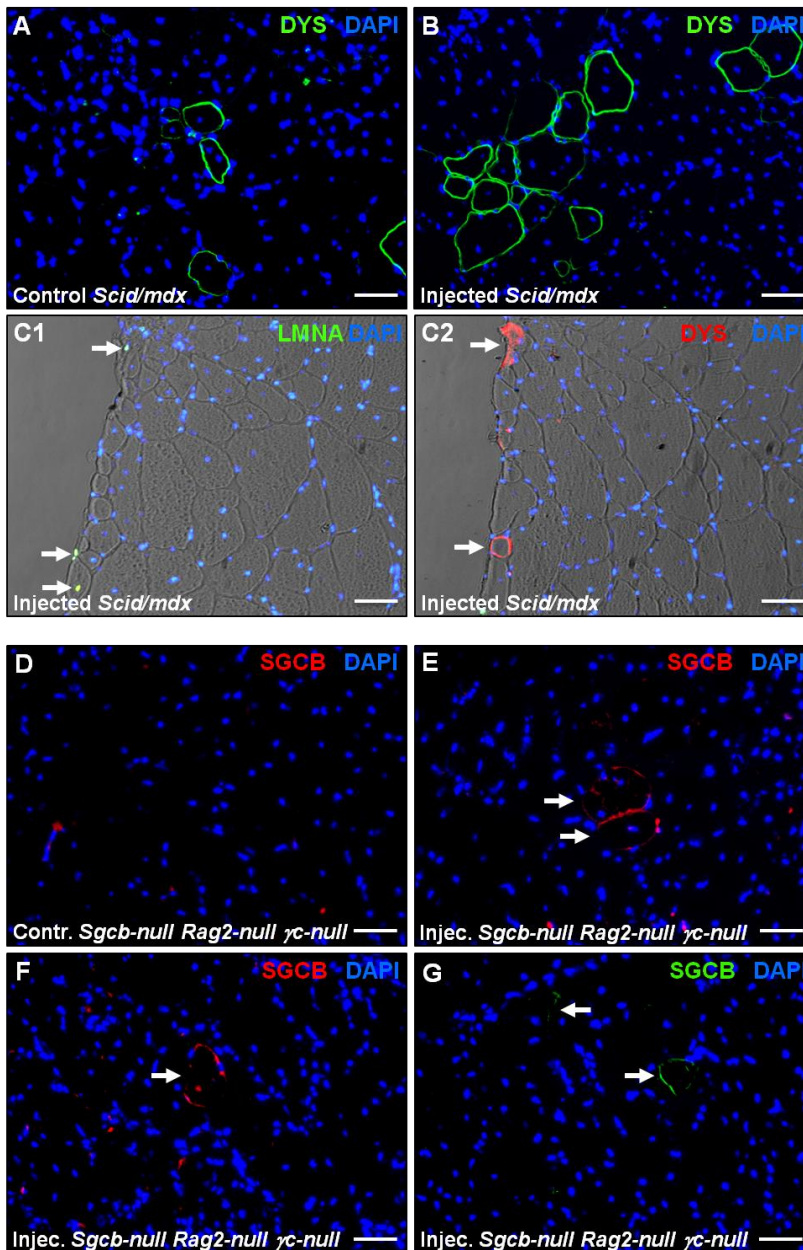


**Figure 26: Effects of DPPSC injection in dystrophic mice. A-B)** Immunofluorescence analyses for dystrophin (green) in control *Scid/mdx* mice (A)

*and DPPSC injected Scid/mdx (B). C Immunofluorescence analyses in two serial slides for human laminin A/C (green) and dystrophin (red) in injected Scid/mdx mice. Bright field allows the identification of the same fibres in the two slides. D-E Immunofluorescence analyses for beta-sarcoglycan (red in D-F, green in G) in control Sgcb-null Rag2-null  $\gamma$ c-null mice (D) and DPPSC injected Sgcb-null Rag2-null  $\gamma$ c-null (E-G). Nuclei are counterstained with DAPI (blue). Scale bars: 50  $\mu$ m.*

Focusing on DPPSC localization in vessel-like structures, we wanted to further evaluate their endothelial and smooth muscle differentiation in skeletal muscles. As said before, in both of the mice models used, DPPSC were detected in the interstitial space between groups of fibres in tubular-like structures. Specifically, in *Scid/mdx* mice, human nuclei were detected in the inner part of the tubular-like structures, in contact with the lumen (Fig. 27A), while others were localized in the middle/outside part of the structure (Fig. 27C). In order to elucidate if these structures were vessels, immunofluorescence analyses for vWF were performed in serial slides and the structures revealed positive for this endothelial marker (Fig. 27B and 27D).



RESULTS

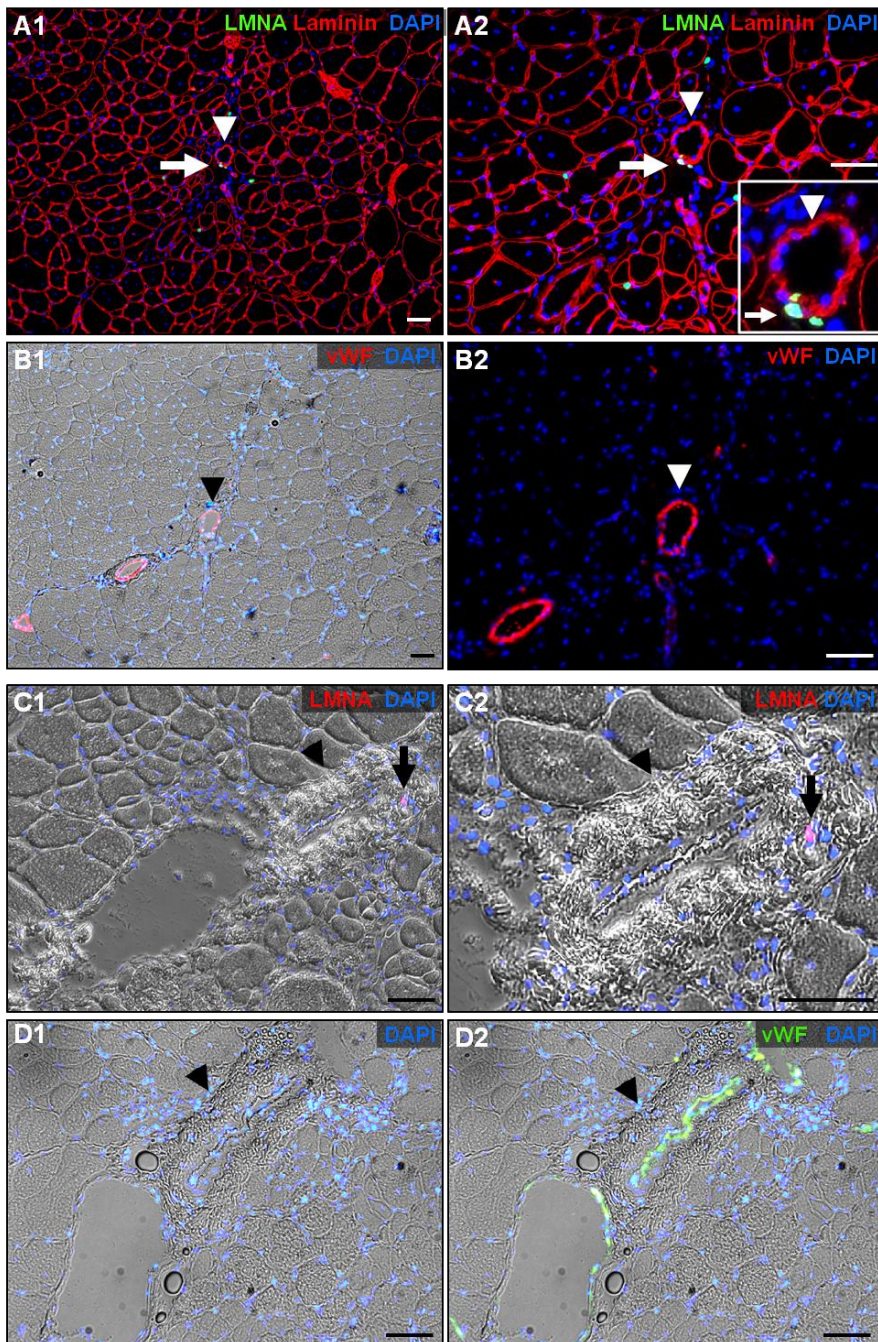


**Figure 27: DPPSC localization in vessel-like structures after injection in Scid/mdx dystrophic mice. A) Immunofluorescence analysis for human specific**

LMNA (green) and laminin (red) in *Scid/mdx*, showing DPPSC localization (arrows) in vessel-like structures (arrow heads). **B)** Immunofluorescence analysis for vWF (red) in a serial slide from **A**, showing the same muscle zone. The same vessel structure is indicated with an arrow head. Bright field can also be observed in **B1**. **C)** Immunofluorescence analysis for human specific LMNA (red) in *Scid/mdx*. Bright field image allows the detection of LMNA in the external part of the vessel-like structure (arrow heads). **D)** Immunofluorescence analysis for vWF (green) in a serial slide from **C**, showing the same muscle zone. The same vessel structure is indicated with an arrow head. Nuclei are counterstained with DAPI (blue). Scale bars: 50  $\mu$ m.

In *Sgcb-null Rag2-null  $\gamma$ c-null* mice, DPPSC were also observed in the inner part of the tubular-like structures (Fig. 28A) and in the middle/outside part of them (Fig. 28B).

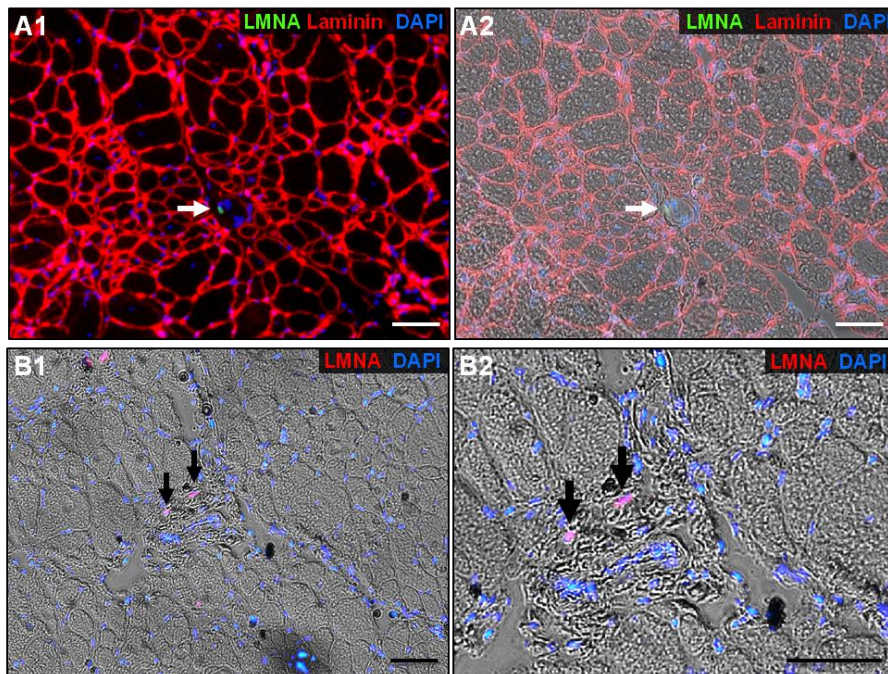


**Figure 28: DPPSC localization in vessel-like structures after injection in *Sgcb-null Rag2-null  $\gamma$ c-null* dystrophic mice. A-B)** Immunofluorescence analyses for human specific LMNA (green) and laminin (red) in *Sgcb-null Rag2-null  $\gamma$ c-null* mice, showing DPPSC localization (white arrows) in vessel-like structures. Bright field can also be observed in **A2**. **B)** Immunofluorescence

**RESULTS**

*analyses for human specific LMNA (red) in Sgcb-null Rag2-null  $\gamma$ c-null mice. Bright field image allows the detection of LMNA (black arrows) in the external part of the vessel-like structures. Nuclei are counterstained with DAPI (blue). Scale bars: 50  $\mu$ m.*

In order to verify the presence of DPPSC in the vessels, immunofluorescence analyses for the endothelial marker vWF or the smooth muscle marker  $\alpha$ SMA were carried out together with human specific lamin A/C. It was possible to localize rare DPPSC integrated in the inner layer of vessels positive for vWF in *Scid/mdx* mice (Fig. 29A), while human nuclei were often localized close to vessels (or in their external part) in *Sgcb-null Rag2-null  $\gamma$ c-null* mice (Fig. 29B). Finally, rare DPPSC were positive for  $\alpha$ SMA in both mice models used, suggesting their contribution to smooth muscle cells (Fig. 29C and 29D).



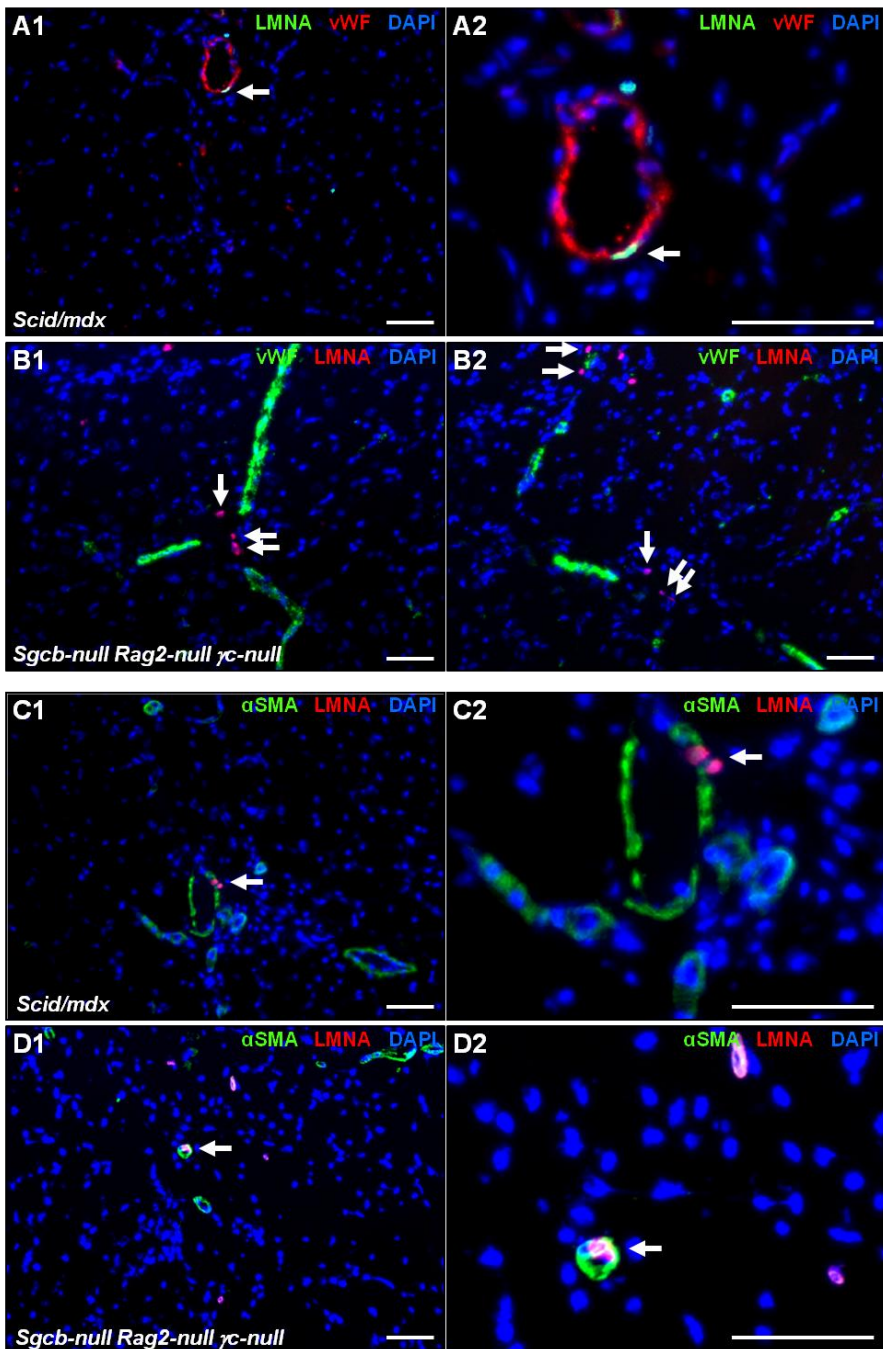


**Figure 29: DPPSC localization in blood vessels after injection in dystrophic mice. A) Immunofluorescence analysis for hLMNA (green) and endothelial marker**

**RESULTS**

*vWF* (red) in *Scid/mdx* mice, showing localization of DPPSC (arrows) in the inner layer of a vessel. **B)** Immunofluorescence analyses for hLMNA (red) and *vWF* (green) in *Sgcb-null Rag2-null  $\gamma$ c-null* mice, showing localization of DPPSC (arrows) in the external part of vessels or close to them. **C-D)** Immunofluorescence analyses for hLMNA (red) and smooth muscle marker  $\alpha$ SMA (green) in *Scid/mdx* mice (**C**) and *Sgcb-null Rag2-null  $\gamma$ c-null* mice (**D**), showing colocalization (arrows). Nuclei are counterstained with DAPI (blue). Scale bars: 50  $\mu$ m.

## **DISCUSSION**

---



## **DPPSC CHARACTERIZATION**

In this study, we present results showing that DPPSC are a source of adult stem cells with unique characteristics. Several stem cells populations have been isolated from human teeth, all of them showing generic MSC-like properties (102, 103). However, DPPSC are the only adult stem cells expressing pluripotent genes providing them a peculiar proliferation capability.

DPPSC are obtained from dental pulp using the same isolation protocol used for DPMSC; therefore, the distinction of these different cell populations must depend on the culture medium and the density at which the cells are seeded. Thus, culture medium and cell density are key elements for maintaining the properties of DPPSC and avoiding DPMSC overgrowth.

In the present study, DPMSC were used as a control population. Since DPPSC and DPMSC are obtained from the same tissue, and DPMSC have been long studied while DPPSC represent a quite new described population, it felt important to establish the differences between them in terms of growth rate or genetic stability, a more controversial concern. Other characteristics, such as differential pluripotency markers expression or osteogenic differentiation capacity have already been addressed in published papers or doctoral thesis (28, 30, 104). However, this study was not focused on the differences between these two populations, but in the characterization itself of DPPSC.

We could observe here, from the primary cultures of several donors until 15 passages, the noticeable differences in morphology between DPPSC and DPMSC. DPPSC are smaller and possess a larger nucleus relative to the volume of the cytoplasm, a characteristic shared with hESC (105), while DPMSC exhibit the typical spindle-shaped morphology of MSC, as previously reported (106). In addition, DPPSC divide faster than DPMSC, resembling the division rate of hESC (107). When we studied the population doubling time of the two populations through passages, we observed that DPMSC decreased their division rate in later passages. Tight dependence of population doublings on passage number and slow decrease of proliferation



## DISCUSSION

potential has already been described in DPMSC (108). In contrast, DPPSC maintained their population doubling time through passages, a characteristic also shared with hESC, which are well known to maintain their pluripotent characteristics stably in spite of an extended period of in vitro cultivation (107).

In previous publications of our laboratory, it was demonstrated that DPPSC have the protein profile SSEA4<sup>+</sup>, OCT3/4<sup>+</sup>, NANOG<sup>+</sup>, Nestin<sup>+</sup>, SOX2<sup>+</sup>, LIN28<sup>+</sup>, CD13<sup>+</sup>, CD105<sup>+</sup>, CD34<sup>-</sup>, CD45<sup>-</sup>, CD90<sup>low</sup>, CD29<sup>+</sup>, CD73<sup>low</sup>, STRO1<sup>low</sup> and CD146<sup>-</sup> (28). To our knowledge, there has not been a published reference to the presence of a population of cells with this protein profile in the dental pulp. In the same work, it was also demonstrated that DPPSC have unique characteristics when compared to other adult stem cells such as DPMSC regarding their higher expression of typical embryonic genes such as OCT3/4, NANOG and SOX2, which are known to be key in maintaining pluripotency (109).

In the present work, we characterized the new DPPSC populations obtained from several donors by gene and protein expression and AP activity. The detection of OCT4 expression by PCR has recently been controversial, due to the presence of transcriptional variants of the OCT4 gene and pseudogenes that encode proteins that do not participate in the pluripotency maintenance (110-116). Therefore, for our analyses, we used the primers from *Guangzu et al.* (110) that only amplify the mRNA variant 1 or OCT4A, which synthesizes the key transcription factor for maintaining self-renewal and pluripotency, and do not amplify the other variants or pseudogenes. We demonstrated for the first time that all DPPSC populations used in this study expressed OCT4A and NANOG at mRNA level for at least 15 passages. The presence of OCT4, NANOG and SOX2 proteins was also confirmed by immunofluorescence analysis. However, so far there is no OCT4A-specific antibody commercially available (110), which causes the detection of other OCT4 isoforms located in the cytoplasm. DPPSC were also characterized by the presence of Alkaline Phosphatase (AP) activity, which is known to be present in pluripotent stem cells such as ESC and iPSC (5, 117).

In this study, we focused on studying whether the pluripotency state of DPPSC was maintained invariable for at least the 15 passages studied or whether the cells

expressed different levels of pluripotency markers through passages. The results demonstrated that DPPSC expression of OCT4A and NANOG varies through the different passages, both increasing from passage 5 to 10 and decreasing from passage 10 to 15.

In previous studies from our group, DPPSC and DPMSC have been demonstrated to coexist in culture (28). Probably, due to the lack of a constricting selection when performing the DPPSC primary culture, other populations such as DPMSC could be present in the culture at a small percentage from the beginning. In those studies, it was also demonstrated that OCT4<sup>+</sup>, SOX<sup>+</sup> cells (DPPSC) were CD73<sup>-</sup>, while OCT4<sup>-</sup>, SOX2<sup>-</sup> cells were CD73<sup>+</sup>. In this regard, in the present study, we hypothesized that the decreasing in OCT4A and NANOG observed at later passages, could be a consequence of the proliferation of the DPMSC present in the culture. Using CD73 as a differential marker for DPMSC, we found that CD73 expression pattern was inversely proportional to OCT4 and NANOG expression, decreasing from passage 5 to 10 and increasing from 10 to 15. With these results, we hypothesize that the DPMSC population present in the culture, although experiencing a slight decrease until passage 10, is able to increase proliferation from passage 10 to 15. This can directly cause that the total population expresses lower levels of OCT4 and NANOG, although it could also be possible that DPMSC negatively influence the DPPSC pluripotency state. For this reason, we propose, as a future protocol, to perform a negative selection for CD73 at passage 10 of the DPPSC cultures. The selection should not be done before since at early passages CD73<sup>-</sup> cells are more likely to give rise to ectodermal-derived tissues (unpublished results) and, therefore, the absence of CD73<sup>+</sup> cells at early passages could hinder the potential of DPPSC cultures to later differentiate into tissues from the mesodermal or endodermal lineages.

For potential clinical applications and development of therapeutic strategies based on DPPSC administrations, the safety and reliability of these cells need to be studied, especially their genetic stability. This important aspect is also supported by MSC literature inconsistencies, where substantial ambiguities and uncertainties concerning their genetic stability exist (118, 119). Similarly, DPMSC have been reported to exhibit karyotypic abnormalities including polyploidy, aneuploidy and ring chromosomes (120).

## DISCUSSION

In the results here presented, we have demonstrated that DPPSC from several donors show no chromosomal abnormalities when cultured *in vitro* for at least 15 passages and we also confirmed that DPMSC from same donors presented aneuploidy. We hypothesize that these chromosomal instabilities in DPMSC could have some relation with the variability observed in their growth rate. In addition, we propose that the technique here used, sCGH, can be used in stem cell research to determine genetic stability of *in vitro* cultured cells, since sCGH allows the detection of genetic abnormalities that could remain hidden with the current protocols, such as karyotype or FISH techniques (101).

Another concern for clinical application is the high number of cells necessary for stem cell therapies or tissue engineering. Since DPPSC current culturing protocol consists on low seeding density and early splitting at 30% of cell confluence, we wanted to test whether DPPSC could be seeded and split at higher densities, allowing the obtainment of more cells using the same resources. However, in previous studies, we have found that the pluripotency state in DPPSC is not definitive as culture conditions have an impact on it (28). In a similar way, Roobrouck *et al.* (121) showed that MSC, MAPC and mesangioblasts (Mab) change their behaviour when cultured in other conditions, altering not only their gene expression pattern but also their subsequent ability to differentiate into different tissues. Cell density is known to affect cell behaviour, especially regarding expression of embryonic genes. BM-MSCs have been shown to express higher levels of OCT4 and NANOG when cultured at low densities (200 cells/cm<sup>2</sup>) in comparison with cultures at higher densities (1000 and 5000 cells/cm<sup>2</sup>) (122). In the present work, we observed that DPPSC seeded and split at higher densities than the established ones, 500 cells/cm<sup>2</sup> and 50% confluence, were able to maintain their growth rate and their OCT4A, NANOG and LIN28 level expression. However, the level of expression of SOX2 was reduced to half. Thomson *et al.* (123) found that OCT4 and SOX2, proteins that maintain ESC identity, also orchestrate germ layer fate commitment: OCT4 suppresses neural ectodermal differentiation and promotes mesendodermal differentiation and SOX2 inhibits mesendodermal differentiation and promotes neural ectodermal differentiation. Wang *et al.* (124) also demonstrated that, instead of being panrepressors of differentiation, each factor

controls specific cell fates: high levels of OCT4 specify mesendoderm, while low levels of OCT4 induce embryonic ectoderm differentiation; NANOG represses embryonic ectoderm differentiation; and SOX2 represses mesendoderm differentiation. With all this, we propose a new DPPSC culturing protocol in which the cells are cultured at higher seeding and splitting densities (500 cells/cm<sup>2</sup> and 50% confluence) when they are planned to be later differentiated into cells from the mesodermal or endodermal lineages, whereas the cells are continued to be cultured following the current protocol (100 cells/cm<sup>2</sup> and 30% confluence) when they are planned to be differentiated into cells from the ectodermal lineage. In the latter regard, when cells are planned to be differentiated to the ectodermal lineage, DPPSC could also be cultured with a seeding density of 150 cells/cm<sup>2</sup> and split at 50% confluence, since cells in these conditions showed maintenance of SOX2 and LIN28 expression levels and decreased expression of OCT4A and NANOG. Nevertheless, analyses for the differential expression of mesendodermal or ectodermal markers should be performed in the cells cultured in the different conditions. In addition, since *Roobrouck et al. (121)* described that changes in culture conditions not only affect expression pattern of the cells but also their differentiation potential, more studies regarding differentiation capacity need to be performed.

Another indispensable factor for DPPSC clinical application is to establish a GMP protocol that allows the isolation and expansion of the cells with defined culture conditions. This has been already done with hESC (125) and other populations of ASC (126). Current techniques for the expansion of stem cells from the dental pulp require the use of foetal bovine serum and animal-derived components. However, animal-derived reagents stage safety issues in clinical therapy (127). In this study, we have established a DPPSC culture media GMP-approved that replaces foetal bovine serum with human serum (at 10%) and that only contains animal-free components. We have demonstrated that this medium allows the isolation of DPPSC and the subsequent culturing of the cells maintaining their morphology, growth rate and genetic stability for 10 passages. We also observed that DPPSC in this conditions increased expression of OCT4A and NANOG, maintained LIN28 levels and decreased SOX2 expression. We proposed that GMP medium supplemented with 10% human serum can be used to

## DISCUSSION

isolate and cultivate DPPSC when the cells are planned to be later differentiated into endodermal and mesodermal lineages. We then hypothesized whether reducing the percentage of serum in the GMP medium, and thus diminishing the quantity of undefined components in the medium, could maintain (or even improve) the properties of DPPSC observed in the GMP medium. We observed that by reducing the serum quantity from 10% to 1%, we could maintain the morphology and growth rate of the cells for 10 passages. After 5 passages of culture, we observed the same pattern of expression of OCT4A and NANOG as when using serum at 10%, but we observed that SOX2 expression was maintained in the same levels as in DPPSC growth media. After 10 passages, the expression of OCT4A and NANOG was down-regulated compared to cells maintained in GMP medium at 10% HS (and OCT4 expression was also lower than cells in the DPPSC medium), whereas SOX2 was up-regulated 4 times compared to cells cultured in DPPSC medium. As described before by *Thomson et al.* (123) and *Wang et al.* (124) about the ectodermal and mesendodermal differentiation promotion and suppression dynamics of SOX2, OCT4 and NANOG, we propose that GMP medium supplemented with 1% human serum can be used to cultivate DPPSC when the cells are planned to be differentiated into the ectodermal lineage. However, more studies regarding DPPSC expression of mesendodermal and ectodermal markers, as well as DPPSC differentiation capacity using GMP growth media need to be performed, eventually evaluating it in combination with the use of higher seeding and splitting densities. In the case of cells cultured in GMP medium at 0.5% HS for 10 passages, our results showed that this serum concentration is too low to maintain DPPSC characteristics, since cells showed more elongated morphology, an increased population doubling time compared to all the other conditions and a decreased level of all pluripotency-related genes tested compared to the cells cultured in the DPPSC medium after 10 passages.

## **DPPSC MESODERMAL DIFFERENTIATION POTENTIAL**

### **Endothelial differentiation**

In this work, we evaluated the DPPSC and DPMSC endothelial differentiation potential and found that DPPSC show greater potential towards the endothelial lineage.

We have compared different *in vitro* protocols of endothelial differentiation from DPPSC and we have established the optimal differentiation protocol to obtain cells that express typical endothelial markers at mRNA and protein levels, such as VEGFR2, CD31, VE-CAD and vWF, and that exhibit the typical endothelial functionality forming tubular-like structures in the matrigel assay. We observed that these features were higher in differentiation protocols that used indirect co-cultures or conditioned medium from an endothelial cell line, HUVEC, probably due to the fact that HUVEC release growth factors and cytokines that promote DPPSC differentiation.

Further experiments to optimise DPPSC endothelial differentiation would be culturing the undifferentiated cells at 500 cells/cm<sup>2</sup> to verify whether the potential induction of mesendodermal lineages better promotes endothelial differentiation. In the same direction, the undifferentiated cells could also be cultured in the GMP growth medium at 10% serum, since it also showed promising results regarding mesendodermal differentiation (123, 124). When cells are changed to the differentiation medium, FBS should also be replaced with human serum. Derivation of vascular endothelial cells from human embryonic stem cells under GMP conditions has already been reported (128) and could be adopted in our cell system.

Another possibility that can be explored in the future to increase endothelial differentiation from DPPSC is the addition of bone morphogenic protein 4 (BMP-4), an inducer of mesoderm, in the first days of the differentiation. It has been reported that in the presence of BMP-4, OCT4 specifies mesendoderm lineage (124). It has also been published that when human ESC are cultured in the presence of BMP-4, this augments their differentiation towards the endothelial lineage (129).

One possible application of the optimised *in vitro* differentiation protocol is the possibility of co-differentiating DPPSC to more than one cell type at the same time,

## DISCUSSION

such as osteogenic and endothelial co-differentiation. One challenge of particular importance in the research of tissue engineering is to enhance vascularization of tissue-engineered bone (130). It has been reported that culture of BM-MSC together with dermal microvascular endothelial cells improved osteogenesis and vascularization of BM-MSC (131). It has also been published that co-culture of DPSC with EC enhances osteo-/odontogenic and angiogenic potential *in vitro*. (132). The co-differentiation of DPPSC into endothelial and osteogenic lineages, therefore, could improve both differentiations.

After this promising *in vitro* differentiation results, we wanted to analyse the *in vivo* differentiation of DPPSC. For that purpose, we used the full thickness wound healing assay described in *Hendrickx et al.* (133) in which we created a wound in the back of nude mice, treated it with undifferentiated tGFP<sup>+</sup> DPPSC and studied the wound closure, revascularization and matrix organization after 11 days. Regarding wound revascularization, unluckily we could not directly check for the co-expression of tGFP and hCD31 positive cells because we could not find a specific enough antibody that worked in our tissue samples. We then checked for the expression of tGFP and  $\alpha$ SMA, which should stain for the coating of the blood vessels (smooth muscle cells). However, we could not detect any tube-like structures positive for  $\alpha$ SMA surrounding tGFP<sup>+</sup> cells. Nevertheless, DPPSC positive effect on angiogenesis and wound healing can be observed in this study. The area of mouse CD31<sup>+</sup> vessels was slightly non-significantly higher in DPPSC-treated wounds and, more interestingly, the area and percentage of mature vessels which were  $\alpha$ SMA-coated were significantly increased, suggesting that the revascularization process was more advanced in DPPSC-treated wounds. The area and percentage of functional vessels were also found to be increased, although values did not reach statistical significance.

In other studies, stem cells such as BM-MSC have been shown to promote angiogenesis in cellular transplants in two distinct fashions: by the so-called paracrine effect stimulating the formation of blood vessels from the host tissue through secretion of angiogenic factors or by differentiating themselves into endothelial cells and thereby actively participating in the newly formed vascular structures (134). Several studies indicate that DPSC also have angiogenic potential *in vivo*. Intramyocardial injection of

GFP-transduced hDPSC in a rat model of myocardial infarction, resulted in an improvement in cardiac function, reduction of the infarct size and a higher neovascularization in cell-treated animals compared to controls (135). In some other preclinical studies, MSC from the umbilical cord demonstrated an enhancement in a regenerative wound microenvironment. The administration of MSC in an animal model of full thickness excisional wound improved wound healing, in terms of an increased accelerated wound closure and collagen synthesis, due to paracrine effects (136). Consistently, we have also demonstrated that DPPSC promote wound closure and matrix organization in the regenerating wound zone. In this regard, all DPPSC-treated wounds showed complete closure in contrast to only 40% of PBS-treated wounds; and epithelium thickness was significantly thinner in DPPSC-treated wounds, more resembling normal tissue. Regarding wound matrix organization, the central part of DPPSC-treated wounds presented higher percentage of total and organized collagen than the central part of PBS-treated wounds; indeed, the centre of DPPSC-treated wounds presented comparable values to the ones observed in the side part of the wounds of the two different groups, more resembling normal tissue. For all this, DPPSC positive effect on angiogenesis and wound healing can be observed in this study.

We hypothesise that DPPSC could not be observed inside the new vessels formed in the wound regenerating area due to the fact that they may need a longer period to differentiate *in vivo* to the endothelial lineage. *In vitro*, their differentiation takes already 28 days, while other differentiations normally take a shorter period. Nevertheless, the wound healing assay has the limitation of having to be stopped at day 10-11, since the wound is already closed at that point and if it continued to regenerate we could not be able to detect the wound area in the subsequent analyses. One alternative could be the utilization of already differentiated DPPSC to the endothelial lineage for the experiment. This approach, however, may not permit to study other beneficial effects that DPPSC have shown to produce in the wound healing (such as wound closure or matrix organization) and, most of all, it would not permit to observe other *in vivo* differentiation potentials of the cells such as the SMC differentiation. To solve this last



## DISCUSSION

concern, the utilization of two different differentiated or pre-differentiated DPPSC populations (one to EC and the other one to SMC) could be explored.

In the other *in vivo* experiment, after injection of DPPSC in the muscle (tibialis anterior) of two models of dystrophic mice for 20-30 days, we observed direct contribution of DPPSC into endothelial cell types. Indeed, DPPSC were detected in the inner part of vessels in dystrophic *Scid/mdx* mice. In dystrophic *Sgcb-null Rag2-null  $\gamma$ c-null* mice, DPPSC were detected in the inner part of vessel-like structures but, unfortunately, specific techniques for the detection of blood vessels didn't detect the cells in the inner part of the same vessel-like structures. However, cells were often detected in the outside part of vessels or very close to them, suggesting a possible involvement in the angiogenesis of regenerative muscles in *Sgcb-null Rag2-null  $\gamma$ c-null* mice. More tissue samples should be tested to be able to detect DPPSC in the inner part of the vessel-like structures and confirm that they are vessels positive for endothelial markers. Similarly to our results, in a previous study by *Pisciotta et al.* (100), it was observed that pre-differentiated human DPSCs to the myogenic lineage were localized in the endothelium of newly generated vasa after their transplantation in *Scid/mdx* mice, supporting the fact that they participated in the neoangiogenesis of the transplanted muscle.

### Smooth muscle differentiation

Functional blood vessels consist of mainly two distinct cell types, i.e., endothelial cells (lining the inside) and vascular smooth muscle cells (surrounding the EC) (50). In this regard, the potential of DPPSC to differentiate to SMC is extremely important for the *in vivo* application of the cells and their potential capacity to form new functional blood vessels.

In this work, we demonstrate that DPPSC are able to differentiate *in vitro* to SMC. The percentages of differentiated cells that express SMC markers are high and seem to vary between cells from different donors but not from different passages. Therefore, DPPSC are able to maintain their smooth muscle differentiation potential through

passages. Differentiation capacity from other DPPSC populations from different donors will be tested in the near future in order to address inter-individual variability. Nevertheless, in the different populations here studied, no statistical differences were observed regarding the co-expression of the two differentiation markers studied, and a very similar percentage of cells expressed at least one differentiation marker in the same proportion; this, as well as the observed morphological change typical of differentiated cells, demonstrates DPPSC capacity to undergo smooth muscle differentiation. In the case of the tGFP<sup>+</sup> population, we hypothesised that the decreased percentage of differentiated cells can be due to alterations in this population as a consequence of the transduction of the tGFP lentiviral vector, due to the stress caused by the procedure itself or due to the integration of the tGFP lentiviral vector in the genome of the cells causing disruptions of genes that are necessary or promote this differentiation.

Many years ago, studies from *Bockman et al.* (137) and *Kirby et al.* (138) suggested that, during embryonic development, ectomesenchymal cells in the cranial neural folds are competent to form SMC. Giving the neuroectodermal origin of DPPSC, this may explain their high capacity to undergo SMC differentiation.

As further experiments, it would also be interesting to cultivate the undifferentiated cells using GMP growth medium supplemented with 10% serum and then change to differentiation medium containing human serum instead of horse serum. Another possibility could be culturing the undifferentiated cells at higher densities (500 cells/cm<sup>2</sup> seeding density and 50% splitting confluence) to see whether it can promote even more SMC differentiation.

In the *in vivo* experiments here presented, DPPSC have shown to differentiate into SMC that surround blood vessels in all the murine models used. In addition, in the wound healing assay, a significant increase in the percentage and area of mature vessels with  $\alpha$ SMA coating was found in the regenerating wound area. DPPSC can be responsible for this either by direct differentiation (as DPPSC were localized in the outer part of vessels expressing  $\alpha$ SMA SMC marker) or by paracrine effect (134). Observing the inter-individual variability in smooth muscle differentiation capacity *in*

## DISCUSSION

*vitro*, we can hypothesise that using another transduced DPPSC population from another donor (with higher smooth muscle differentiation potential *in vitro*) could have led to better *in vivo* results, but cells from other donors were not so successfully transduced with the lentivirus vector containing tGFP, and that is why they were not used for the *in vivo* experiments. For future experiments, more lentiviral transductions and new *in vivo* experiments can be performed in this regard.

### **Skeletal muscle differentiation**

In the present study, we also evaluated the myogenic potential of DPPSC *in vitro* and *in vivo*.

In the *in vitro* differentiation, we aimed to determine the optimal conditions for achieving the myogenic commitment testing different protocols. The results from co-culture experiments demonstrate that DPPSC are capable of fusing with mouse C2C12 cells generating hybrid myotubes after 5 days in differentiation conditions. The myogenic potential of DPPSC at passage 5 and 10 was tested, showing comparable results. DPPSC populations from 3 different donors were used to test DPPSC myogenic potential and all of them showed similar capacity. We also observed that the presence of DPPSC contributes to a better differentiation potential of C2C12 cells, revealed by the increased fusion index and the number of MyHC<sup>+</sup> myotubes.

DPPSC cultures subjected for 7 days to different myogenic differentiation protocols did not clearly show the ability to fuse, although some multinucleated MyHC<sup>+</sup> DPPSC were detected upon serum starvation. In the case of conditioned media, DPPSC showed changes in cell morphology and became more elongated resembling myotubes, although the high density of cells prevented a clear localization of human nuclei. In this regard, the co-cultures system seems to clearly promote the ability of DPPSC to differentiate to skeletal muscle *in vitro*, probably due to released paracrine factors by C2C12 cells.

In a previous study using DPMSC, cells were also able to fuse with C2C12 cells forming hybrid myotubes after 14 days of myogenic induction (139). Similarly to our results, DPMSC were also unable to form multinucleated myotubes when differentiated

alone or in conditioned medium for 14 days. However, at day 28 of differentiation, DPMSCs with or without conditioned media generated multinucleated myotubes under the treatment of 5-Azacytidine, a potent demethylating agent. For further experiments, strategies to optimise DPPSC myogenic differentiation *in vitro* could be the extension of the differentiation time from 7 days up to 28 days and the use of demethylating agents. As in the other mesodermal lineage differentiations, it would also be interesting to cultivate the undifferentiated cells using GMP growth medium supplemented with 10% serum and using higher densities (500 cells/cm<sup>2</sup> seeding density and 50% splitting confluence) to induce mesendodermal lineages.

Two different murine models of muscular dystrophies were used in this study to test the *in vivo* myogenic potential of DPPSC: *Scid/mdx mice*, a model for DMD (the most severe and common muscular dystrophy), and *Sgcb-null Rag2-null γc-null mice*, a model for limb-girdle muscular dystrophy type 2E. Our results showed that DPPSC can contribute to regenerate muscle fibres *in vivo* in intramuscularly injected dystrophic mice. In fact, human nuclei were detected inside the centre-nucleated muscle fibres. We also detected the presence of beta-sarcoglycan positive fibres in injected *Sgcb-null Rag2-null γc-null mice* and an increased proportion of dystrophin positive myofibers in injected *Scid/mdx* compared to the controls (dystrophic mdx muscles present rare dystrophin positive fibres (140)). Serial sections showed the presence of DPPSC nuclei in the area of dystrophin positive fibers, suggesting a direct contribution of DPPSC to restore the missing protein in the injected dystrophic mice.

In addition, DPPSC were also found, among other locations, in the basal lamina close to the fibres, where satellite cells (the adult myogenic progenitor cells) reside (100, 141-143). In this regard, we hypothesized that DPPSC situated in the basal lamina could potentially act as satellite cells and help keeping up with the muscle fibre regeneration for longer periods of time. However, this aspect needs further investigation.

Other studies showed that MSC possessed the capacity to differentiate, at least in part, into muscle lineages (144-146) and in *Pisciotta et al.* (100), pre-differentiated DPMSCs regenerated dystrophin-positive fibres in treated *Scid/mdx mice* with limited capacity.

## DISCUSSION

However, in the present study, for the first time we provided evidence that DPPSC also contribute to myogenic regeneration when transplanted in two different murine models, the widely studied *mdx* mice and in a more severe dystrophic animal model, *Sgcb-null Rag2-null  $\gamma$ C-null* mice (147).

In future experiments, we propose to study the DPPSC effects in dystrophic mice when the cells are injected after a short-term myogenic induction. This approach, however, would not permit to take advantage of the angiogenic effect of DPPSC. In this regard, simultaneous injections of undifferentiated and pre-differentiated DPPSC could also be explored.

Taken together, our results showed that DPPSC own mesodermal differentiation potential *in vitro* and *in vivo*, similar to DPMSC; however, they are superior compared to DPMSC in terms of population doubling time, genetic stability and expansion ability, tested also in GMP conditions.

# **CONCLUSIONS**

---



1. DPPSC have better population doubling time than DPMSC: they divide faster and the average division rate is stable at least up to 15 passages.
2. DPPSC show no chromosomal abnormalities when cultured *in vitro* for at least 15 passages confirmed in several DPPSC populations isolated from 10 different donors.
3. DPPSC have pluripotency potential. They express the pluripotency marker OCT4A, confirmed by qRT-PCR analysis using specific primers that do not detect OCT4 isoforms or pseudogenes not involved in pluripotency.
4. The pluripotency capacity of DPPSC changes through cell passages. Pluripotency markers OCT4A and NANOG are expressed at least up to 15 passages, with the highest expression at passage 10.
5. Expression of CD73 through passages in the DPPSC population is inversely proportional to the expression of the pluripotency markers OCT4A and NANOG.
6. DPPSC pluripotency capacity is influenced by culture conditions such as the cellular seeding density and splitting confluence. OCT4A and NANOG are up-regulated when cultured at higher densities (500 cells/cm<sup>2</sup> and 50% confluence), while SOX2 is down-regulated.
7. DPPSC can be cultured in a GMP-approved growth medium that maintains the pluripotency capacity of the cells and facilitates their future application in regenerative medicine. Using GMP growth medium supplemented with 10% serum, OCT4A and NANOG are up-regulated, whereas SOX2 is down-regulated. Using GMP growth medium supplemented with 1% serum, SOX2 and NANOG are up-regulated, whereas OCT4A is down-regulated at later passages.
8. DPPSC can differentiate into endothelial cells *in vitro* that express typical endothelial markers and functionality.
9. DPPSC can differentiate into endothelial cells *in vivo* present in the inner layer of vessels in the skeletal muscle of dystrophic mice *Scid/mdx*. DPPSC seem to also be able to differentiate to endothelial cells present in the inner layer of vessel-like structures in the skeletal muscle of dystrophic mice *Sgcb-null Rag2-null γc-null*.



## CONCLUSIONS

10. DPPSC can differentiate into smooth muscle cells *in vitro* that present typical morphology and smooth muscle markers expression. Their differentiation potential is maintained through passages until at least passage 10.
11. DPPSC can differentiate into smooth muscle cells *in vivo* in the regenerating wound area of *Foxn1* mice and in dystrophic skeletal muscles of *Scid/mdx* and *Sgcb-null Rag2-null  $\gamma$ C-null* mice.
12. DPPSC positively contribute to wound closure, revascularization and matrix organization in *Foxn1* mice subjected to a wound healing assay.
13. DPPSC can differentiate into skeletal muscle cells *in vitro* when co-cultured with C2C12 cells. DPPSC are able to fuse with C2C12 cells and the hybrid multinucleated cells express typical skeletal muscle markers. DPPSC myogenic potential is maintained until at least passage 10.
14. DPPSC can differentiate into skeletal muscle cells *in vivo*. DPPSC can fuse and contribute to muscle fibre regeneration in a mouse model of Duchenne Muscular Dystrophy (*Scid/mdx*) and they seem to partially restore the dystrophin protein. DPPSC can also fuse and contribute to muscle fibre regeneration in a mouse model of Limb-Girdle Muscular Dystrophy Type 2E (*Sgcb-null Rag2-null  $\gamma$ C-null*) and they seem to partially restore the beta-sarcoglycan protein.

# **BIBLIOGRAPHY**

---



1. Fuchs E, Segre JA. Stem cells: a new lease on life. *Cell*. 2000;100(1):143-55.
2. Bhattacharya N, Stubblefield PG. *Regenerative Medicine: Using Non-Fetal Sources of Stem Cells*: Springer; 2012 Nov 7.
3. Mimeault M, Hauke R, Batra SK. Stem cells: a revolution in therapeutics-recent advances in stem cell biology and their therapeutic applications in regenerative medicine and cancer therapies. *Clinical pharmacology and therapeutics*. 2007;82(3):252-64.
4. Medvedev SP, Shevchenko AI, Zakian SM. Induced Pluripotent Stem Cells: Problems and Advantages when Applying them in Regenerative Medicine. *Acta naturae*. 2010;2(2):18-28.
5. Takahashi K, Tanabe K, Ohnuki M, Narita M, Ichisaka T, Tomoda K, et al. Induction of pluripotent stem cells from adult human fibroblasts by defined factors. *Cell*. 2007;131(5):861-72.
6. Mimeault M, Batra SK. Concise review: recent advances on the significance of stem cells in tissue regeneration and cancer therapies. *Stem cells*. 2006;24(11):2319-45.
7. Baldwin T. Morality and human embryo research. Introduction to the Talking Point on morality and human embryo research. *EMBO Reports*. 2009;10(4):299-300.
8. Richards M, Tan SP, Tan JH, Chan WK, Bongso A. The transcriptome profile of human embryonic stem cells as defined by SAGE. *Stem cells*. 2004;22(1):51-64.
9. Yu J, Vodyanik MA, Smuga-Otto K, Antosiewicz-Bourget J, Frane JL, Tian S, et al. Induced pluripotent stem cell lines derived from human somatic cells. *Science (New York, NY)*. 2007;318(5858):1917-20.
10. Watts C, McConkey H, Anderson L, Caldwell M. Anatomical perspectives on adult neural stem cells. *Journal of anatomy*. 2005;207(3):197-208.
11. Kim CF, Jackson EL, Woolfenden AE, Lawrence S, Babar I, Vogel S, et al. Identification of bronchioalveolar stem cells in normal lung and lung cancer. *Cell*. 2005;121(6):823-35.

BIBLIOGRAPHY

12. Leri A, Kajstura J, Anversa P. Cardiac stem cells and mechanisms of myocardial regeneration. *Physiological reviews*. 2005;85(4):1373-416.
13. Schmelzer E, Zhang L, Bruce A, Wauthier E, Ludlow J, Yao HL, et al. Human hepatic stem cells from fetal and postnatal donors. *The Journal of experimental medicine*. 2007;204(8):1973-87.
14. Tumber T, Guasch G, Greco V, Blanpain C, Lowry WE, Rendl M, et al. Defining the epithelial stem cell niche in skin. *Science (New York, NY)*. 2004;303(5656):359-63.
15. Lavker RM, Tseng SC, Sun TT. Corneal epithelial stem cells at the limbus: looking at some old problems from a new angle. *Experimental eye research*. 2004;78(3):433-46.
16. Fuchs E, Tumber T, Guasch G. Socializing with the neighbors: stem cells and their niche. *Cell*. 2004;116(6):769-78.
17. Friedenstein AJ, Petrakova KV, Kurolesova AI, Frolova GP. Heterotopic of bone marrow. Analysis of precursor cells for osteogenic and hematopoietic tissues. *Transplantation*. 1968;6(2):230-47.
18. Zuk PA, Zhu M, Ashjian P, De Ugarte DA, Huang JI, Mizuno H, et al. Human adipose tissue is a source of multipotent stem cells. *Molecular biology of the cell*. 2002;13(12):4279-95.
19. In 't Anker PS, Scherjon SA, Kleijburg-van der Keur C, de Groot-Swings GM, Claas FH, Fibbe WE, et al. Isolation of mesenchymal stem cells of fetal or maternal origin from human placenta. *Stem cells*. 2004;22(7):1338-45.
20. Sharma RR, Pollock K, Hubel A, McKenna D. Mesenchymal stem or stromal cells: a review of clinical applications and manufacturing practices. *Transfusion*. 2014;54(5):1418-37.
21. Gronthos S, Mankani M, Brahimi J, Robey PG, Shi S. Postnatal human dental pulp stem cells (DPSCs) in vitro and in vivo. *Proceedings of the National Academy of Sciences of the United States of America*. 2000;97(25):13625-30.

22. Miura M, Gronthos S, Zhao M, Lu B, Fisher LW, Robey PG, et al. SHED: stem cells from human exfoliated deciduous teeth. *Proceedings of the National Academy of Sciences of the United States of America*. 2003;100(10):5807-12.
23. Sonoyama W, Liu Y, Yamaza T, Tuan RS, Wang S, Shi S, et al. Characterization of the apical papilla and its residing stem cells from human immature permanent teeth: a pilot study. *Journal of endodontics*. 2008;34(2):166-71.
24. Seo BM, Miura M, Gronthos S, Bartold PM, Batouli S, Brahim J, et al. Investigation of multipotent postnatal stem cells from human periodontal ligament. *Lancet*. 2004;364(9429):149-55.
25. Vollner F, Driemel O, Reichert T, Morsczeck C. Isolation and characterization of dental follicle precursor cells (DFPCs). *Journal of stem cells & regenerative medicine*. 2007;2(1):130.
26. Davies OG, Cooper PR, Shelton RM, Smith AJ, Scheven BA. A comparison of the in vitro mineralisation and dentinogenic potential of mesenchymal stem cells derived from adipose tissue, bone marrow and dental pulp. *Journal of bone and mineral metabolism*. 2014.
27. Sloan AJ, Waddington RJ. Dental pulp stem cells: what, where, how? *International journal of paediatric dentistry / the British Paedodontic Society [and] the International Association of Dentistry for Children*. 2009;19(1):61-70.
28. Atari M, Gil-Recio C, Fabregat M, Garcia-Fernandez D, Barajas M, Carrasco MA, et al. Dental pulp of the third molar: a new source of pluripotent-like stem cells. *Journal of cell science*. 2012;125(Pt 14):3343-56.
29. Atari M, Barajas M, Hernandez-Alfaro F, Gil C, Fabregat M, Ferrer Padro E, et al. Isolation of pluripotent stem cells from human third molar dental pulp. *Histology and histopathology*. 2011;26(8):1057-70.
30. Atari M, Caballe-Serrano J, Gil-Recio C, Giner-Delgado C, Martinez-Sarra E, Garcia-Fernandez DA, et al. The enhancement of osteogenesis through the use of dental pulp pluripotent stem cells in 3D. *Bone*. 2012;50(4):930-41.

## BIBLIOGRAPHY

31. Kucia M, Reza R, Campbell FR, Zuba-Surma E, Majka M, Ratajczak J, et al. A population of very small embryonic-like (VSEL) CXCR4(+)SSEA-1(+)Oct-4+ stem cells identified in adult bone marrow. *Leukemia*. 2006;20(5):857-69.
32. Jiang Y, Jahagirdar BN, Reinhardt RL, Schwartz RE, Keene CD, Ortiz-Gonzalez XR, et al. Pluripotency of mesenchymal stem cells derived from adult marrow. *Nature*. 2002;418(6893):41-9.
33. Petrini M, Pacini S, Trombi L, Fazzi R, Montali M, Ikehara S, et al. Identification and purification of mesodermal progenitor cells from human adult bone marrow. *Stem cells and development*. 2009;18(6):857-66.
34. D'Ippolito G, Diabira S, Howard GA, Menei P, Roos BA, Schiller PC. Marrow-isolated adult multilineage inducible (MIAMI) cells, a unique population of postnatal young and old human cells with extensive expansion and differentiation potential. *Journal of cell science*. 2004;117(Pt 14):2971-81.
35. Benton G, George J, Kleinman HK, Arnaoutova IP. Advancing science and technology via 3D culture on basement membrane matrix. *Journal of cellular physiology*. 2009;221(1):18-25.
36. Maltman DJ, Przyborski SA. Developments in three-dimensional cell culture technology aimed at improving the accuracy of in vitro analyses. *Biochemical Society transactions*. 2010;38(4):1072-5.
37. Mason C, Dunnill P. A brief definition of regenerative medicine. *Regenerative medicine*. 2008;3(1):1-5.
38. Yannas IV. *Tissue and Organ Regeneration in Adults*: Springer Publishing; 2007.
39. Bajada S, Mazakova I, Ashton BA, J.B. R, N. A. *Stem Cells in Regenerative Medicine*. *Topics in Tissue Engineering*. 4: N Ashammakhi, R Reis, & F Chiellini.
40. Greenwood HL, Thorsteinsdottir H, Perry G, Renihan J, Singer PA, Daar AS. Regenerative medicine: new opportunities for developing countries. *J Biotechnol*. 2006;8(1-2):60-77.

41. Muneoka K, Allan CH, Yang X, Lee J, Han M. Mammalian regeneration and regenerative medicine. Birth defects research Part C, Embryo today : reviews. 2008;84(4):265-80.
42. Riazi AM, Kwon SY, Stanford WL. Stem cell sources for regenerative medicine. Methods in molecular biology. 2009;482:55-90.
43. Rotter N, Oder J, Schlenke P, Lindner U, Bohrsen F, Kramer J, et al. Isolation and characterization of adult stem cells from human salivary glands. Stem cells and development. 2008;17(3):509-18.
44. Patsch C, Challet-Meylan L, Thoma EC, Urich E, Heckel T, O'Sullivan JF, et al. Generation of vascular endothelial and smooth muscle cells from human pluripotent stem cells. Nature cell biology. 2015;17(8):994-1003.
45. Majesky MW. Developmental basis of vascular smooth muscle diversity. Arteriosclerosis, thrombosis, and vascular biology. 2007;27(6):1248-58.
46. Tortora G, Derrickson B. Chapter 21: The cardiovascular system: Blood vessels and hemodynamics. Principles of Anatomy and Physiology: John Wiley & Sons, Inc.; 2009.
47. Luo Z, Wang G, Wang W, Xiao Q, Xu Q. Signalling pathways that regulate endothelial differentiation from stem cells. Frontiers in bioscience (Landmark edition). 2011;16:472-85.
48. Grotendorst GR, Seppa HE, Kleinman HK, Martin GR. Attachment of smooth muscle cells to collagen and their migration toward platelet-derived growth factor. Proceedings of the National Academy of Sciences of the United States of America. 1981;78(6):3669-72.
49. Hirschi KK, Majesky MW. Smooth muscle stem cells. The anatomical record Part A, Discoveries in molecular, cellular, and evolutionary biology. 2004;276(1):22-33.
50. Luttun A, Ross JJ, Verfaillie C, Aranguren XL, Prosper F. Differentiation of multipotent adult progenitor cells into functional endothelial and smooth muscle cells.



BIBLIOGRAPHY

Current protocols in immunology / edited by John E Coligan [et al]. 2006;Chapter 22:Unit 22F.9.

51. Carmeliet P. Angiogenesis in life, disease and medicine. *Nature*. 2005;438(7070):932-6.

52. Kane NM, Meloni M, Spencer HL, Craig MA, Strehl R, Milligan G, et al. Derivation of endothelial cells from human embryonic stem cells by directed differentiation: analysis of microRNA and angiogenesis in vitro and in vivo. *Arteriosclerosis, thrombosis, and vascular biology*. 2010;30(7):1389-97.

53. Bronckaers A, Hilkens P, Fanton Y, Struys T, Gervois P, Politis C, et al. Angiogenic properties of human dental pulp stem cells. *PloS one*. 2013;8(8):e71104.

54. Katz B. The terminations of the afferent nerve fibre in the muscle spindle of the frog. *Philos Trans Royal Soc Lond [Biol]*. 1961;243:221-40.

55. Mauro A. Satellite cell of skeletal muscle fibers. *The Journal of biophysical and biochemical cytology*. 1961;9:493-5.

56. Hawke TJ, Garry DJ. Myogenic satellite cells: physiology to molecular biology. *Journal of applied physiology (Bethesda, Md : 1985)*. 2001;91(2):534-51.

57. Yablonka-Reuveni Z, Day K. Chapter 11: Skeletal muscle stem cells in the spotlight: the satellite cell. *Regenerating the Heart: Stem Cells and the Cardiovascular System* Springer, Humana Press; 2011. p. 173-200.

58. Lodish H, Berk A, Zipursky SL, Matsudaira P, Baltimore D, Darnell J. *Molecular Cell Biology*: W. H. Freeman; 2013.

59. Watanabe M, Shin'oka T, Tohyama S, Hibino N, Konuma T, Matsumura G, et al. Tissue-engineered vascular autograft: inferior vena cava replacement in a dog model. *Tissue engineering*. 2001;7(4):429-39.

60. Meinhart JG, Deutsch M, Fischlein T, Howanietz N, Froschl A, Zilla P. Clinical autologous in vitro endothelialization of 153 infrainguinal ePTFE grafts. *The Annals of thoracic surgery*. 2001;71(5 Suppl):S327-31.

61. Seifalian AM, Tiwari A, Hamilton G, Salacinski HJ. Improving the clinical patency of prosthetic vascular and coronary bypass grafts: the role of seeding and tissue engineering. *Artificial organs*. 2002;26(4):307-20.
62. James D, Nam HS, Seandel M, Nolan D, Janovitz T, Tomishima M, et al. Expansion and maintenance of human embryonic stem cell-derived endothelial cells by TGFbeta inhibition is Id1 dependent. *Nature biotechnology*. 2010;28(2):161-6.
63. Levenberg S, Golub JS, Amit M, Itskovitz-Eldor J, Langer R. Endothelial cells derived from human embryonic stem cells. *Proceedings of the National Academy of Sciences of the United States of America*. 2002;99(7):4391-6.
64. Vodyanik MA, Bork JA, Thomson JA, Slukvin, II. Human embryonic stem cell-derived CD34+ cells: efficient production in the coculture with OP9 stromal cells and analysis of lymphohematopoietic potential. *Blood*. 2005;105(2):617-26.
65. Li Z, Suzuki Y, Huang M, Cao F, Xie X, Connolly AJ, et al. Comparison of reporter gene and iron particle labeling for tracking fate of human embryonic stem cells and differentiated endothelial cells in living subjects. *Stem cells*. 2008;26(4):864-73.
66. Wang H, Charles PC, Wu Y, Ren R, Pi X, Moser M, et al. Gene expression profile signatures indicate a role for Wnt signaling in endothelial commitment from embryonic stem cells. *Circulation research*. 2006;98(10):1331-9.
67. Wang ZZ, Au P, Chen T, Shao Y, Daheron LM, Bai H, et al. Endothelial cells derived from human embryonic stem cells form durable blood vessels in vivo. *Nature biotechnology*. 2007;25(3):317-8.
68. Sumi T, Tsuneyoshi N, Nakatsuji N, Suemori H. Defining early lineage specification of human embryonic stem cells by the orchestrated balance of canonical Wnt/beta-catenin, Activin/Nodal and BMP signaling. *Development (Cambridge, England)*. 2008;135(17):2969-79.
69. Inman GJ, Nicolas FJ, Callahan JF, Harling JD, Gaster LM, Reith AD, et al. SB-431542 is a potent and specific inhibitor of transforming growth factor-beta superfamily type I activin receptor-like kinase (ALK) receptors ALK4, ALK5, and ALK7. *Molecular pharmacology*. 2002;62(1):65-74.

BIBLIOGRAPHY

70. Orlova VV, Drabsch Y, Freund C, Petrus-Reurer S, van den Hil FE, Muenthaisong S, et al. Functionality of endothelial cells and pericytes from human pluripotent stem cells demonstrated in cultured vascular plexus and zebrafish xenografts. *Arteriosclerosis, thrombosis, and vascular biology*. 2014;34(1):177-86.
71. Colazzo F, Chester AH, Taylor PM, Yacoub MH. Induction of mesenchymal to endothelial transformation of adipose-derived stem cells. *The Journal of heart valve disease*. 2010;19(6):736-44.
72. Konno M, Hamazaki TS, Fukuda S, Tokuhara M, Uchiyama H, Okazawa H, et al. Efficiently differentiating vascular endothelial cells from adipose tissue-derived mesenchymal stem cells in serum-free culture. *Biochemical and biophysical research communications*. 2010;400(4):461-5.
73. Caplan AI. Review: mesenchymal stem cells: cell-based reconstructive therapy in orthopedics. *Tissue engineering*. 2005;11(7-8):1198-211.
74. Oswald J, Boxberger S, Jorgensen B, Feldmann S, Ehninger G, Bornhauser M, et al. Mesenchymal stem cells can be differentiated into endothelial cells in vitro. *Stem cells*. 2004;22(3):377-84.
75. Pittenger MF, Mackay AM, Beck SC, Jaiswal RK, Douglas R, Mosca JD, et al. Multilineage potential of adult human mesenchymal stem cells. *Science (New York, NY)*. 1999;284(5411):143-7.
76. Fischer LJ, McIlhenny S, Tulenko T, Golesorkhi N, Zhang P, Larson R, et al. Endothelial differentiation of adipose-derived stem cells: effects of endothelial cell growth supplement and shear force. *The Journal of surgical research*. 2009;152(1):157-66.
77. Culmes M, Eckstein HH, Burgkart R, Nussler AK, Guenther M, Wagner E, et al. Endothelial differentiation of adipose-derived mesenchymal stem cells is improved by epigenetic modifying drug BIX-01294. *European journal of cell biology*. 2013;92(2):70-9.

78. Heeschen C, Chang E, Aicher A, Cooke JP. Endothelial progenitor cells participate in nicotine-mediated angiogenesis. *Journal of the American College of Cardiology*. 2006;48(12):2553-60.
79. Huang PP, Yang XF, Li SZ, Wen JC, Zhang Y, Han ZC. Randomised comparison of G-CSF-mobilized peripheral blood mononuclear cells versus bone marrow-mononuclear cells for the treatment of patients with lower limb arteriosclerosis obliterans. *Thrombosis and haemostasis*. 2007;98(6):1335-42.
80. Li Z, Han Z, Wu JC. Transplantation of human embryonic stem cell-derived endothelial cells for vascular diseases. *Journal of cellular biochemistry*. 2009;106(2):194-9.
81. Yang C, Zhang ZH, Li ZJ, Yang RC, Qian GQ, Han ZC. Enhancement of neovascularization with cord blood CD133+ cell-derived endothelial progenitor cell transplantation. *Thrombosis and haemostasis*. 2004;91(6):1202-12.
82. Li Z, Wilson KD, Smith B, Kraft DL, Jia F, Huang M, et al. Functional and transcriptional characterization of human embryonic stem cell-derived endothelial cells for treatment of myocardial infarction. *PloS one*. 2009;4(12):e8443.
83. Tepper OM, Galiano RD, Capla JM, Kalka C, Gagne PJ, Jacobowitz GR, et al. Human endothelial progenitor cells from type II diabetics exhibit impaired proliferation, adhesion, and incorporation into vascular structures. *Circulation*. 2002;106(22):2781-6.
84. Owens GK, Kumar MS, Wamhoff BR. Molecular regulation of vascular smooth muscle cell differentiation in development and disease. *Physiological reviews*. 2004;84(3):767-801.
85. Shi N, Chen SY. From nerve to blood vessel: a new role of Olfm2 in smooth muscle differentiation from human embryonic stem cell-derived mesenchymal cells. *Journal of biomedical research*. 2015;29(4):261-3.
86. Xie C, Ritchie RP, Huang H, Zhang J, Chen YE. Smooth muscle cell differentiation in vitro: models and underlying molecular mechanisms. *Arteriosclerosis, thrombosis, and vascular biology*. 2011;31(7):1485-94.

BIBLIOGRAPHY

87. Mahoney WM, Schwartz SM. Defining smooth muscle cells and smooth muscle injury. *The Journal of clinical investigation*. 2005;115(2):221-4.
88. Yoshida T, Owens G. Molecular determinants of vascular smooth muscle cell diversity. *Circulation research*. 2005;96(3):280-91.
89. Miller RG, Sharma KR, Pavlath GK, Gussoni E, Mynhier M, Lanctot AM, et al. Myoblast implantation in Duchenne muscular dystrophy: the San Francisco study. *Muscle & nerve*. 1997;20(4):469-78.
90. Skuk D, Goulet M, Tremblay JP. Use of repeating dispensers to increase the efficiency of the intramuscular myogenic cell injection procedure. *Cell transplantation*. 2006;15(7):659-63.
91. Fan Y, Maley M, Beilharz M, Grounds M. Rapid death of injected myoblasts in myoblast transfer therapy. *Muscle & nerve*. 1996;19(7):853-60.
92. Guerette B, Skuk D, Celestin F, Huard C, Tardif F, Asselin I, et al. Prevention by anti-LFA-1 of acute myoblast death following transplantation. *Journal of immunology (Baltimore, Md : 1950)*. 1997;159(5):2522-31.
93. Bongso A, Lee E. *Stem Cells: From Bench to Bedside*. Stem cells: their definition, classification and sources. Singapur2005.
94. Meirelles Lda S, Nardi NB. Methodology, biology and clinical applications of mesenchymal stem cells. *Frontiers in bioscience (Landmark edition)*. 2009;14:4281-98.
95. Keating A. Mesenchymal stromal cells: new directions. *Cell stem cell*. 2012;10(6):709-16.
96. Uccelli A, Benvenuto F, Laroni A, Giunti D. Neuroprotective features of mesenchymal stem cells. *Best practice & research Clinical haematology*. 2011;24(1):59-64.
97. Meng J, Adkin CF, Arechavala-Gomez V, Boldrin L, Muntoni F, Morgan JE. The contribution of human synovial stem cells to skeletal muscle regeneration. *Neuromuscular disorders : NMD*. 2010;20(1):6-15.

98. Lin H, Otsu M, Nakauchi H. Stem cell therapy: an exercise in patience and prudence. *Philos Trans R Soc Lond B Biol Sci.* 2013;368(1609).
99. Ra JC, Shin IS, Kim SH, Kang SK, Kang BC, Lee HY, et al. Safety of intravenous infusion of human adipose tissue-derived mesenchymal stem cells in animals and humans. *Stem cells and development.* 2011;20(8):1297-308.
100. Pisciotta A, Riccio M, Carnevale G, Lu A, De Biasi S, Gibellini L, et al. Stem cells isolated from human dental pulp and amniotic fluid improve skeletal muscle histopathology in mdx/SCID mice. *Stem cell research & therapy.* 2015;6:156.
101. Rius M, Obradors A, Daina G, Cuzzi J, Marques L, Calderon G, et al. Reliability of short comparative genomic hybridization in fibroblasts and blastomeres for a comprehensive aneuploidy screening: first clinical application. *Human reproduction.* 2010;25(7):1824-35.
102. Rodriguez-Lozano FJ, Bueno C, Insausti CL, Meseguer L, Ramirez MC, Blanquer M, et al. Mesenchymal stem cells derived from dental tissues. *International endodontic journal.* 2011;44(9):800-6.
103. Laino G, d'Aquino R, Graziano A, Lanza V, Carinci F, Naro F, et al. A new population of human adult dental pulp stem cells: a useful source of living autologous fibrous bone tissue (LAB). *Journal of bone and mineral research : the official journal of the American Society for Bone and Mineral Research.* 2005;20(8):1394-402.
104. Gil-Recio C. Obtaining hepatocyte-like cells from dental pulp pluripotent-like stem cells. Barcelona: UIC Barcelona; 2015.
105. Cohen S, Itskovitz-Eldor J, Leshanski L. Tissue engineering and regenerative medicine. In: Lanza R, Klimanskaya I, editors. *Stem Cell Tools and Other Experimental Protocols (Methods in Enzymology).* 420: Academic Press (Elsevier); 2006.
106. Vaananen HK. Mesenchymal stem cells. *Annals of medicine.* 2005;37(7):469-79.

BIBLIOGRAPHY

107. Park YB, Kim YY, Oh SK, Chung SG, Ku SY, Kim SH, et al. Alterations of proliferative and differentiation potentials of human embryonic stem cells during long-term culture. *Experimental & Molecular Medicine*. 2008;40(1):98-108.
108. Suchanek J, Soukup T, Ivancakova R, Karbanova J, Hubkova V, Pytlík R, et al. Human dental pulp stem cells--isolation and long term cultivation. *Acta medica (Hradec Kralove) / Universitas Carolina, Facultas Medica Hradec Kralove*. 2007;50(3):195-201.
109. Chambers I, Tomlinson SR. The transcriptional foundation of pluripotency. *Development (Cambridge, England)*. 2009;136(14):2311-22.
110. Xu G, Yang L, Zhang W, Wei X. All the Tested Human Somatic Cells Express Both Oct4A and Its Pseudogenes but Express Oct4A at Much Lower Levels Compared with Its Pseudogenes and Human Embryonic Stem Cells. *Stem cells and development*. 2015;24(13):1546-57.
111. Cauffman G, Liebaers I, Van Steirteghem A, Van de Velde H. POU5F1 isoforms show different expression patterns in human embryonic stem cells and preimplantation embryos. *Stem cells*. 2006;24(12):2685-91.
112. Lee J, Kim HK, Rho JY, Han YM, Kim J. The human OCT-4 isoforms differ in their ability to confer self-renewal. *The Journal of biological chemistry*. 2006;281(44):33554-65.
113. Wang X, Dai J. Concise review: isoforms of OCT4 contribute to the confusing diversity in stem cell biology. *Stem cells*. 2010;28(5):885-93.
114. Wang X, Zhao Y, Xiao Z, Chen B, Wei Z, Wang B, et al. Alternative translation of OCT4 by an internal ribosome entry site and its novel function in stress response. *Stem cells*. 2009;27(6):1265-75.
115. Gao Y, Wei J, Han J, Wang X, Su G, Zhao Y, et al. The novel function of OCT4B isoform-265 in genotoxic stress. *Stem cells*. 2012;30(4):665-72.
116. Seo KW, Lee SR, Bhandari DR, Roh KH, Park SB, So AY, et al. OCT4A contributes to the stemness and multi-potency of human umbilical cord blood-derived

multipotent stem cells (hUCB-MSCs). *Biochemical and biophysical research communications*. 2009;384(1):120-5.

117. Pera MF, Reubinoff B, Trounson A. Human embryonic stem cells. *Journal of cell science*. 2000;113 ( Pt 1):5-10.

118. Dahl JA, Duggal S, Coulston N, Millar D, Melki J, Shahdadfar A, et al. Genetic and epigenetic instability of human bone marrow mesenchymal stem cells expanded in autologous serum or fetal bovine serum. *The International journal of developmental biology*. 2008;52(8):1033-42.

119. Sensebe L, Tarte K, Galipeau J, Krampera M, Martin I, Phinney DG, et al. Limited acquisition of chromosomal aberrations in human adult mesenchymal stromal cells. *Cell stem cell*. 2012;10(1):9-10; author reply -1.

120. Duailibi MT, Kulikowski LD, Duailibi SE, Lipay MV, Melaragno MI, Ferreira LM, et al. Cytogenetic instability of dental pulp stem cell lines. *Journal of molecular histology*. 2012;43(1):89-94.

121. Roobrouck VD, Clavel C, Jacobs SA, Ulloa-Montoya F, Crippa S, Sohni A, et al. Differentiation potential of human postnatal mesenchymal stem cells, mesoangioblasts, and multipotent adult progenitor cells reflected in their transcriptome and partially influenced by the culture conditions. *Stem cells*. 2011;29(5):871-82.

122. Lee MW, Kim DS, Yoo KH, Kim HR, Jang IK, Lee JH, et al. Human bone marrow-derived mesenchymal stem cell gene expression patterns vary with culture conditions. *Blood research*. 2013;48(2):107-14.

123. Thomson M, Liu SJ, Zou LN, Smith Z, Meissner A, Ramanathan S. Pluripotency factors in embryonic stem cells regulate differentiation into germ layers. *Cell*. 2011;145(6):875-89.

124. Wang Z, Oron E, Nelson B, Razis S, Ivanova N. Distinct lineage specification roles for NANOG, OCT4, and SOX2 in human embryonic stem cells. *Cell stem cell*. 2012;10(4):440-54.



BIBLIOGRAPHY

125. Lu J, Hou R, Booth CJ, Yang SH, Snyder M. Defined culture conditions of human embryonic stem cells. *Proceedings of the National Academy of Sciences of the United States of America*. 2006;103(15):5688-93.
126. Hirata TM, Ishkitiev N, Yaegaki K, Calenic B, Ishikawa H, Nakahara T, et al. Expression of multiple stem cell markers in dental pulp cells cultured in serum-free media. *Journal of endodontics*. 2010;36(7):1139-44.
127. Khanna-Jain R, Vanhatupa S, Vuorinen A, Sandor G, Suuronen R, Mannerstrom B, et al. Growth and Differentiation of Human Dental Pulp Stem Cells Maintained in Fetal Bovine Serum, Human Serum and Serum-free/Xeno-free Culture Media. *Journal of Stem Cell Research & Therapy*. 2012;2(4).
128. Kaupisch A, Kennedy L, Stelmanis V, Tye B, Kane NM, Mountford JC, et al. Derivation of vascular endothelial cells from human embryonic stem cells under GMP-compliant conditions: towards clinical studies in ischaemic disease. *Journal of cardiovascular translational research*. 2012;5(5):605-17.
129. Goldman O, Feraud O, Boyer-Di Ponio J, Driancourt C, Clay D, Le Bousse-Kerdiles MC, et al. A boost of BMP4 accelerates the commitment of human embryonic stem cells to the endothelial lineage. *Stem cells*. 2009;27(8):1750-9.
130. Cancedda R, Giannoni P, Mastrogiacomo M. A tissue engineering approach to bone repair in large animal models and in clinical practice. *Biomaterials*. 2007;28(29):4240-50.
131. Kaigler D, Krebsbach PH, West ER, Horger K, Huang YC, Mooney DJ. Endothelial cell modulation of bone marrow stromal cell osteogenic potential. *FASEB journal : official publication of the Federation of American Societies for Experimental Biology*. 2005;19(6):665-7.
132. Dissanayaka WL, Zhan X, Zhang C, Hargreaves KM, Jin L, Tong EH. Coculture of dental pulp stem cells with endothelial cells enhances osteo-/odontogenic and angiogenic potential in vitro. *Journal of endodontics*. 2012;38(4):454-63.

133. Hendrickx B, Verdonck K, Van den Berge S, Dickens S, Eriksson E, Vranckx JJ, et al. Integration of blood outgrowth endothelial cells in dermal fibroblast sheets promotes full thickness wound healing. *Stem cells*. 2010;28(7):1165-77.
134. Sieveking DP, Ng MK. Cell therapies for therapeutic angiogenesis: back to the bench. *Vascular medicine (London, England)*. 2009;14(2):153-66.
135. Gandia C, Arminan A, Garcia-Verdugo JM, Lledo E, Ruiz A, Minana MD, et al. Human dental pulp stem cells improve left ventricular function, induce angiogenesis, and reduce infarct size in rats with acute myocardial infarction. *Stem cells*. 2008;26(3):638-45.
136. Batsali AK, Kastrinaki MC, Papadaki HA, Pontikoglou C. Mesenchymal stem cells derived from Wharton's Jelly of the umbilical cord: biological properties and emerging clinical applications. *Current stem cell research & therapy*. 2013;8(2):144-55.
137. Bockman DE, Redmond ME, Waldo K, Davis H, Kirby ML. Effect of neural crest ablation on development of the heart and arch arteries in the chick. *The American journal of anatomy*. 1987;180(4):332-41.
138. Kirby ML. Plasticity and predetermination of mesencephalic and trunk neural crest transplanted into the region of the cardiac neural crest. *Developmental biology*. 1989;134(2):402-12.
139. Nakatsuka R, Nozaki T, Uemura Y, Matsuoka Y, Sasaki Y, Shinohara M, et al. 5-Aza-2'-deoxycytidine treatment induces skeletal myogenic differentiation of mouse dental pulp stem cells. *Archives of oral biology*. 2010;55(5):350-7.
140. Fanin M, Danieli GA, Cadaldini M, Miorin M, Vitiello L, Angelini C. Dystrophin-positive fibers in Duchenne dystrophy: origin and correlation to clinical course. *Muscle & nerve*. 1995;18(10):1115-20.
141. Miller JB, Schaefer L, Dominov JA. Seeking muscle stem cells. *Current topics in developmental biology*. 1999;43:191-219.
142. Lund TC, Grange RW, Lowe DA. Telomere shortening in diaphragm and tibialis anterior muscles of aged mdx mice. *Muscle & nerve*. 2007;36(3):387-90.

BIBLIOGRAPHY

143. Lu A, Poddar M, Tang Y, Proto JD, Sohn J, Mu X, et al. Rapid depletion of muscle progenitor cells in dystrophic mdx/utrophin<sup>-/-</sup> mice. *Human molecular genetics*. 2014;23(18):4786-800.
144. Ferrari G, Cusella-De Angelis G, Coletta M, Paolucci E, Stornaiuolo A, Cossu G, et al. Muscle regeneration by bone marrow-derived myogenic progenitors. *Science (New York, NY)*. 1998;279(5356):1528-30.
145. Saito T, Dennis JE, Lennon DP, Young RG, Caplan AI. Myogenic Expression of Mesenchymal Stem Cells within Myotubes of mdx Mice in Vitro and in Vivo. *Tissue engineering*. 1995;1(4):327-43.
146. Gussoni E, Soneoka Y, Strickland CD, Buzney EA, Khan MK, Flint AF, et al. Dystrophin expression in the mdx mouse restored by stem cell transplantation. *Nature*. 1999;401(6751):390-4.
147. Quattrocchi M, Swinnen M, Giacomazzi G, Camps J, Barthelemy I, Ceccarelli G, et al. Mesodermal iPSC-derived progenitor cells functionally regenerate cardiac and skeletal muscle. *The Journal of clinical investigation*. 2015;125(12):4463-82.

# **APPENDIX - SUPPLEMENTARY DATA**

---



## Supplementary figures and tables



**Figure S1: Genetic stability of DPPSC.** Short-Comparative Genomic Hybridization in DPPSC at passage 15 from 6 different donors showing no

## APPENDIX – SUPPLEMENTARY DATA

*chromosomal abnormalities. Some chromosome regions, including centromeric, peri-centromeric, heterochromatic and telomeric regions are excluded from sCGH analysis since they are artefactual, as well as chromosome 1p, 16, 17, 19 and 22 and p-arms of acrocentric chromosomes (most of these regions are shown in grey). The DNA control used for the hybridization was XXY, therefore male donors present a loss in chromosome X (highlighted in green) and female donors in chromosome Y (not highlighted since chromosome Y can be artefactual).*

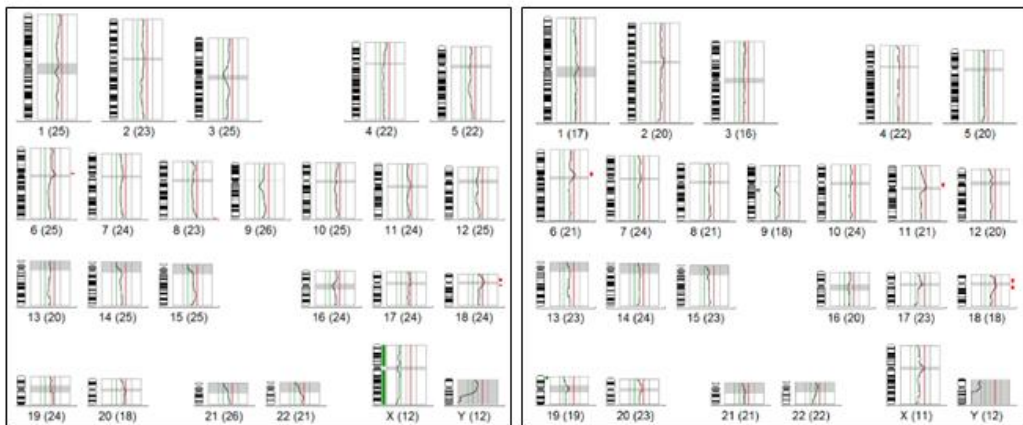


**Figure S2: Genetic stability of DPPSC.** Short-Comparative Genomic Hybridization in DPPSC at passage 15 from 2 different donors showing no chromosomal abnormalities. Some chromosome regions, including centromeric, peri-centromeric, heterochromatic and telomeric regions are excluded from sCGH analysis since they are artefactual, as well as chromosome 1p, 16, 17, 19 and 22 and p-arms of acrocentric chromosomes (most of these regions are shown in grey). The DNA control used for the hybridization was XXY, therefore male donors present a loss in chromosome X (highlighted in green) and female donors in chromosome Y (not highlighted since chromosome Y can be artefactual).

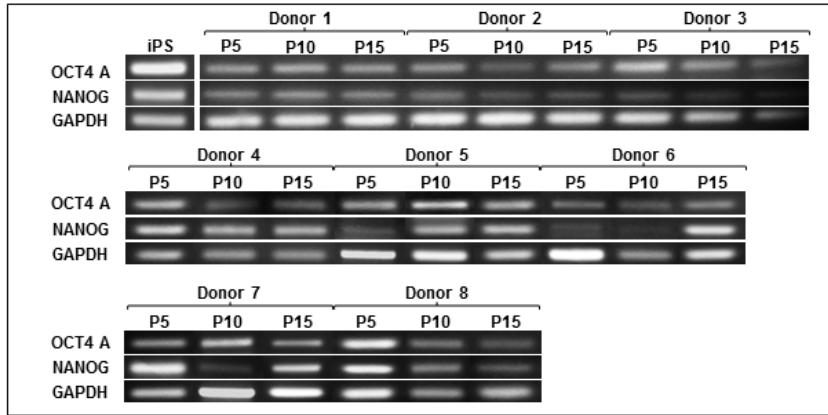


**Figure S3: RT-PCR analyses of pluripotent markers in undifferentiated DPPSC.** Analyses of mRNA expression of the pluripotency markers OCT4A and NANOG by RT-PCR in DPPSC from 8 different donors at passage 5, 10 and 15. GAPDH was used as housekeeping gene and human iPS cells were used as a positive control.

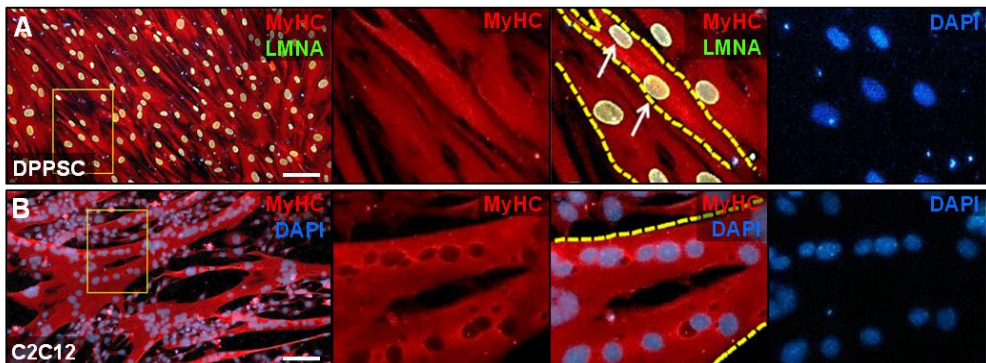


**Figure S4: In vitro myogenic differentiation of DPPSC to skeletal muscle. A)** Immunofluorescence analysis of DPPSC differentiated for 7 days to skeletal muscle. Myosin Heavy Chain is shown in red and human specific marker for Lamin A/C in green. Yellow lines show the presence of myotubes with more than one nucleus inside. The nuclei are indicated with white arrows. **B)** Immunofluorescence analysis of the mouse myoblast cell line C2C12 differentiated for 7 days to skeletal muscle. Myosin Heavy Chain is shown in red. An example of a myotube is also indicated with yellow lines. Nuclei are counterstained with DAPI in blue. Scale bars: 100μm.



## APPENDIX – SUPPLEMENTARY DATA

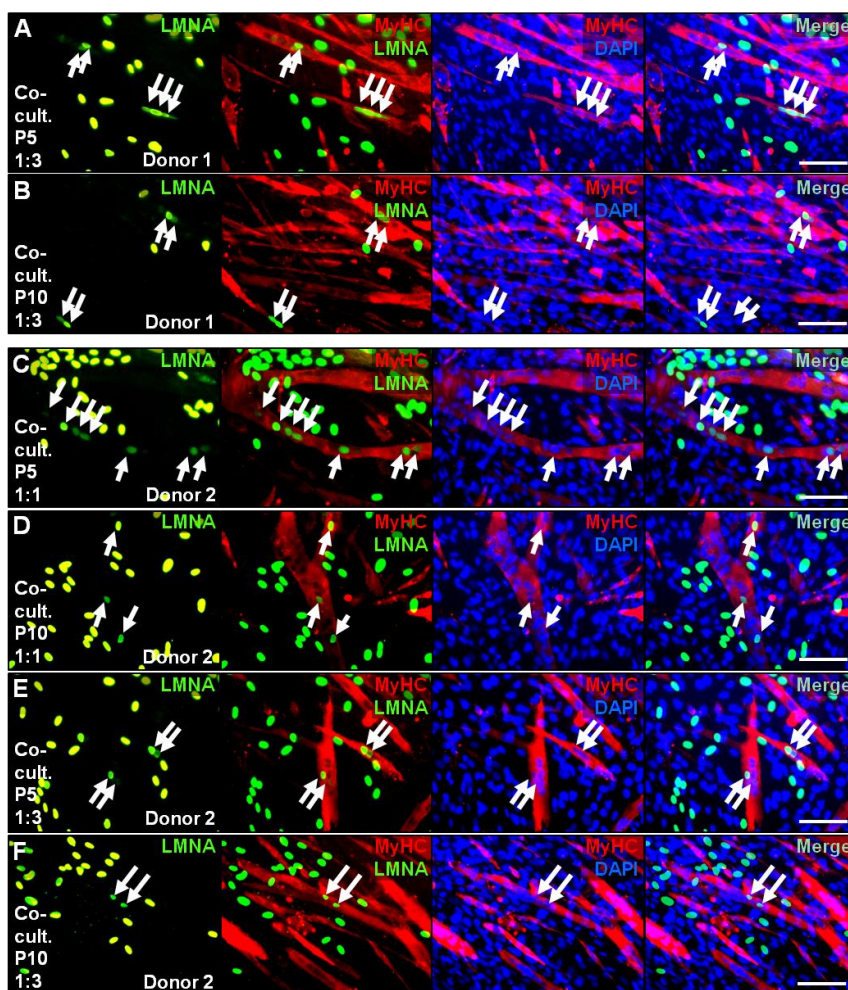


**Figure S5: In vitro myogenic differentiation of DPPSC to skeletal muscle co-cultured with C2C12 cells. A-B)** DPPSC from passage 5 (A) and 10 (B) from the same donor as Fig. 20 co-cultured with C2C12 cells 1:3 for 5 days. White arrows indicate the presence of human nuclei (stained for human-specific Lamin A/C in green), inside the hybrid myotubes expressing Myosin Heavy Chain (red). **C-F)** DPPSC from another donor at passage 5 (C, E) and 10 (D, F) co-cultured with C2C12 cells 1:1 (C, D) and 1:3 (E, F) for 5 days. White arrows indicate the presence of human nuclei (stained for human-specific Lamin A/C in green), inside the formed myotubes expressing Myosin Heavy Chain (red). Nuclei are counterstained with DAPI in blue. Scale bars: 100µm.

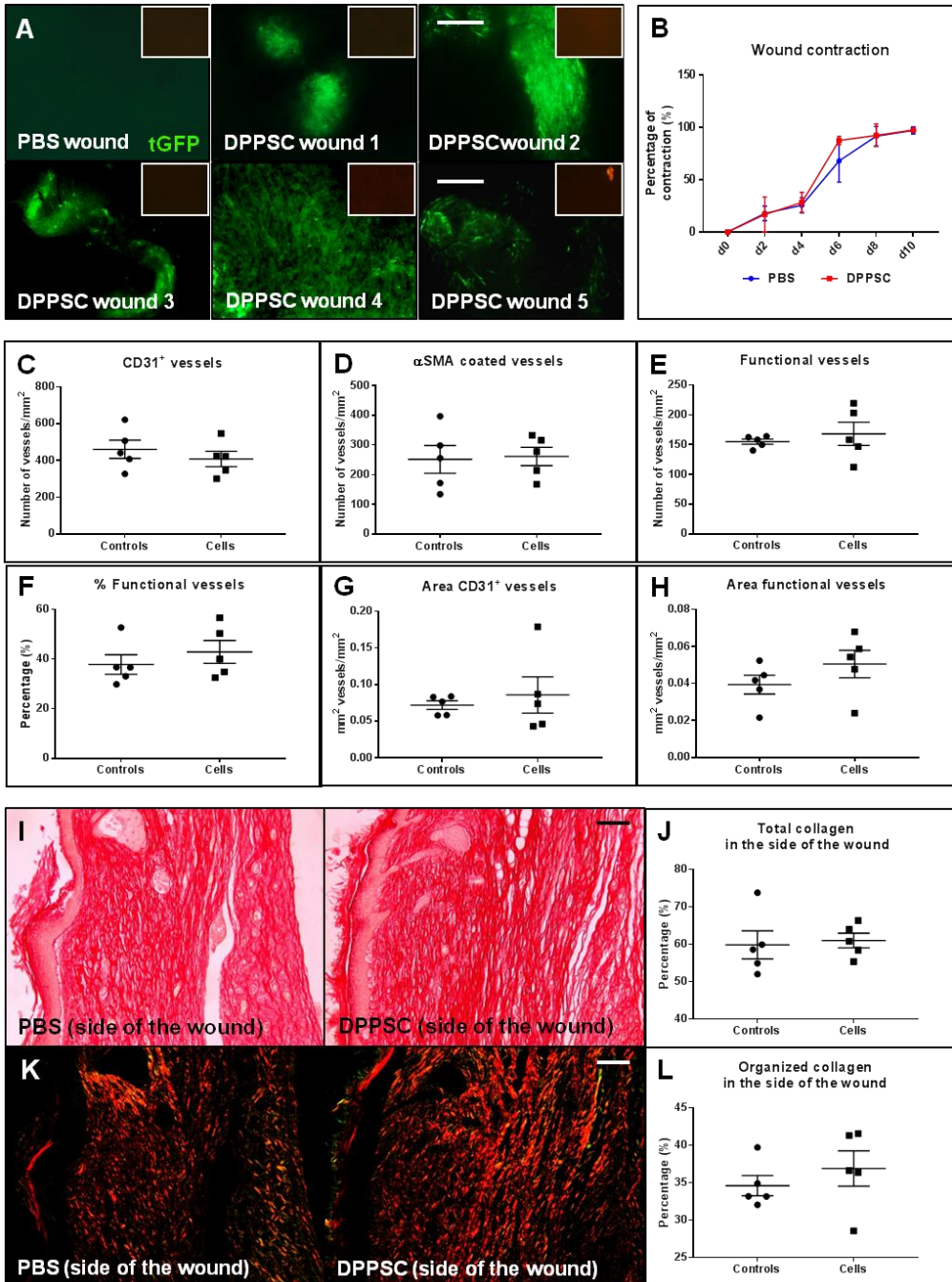


**Figure S6: Cell engraftment and effects of DPPSC treatment in the wound healing assay. A) Turbo GFP expression of DPPSC in the wounds at day 11.**

## APPENDIX – SUPPLEMENTARY DATA

*Unspecific fluorescence in the PBS or DPPSC treated mice can be observed in the TRITC channel (upper right picture). Scale bars: 2mm. **B**) Wound contraction from day 0 until day 10 in PBS or DPPSC treated wounds, showing no significant differences ( $p>0.05$ ,  $n=5$  for each group). **C-E**) Number of vessels CD31<sup>+</sup> (**C**),  $\alpha$ SMA-coated (**D**) and functionally active (**E**) per mm<sup>2</sup> of tissue, showing no significant differences ( $p>0.05$ ,  $n=5$  for each group). **F**) Quantification of functional vessels in PBS and DPPSC treated wounds, showing no significant differences ( $p>0.05$ ,  $n=5$  for each group). **G-H**) Quantification of CD31<sup>+</sup> area (**G**) and functional vessels area (**H**) in PBS or DPPSC treated wounds, showing no significant differences ( $p>0.05$ ,  $n=5$  for each group). **I**) Sirius Red staining of the side part of wounds treated with PBS or DPPSC for the analysis of total collagen in the wound matrix. Scale bars: 200  $\mu$ m. **J**) Quantification of the total collagen present in the side part of the wounds treated with PBS or DPPSC, showing no significant differences ( $p>0.05$ ,  $n=5$  for each group). **K**) Sirius Red staining of the same sections as in H using polarized light for the analysis of organized collagen (observed in red) in the wound matrix. Scale bars: 200  $\mu$ m. **L**) Quantification of the organized collagen present in the side part of the wounds treated with PBS or DPPSC, showing no significant differences ( $p>0.05$ ,  $n=5$  for each group).*

Donor	Gender	Age (years)	Molar(s)	Pathology (caries, periodontal disease, pericoronitis)	Date of extraction (dd/mm/yy)
1	XY	16	18,28,38,48	-	27/04/2012
2	XX	17	38	-	21/12/2012
3	XY	19	38	-	21/12/2012
4	XX	16	48	-	21/12/2012
5	XX	14	38,48	-	18/10/2013
6	XY	16	38,48	-	25/10/2013
7	XX	15	18,28	-	08/11/2013
8	XX	15	38,48	-	10/01/2014
9	XY	16	38,48	-	10/01/2014
10	XX	15	38,48	-	10/01/2014
11	XY	21	38	-	14/11/2014
12	XX	15	38	-	06/02/2015
13	XY	15	38,48	-	17/07/2015
14	XX	14	38,48	-	17/07/2015
15	XX	16	38,48	-	17/07/2015

**Supplementary Table 1:** Clinical information on the patients and third molars used for this study.

## Ethics Committee approvals



### CARTA APROVACIÓ PROJECTE PEL CER

Codi de l'estudi: BIO-ELB-2013-04

Versió del protocol: 1.1

Data de la versió: 09/01/14

Títol: "Caracterización celular de las Dental Pulp Pluripotent Stem Cells (DPPSC) y su potencial de diferenciación mesodérmica"

Sant Cugat del Vallès, 14 de gener de 2014

**Investigadora: Ester Martínez Sarrà**

**Títol de l'estudi: "Caracterización celular de las Dental Pulp Pluripotent Stem Cells (DPPSC) y su potencial de diferenciación mesodérmica"**

Benvolgut(da),

Valorat el projecte presentat, el CER de la Universitat Internacional de Catalunya, considera que, des del punt de vista ètic, reuneix els criteris exigits per aquesta institució i, per tant, ha

**RESULT FAVORABLEMENT**

emetre aquest CERTIFICAT D'APROVACIÓ per part del Comitè d'Ètica de la Recerca, per que pugui ser presentat a les instàncies que així ho requereixin.

Em permeto recordar-li que si en el procés d'execució es produís algun canvi significatiu en els seus plantejaments, hauria de ser sotmès novament a la revisió i aprovació del CER.


Atentament,



**Dr. Josep Argemí**  
**President CER-UIC**



De ondertekende aanvraagformulieren sturen naar: Erna Dewil, Proefdierencentrum, Herestraat 49  
bus 501, 3000 Leuven. [ecd@pfd.kuleuven.be](mailto:ecd@pfd.kuleuven.be)  
Document geldig van/valid from: 15/03/2014



**FORMULIER ETHISCHE COMMISSIE**  
**Form Ethical Committee**

KATHOLIEKE  
UNIVERSITEIT  
LEUVEN

**Gebruiker (User):** Aernout Luttun (ZAP lid van het Departement Cardiovasculaire Wetenschappen)  
**Erkenningsnummer Gebruiker (license number):** LA1210253 (Departement Cardiovasculaire Wetenschappen)

**Projectverantwoordelijke of proefleider (ZAP) (PI):**

Naam/Name	Voornaam/first name	Diploma /degree	Certificaat proefdierkunde/certificate lab animal science
LUTTUN	Aernout	PharmD/PhD	<input checked="" type="checkbox"/>

**Uitvoerende onderzoeker(s) (AAP/BAP) (researchers and technicians):**

Naam/Name	Voornaam/First name	Diploma/degree	Certificaat proefdierkunde/certificate lab animal science
Luttun	Aernout	PharmD/PhD	<input checked="" type="checkbox"/>
Caluwé	Ellen	Laborant	<input checked="" type="checkbox"/>
Van Houtven	Ellen	Laborant	<input checked="" type="checkbox"/>
Lox	Marleen	Laborant	<input checked="" type="checkbox"/>

**Proefdierantenne (animal antenna):**

Naam/Name	Voornaam/first name	Diploma /degree	Certificaat proefdierkunde/certificate lab animal science
Lox	Marleen	Laborant	<input checked="" type="checkbox"/>

Nieuw project (new project)       Verbonden aan een project (Nr. ....)/linked to project P...

**Titel van het onderzoeksproject (title of the research project):**

Studie van het wondhelend effect van MultiStem® cellen gederiveerd en gekweekt in serum-vrij medium.  
Evaluation of the healing effect of MultiStem® cells derived and cultured under serum-free conditions on wounds.

**Duur van het project (maximum 5 jaar) (duration of the project, max 5 years)**  
 Begindatum (start date): 01/02/2015      Einddatum (end date): 31/01/2020

Handtekening van de projectverantwoordelijke/signature PI      Datum/date 7/01/2015

**Binnen het project te gebruiken proefdieren (raming van het aantal benodigde dieren voor de bovenvermelde duur van het project) en inschatting van duur van de proef, duur en graad van pijn, lijden en letsel (zie Referentielijst) (species, strain, number of animals to be used, mean duration of the experiment, mean duration of pain, suffering and lasting harm, estimate of pain, suffering and lasting harm)**

Aantal (number)	Diersoort en stam (species and strain)	Gemiddelde duur van de proef (dagen, weken, maanden) <i>Mean duration of the experiment</i>	Gemiddelde duur van pijn, lijden en letsel (dagen, weken, maanden) <i>Mean duration of pain, suffering and lasting harm</i>	Graad van pijn, lijden en letsel (geen, gering, matig, ernstig, ondefiniceerbaar) <i>Estimate of pain, suffering and lasting harm (none, low, moderate, severe, undefinable)</i>
430	Adult athymic nu:nu mice	5-10 days	5-10 days	severe

APPENDIX – SUPPLEMENTARY DATA

P095/2012

De ondertekende aanvraagformulieren sturen naar: Ema Dewil, Proefdierencentrum, Herestraat 49 bus 501, 3000 Leuven.

Gelieve ons te verwittigen als het project effectief van start gaat, zodat een projectnummer kan toegekend worden



KATHOLIEKE  
UNIVERSITEIT  
LEUVEN

### FORMULIER ETHISCHE COMMISSIE

Laboratorium: Translational Cardiomyology Laboratory  
 Erkenningsnummer laboratorium: Stem Cell Institute Leuven - Dept of Development and Regeneration  
 Laboratoriumdirecteur:

Naam	Voornaam	Diploma	
Sampaolesi	Maurilio	PhD	

Proefvelders (ZAP):

Naam	Voornaam	Diploma	Certificaat proffilerkunde
Sampaolesi	Maurilio	PhD	<input checked="" type="checkbox"/>
.....	.....	.....	<input type="checkbox"/>
.....	.....	.....	<input type="checkbox"/>

Uitvoerende onderzoeker(s) (AAP/BAP):

Naam	Voornaam	Diploma	Certificaat proffilerkunde
Perini Haria / Quattrocelli Mattia		master thesis	<input checked="" type="checkbox"/>
Berardi Emanuele / Poes Matthias		PhD / master thesis	<input type="checkbox"/>

Nieuw project       Verlenging van een project (Nr. 068/2008)       Wijziging van een project (Nr.....)

(nieuwe titel, nieuw projectnummer)      (nieuwe titel, nieuw projectnummer)      (zelfde titel, zelfde projectnummer)

**Titel van het onderzoeksproject:**

Reprogramming adult stem cells: multipotent versus pluripotent potential in myogenic differentiation

**Duur van het project (maximum 4 jaar)**  
 Begindatum: 21/05/2012      Einddatum: 21/05/2016

Handtekening van de laboratoriumdirecteur:       Datum: 18/04/2012

---

**Advies (voorbehouden aan de Ethische Commissie):**  
 gunstig       gunstig mits aanpassingen       ongunstig      Datum: 31 VII 2012

**Inschatting van pijn, lijden of letsel door de Ethische Commissie:**  
 geen       gering       matig       ernstig       ondefinieerbaar

**Commentaar en opmerkingen:**

  
 De Voorzitter

  
 De Leden

## Doctorate School Academic Committee approvals



Barcelona, 21 de octubre de 2013

Sra. Ester Martínez Sarrà  
Anselm Clavé 207 Casa B  
08186 Lliçà d'Amunt

Estimada Sra.

Por la presente, le comunico que la Comisión Académica del Doctorado en Ciencias de la Salud, en la su sesión del 8 de octubre de 2013, y una vez estudiada su solicitud ha acordado:

Se acuerda admitir a la Sra. Ester Martínez Sarrà al Periodo de Investigación del Doctorado de Odontología.

Se acuerda aprobar el Proyecto de Tesis titulado "Caracterización celular de los Dental Pulp Pluripotent Stem Cells (DPPSC) y su potencial de diferenciación mesodérmica", y nombrar al Dr. Maher Al Atari como Director de la Tesis.

Adicionalmente, se le informa que la normativa de la UIC establece que debe obtener una evaluación favorable del Comité de Ética en la Investigación, antes de la puesta en marcha de la investigación. Deberá aportar este informe cuando lo obtenga.

Aprovecho la oportunidad para saludarla cordialmente,

Jaime Oliver Serrano  
Secretario Comisión Académica  
Doctorado en Ciencias de la Salud



**VICERECTORAT DE RECERCA**



REGISTRE GENERAL

Sortida  
5855  
Data  
21 10 13



APPENDIX – SUPPLEMENTARY DATA



ESTER MARTÍNEZ SARRÀ  
ANSELM CLAVÉ, 207 B  
08186 - LLIÇA D'AMUNT

Benvolguda Ester,

amb la present et comunico que la Comissió Acadèmica de Doctorat en Salut, en la passada edició del 5 de maig de 2015, va aprovar la teva petició de canvi d'expedient al Programa de Recerca en Salut. T'adjuntem la matrícula d'aquest curs acadèmic del que caldria fer el pagament de l'assegurança escolar.

Atentament,



Esther Belvis  
Secretària Tècnica de l'Escola de Doctorat  
Escola de Doctorat

Barcelona, 18 de maig de 2015



